[American Journal of Science, Vol. 312, October, 2012, P. 817–884, DOI 10.2475/08.2012.01]

American Journal of Science

CONSTRAINTS ON NEOPROTEROZOIC PALEOGEOGRAPHY AND PALEOZOIC OROGENESIS FROM PALEOMAGNETIC RECORDS OF THE BITTER SPRINGS FORMATION, AMADEUS BASIN, CENTRAL AUSTRALIA

NICHOLAS L. SWANSON-HYSELL*,†, ADAM C. MALOOF*, JOSEPH L. KIRSCHVINK**, DAVID A. D. EVANS***, GALEN P. HALVERSON§, and MATTHEW T. HURTGEN§§

ABSTRACT. The supercontinent Rodinia is hypothesized to have been assembled and positioned in tropical latitudes by the early Neoproterozoic Era. Paleomagnetic data from limestones of Svalbard and basaltic dikes of South China have been interpreted to record rapid changes in paleogeography driven by true polar wander that may have rotated the supercontinent in association with the ~800 Ma Bitter Springs carbon isotope event. To further constrain early Neoproterozoic paleogeography and to test proposed rapid rotations, we have developed sequence- and chemostratigraphically constrained paleomagnetic data from the Bitter Springs Formation of the Amadeus Basin of central Australia. A new paleomagnetic pole for the post–Bitter Springs stage ~770 Ma Johnny's Creek Member (Bitter Springs Formation) provides a positive test for a long-lived history of Australia and Laurentia in a single supercontinent as its similar position to late Mesoproterozoic north Australia poles reproduces the closure of the Laurentian "Grenville Loop." This new pole also provides support for the hypothesis that there was significant rotation between north and south+west Australia at the end of the Neoproterozoic as this rotation brings the south+west Australia ~755 Ma Mundine Well pole into much closer proximity to the north Australia Johnny's Creek pole. Syn–Bitter Springs stage carbonates of the Love's Creek Member of the formation contain a well-behaved remanence held by magnetite. The direction of this remanent magnetization falls on the Cambrian portion of Australia's apparent polar wander path suggesting that the magnetite may have formed authigenically at that time. If primary, the Love's Creek direction is consistent with the true polar wander hypothesis for the Bitter Springs stage, is internally consistent with the relative sea level changes inferred from the formation, and can constrain Australia to a SouthWest North America East AnTarctica (SWEAT) fit. A remanence held by pyrrhotite in carbonates of the Bitter Springs Formation corresponds to the apparent polar wander path of Australia at ~350 Ma. This component can be used to constrain the history of the Devonian-Carboniferous Alice Springs Orogeny as it demonstrates that regional folding of basinal sediments occurred prior to ~350 Ma, but that the latest stages of tectonism in the hinterland drove fluids through the sediments that altered redox conditions to favor pyrrhotite precipitation.

* Department of Geosciences, Princeton University, Guyot Hall, Washington Road, Princeton, New Jersey 08544, USA
** Division of Geological & Planetary Sciences, California Institute of Technology, 1200 East California Boulevard, Pasadena, California 91125, USA
*** Department of Geology & Geophysics, Yale University, New Haven, Connecticut 06520, USA
§ Department of Earth & Planetary Sciences, McGill University, Montreal, Quebec H3A 2A7, Canada
§§ Department of Earth & Planetary Sciences, Northwestern University, 1850 Campus Drive, Evanston, Illinois, 60208 USA
† Corresponding author's present addresses: Department of Earth and Planetary Science, University of California, Berkeley, 307 McCone Hall, Berkeley, California 94720-4767 and Winchell School of Earth Sciences, 100 Union Street SE, University of Minnesota, Minneapolis, Minnesota 55455; Email address: swanson-hysell@berkeley.edu

Key words: Neoproterozoic, Australia, paleomagnetism, paleogeography, Rodinia, Bitter Springs Formation, Alice Springs orogeny

INTRODUCTION

The Rodinia supercontinent is the most salient boundary condition controlling the evolution of the Earth system at the Mesoproterozoic to Neoproterozoic transition (~1 Ga) and throughout the Neoproterozoic Era as Rodinia rifted apart. This rifting then led to many of the spalled cratons reassembling as Gondwana (Hoffman, 1991). Major questions remain about the intervening paleogeography: Was Rodinia coherent for only the very beginning of the era, or was it intact into the Cryogenian? Was there large-scale true polar wander associated with the ~800 Ma Bitter Springs carbon isotope stage as suggested by paleomagnetic data from limestones of Svalbard and basaltic dikes of South China (Li and others, 2004b; Maloof and others, 2006)? How did changing paleogeography influence the global carbon cycle, low-latitude glaciation, and the evolution of animals?

Two primary geological observations first led to the reconstruction of a late Mesoproterozoic to early Neoproterozoic supercontinent: (1) the presence of ~1100 Ma (Grenville *sensu lato*) orogenic belts in Antarctica, Amazonia, Australia, Baltica, Congo, India, Kalahari and Laurentia (Hoffman, 1991; Moores, 1991; Li and others, 2008) and (2) the fact that Laurentia is surrounded by rifted margins of Neoproterozoic-Cambrian age (Bond and others, 1984; Hoffman, 1991). Since Laurentia is believed to be the keystone continent in Rodinia, there has been much discussion of the relative position between it and other constituents that are hypothesized to have been adjoined to its margins. A particularly vigorous debate is concerned with the relative positions of Laurentia and Australia/East Antarctica in the supercontinent.

Building on a connection postulated by Bell and Jefferson (1987), the first reconstructions of Rodinia connected Grenville-aged orogenic belts such that East Antarctica flanked southwestern North America (this model is called SWEAT; South-West North America East AnTarctica; Hoffman, 1991; Moores, 1991; Dalziel, 1991). In the original SWEAT model, Australia is located adjacent to northwestern Canada; a relationship that is strengthened by the presence of rift basins of similar age, orientation and stratigraphy on both continents (the Mackenzie Mountain Fold Belt in Northwest Canada and the Adelaide Rift Complex in South Australia; Rainbird and others, 1996; Preiss, 2000). The subsequent alternative reconstruction of AUSWUS (Australia South West United States) was proposed on the basis of pattern matching of crustal $^{87}Sr/^{86}Sr$ isopleths, correlation of lineaments between Australia and Laurentia and terrane matching between the distinctive Mojavia and Broken Hill provinces (Brookfield, 1993; Karlstrom and others, 1999, 2001; Burrett and Berry, 2000). Another variation on this theme of Australia as the conjugate margin to North America was proposed by Wingate and others (2002) on the basis of a paleomagnetic pole for the 1070 Ma Bangemall Basin Sills that was interpreted, in conjunction with poles from the well-constrained North American "Keweenawan Track," to be incompatible with either SWEAT or AUSWUS. This reconstruction was termed AUSMEX (Australia-Mexico) and aligned interpreted Grenville-aged metamorphism in Australia with southernmost Laurentia. Other reconstructions have argued that other continents were linked to the western margin of North America such as: Siberia (Kirschvink, 1992b; Sears and Price, 2000), Congo (Maloof and others, 2006), West Africa (Evans, 2009) and South China (Li and others, 2008). The model in which South China was a conjugate margin of western Laurentia has been termed the "missing-link" model as China fills a proposed gap between west Laurentia and Australia (Li and others, 1995, 2008).

Paleogeography sets the boundary conditions for many aspects of Earth system evolution. The latitudinal distribution of the continents and their configuration has

significant effects on the physics of Earth's surface through its control on ocean/atmosphere circulation and global albedo (Barron, 1981). Paleogeography also can exert powerful controls on the carbon cycle through processes such as silicate weathering and the land-area carbon cycle feedback during ice ages (Walker and others, 1981; Marshall and others, 1988), and the enhancement of organic carbon burial on tropical continental shelves (Schrag and others, 2002; Maloof and others, 2006). Rodinia's location and the timing/style of its break-up have been hypothesized to have been a dominant control on the large-scale variations in climate and biogeochemical cycling during the Neoproterozoic Era (for example "snowball Earth" events; fig. 1; Kirschvink, 1992a; Hoffman and others, 1998; Hoffman, 1999; Schrag and others, 2002; Lewis and others, 2004; Donnadieu and others, 2004), that themselves are hypothesized to have played a central role in the evolution of animals (Hoffman and others, 1998; Narbonne and Gehling, 2003; Canfield and others, 2007). These strong ties between changing continental positions and other aspects of Earth's evolving surface environment have been one of the prime motivators driving continued research that seeks to test and refine late Proterozoic paleogeographic models.

In order to evaluate hypotheses about the initial configuration and location of the supercontinent and the timing of its breakup, it is essential to obtain more paleomagnetic poles from across the Mesoproterozoic-Neoproterozoic transition at increasingly higher spatial and temporal resolution. The continuity of continental connections that is predicted by a supercontinent model sets up the testable hypothesis that paleomagnetic poles from the member continents trace out similar apparent polar wander paths (APWP). New paleomagnetic data sets from sedimentary lithologies can add to the paleomagnetic data base and have the additional advantage that they present the opportunity to directly pair records of paleolatitude and paleogeography to sedimentary records of changing climate and biogeochemical cycling—without the uncertainties that stem from spatial and temporal correlations. Furthermore, stratigraphic context enables tests of hypotheses that are reliant on high-resolution time series records of paleomagnetic directions such as rapid true polar wander.

Developing convincing records of primary paleomagnetic remanence in sedimentary rocks may be complicated by the secondary growth of iron oxides and sulfides that can partially or completely obscure the remanence direction held by primary ferromagnetic grains. An additional complexity of inclination shallowing can arise in lithologies where the magnetization is carried by a detrital remanent magnetization and where there has been significant post-depositional compaction. As a result of these potential complexities, it is essential to pair high-resolution study of ancient sedimentary paleomagnetic remanence direction with both field tests and rock magnetic experiments that determine the carriers of the remanence magnetization and constrain the timing of remanence acquisition. In this contribution, such a multidisciplinary approach is employed for sediments from the early Neoproterozoic Bitter Springs Formation of central Australia. Primary remanence directions from the Bitter Springs Formation would provide important constraints on the positioning of northern Australia in Rodinia and a direct test of the Maloof and others (2006) hypothesis that there was large-scale rotation of continental landmasses as a result of true polar wander associated with the ~800 Ma Bitter Springs Stage carbon cycle event. Furthermore, the interpretation that north and south+west Australia may have undergone late Neoproterozoic relative rotation (Li and Evans, 2011) underscores the need to develop more Neoproterozoic paleomagnetic poles from north Australia to improve the currently sparse database (fig. 1).

The Neoproterozoic Bitter Springs Stage and the True Polar Wander Hypothesis

Carbonates of Neoproterozoic age (1000 to 542 Ma) typically are enriched in ^{13}C with $\delta^{13}C$ values of ~5 per mil (Halverson and others, 2005). This high steady-state

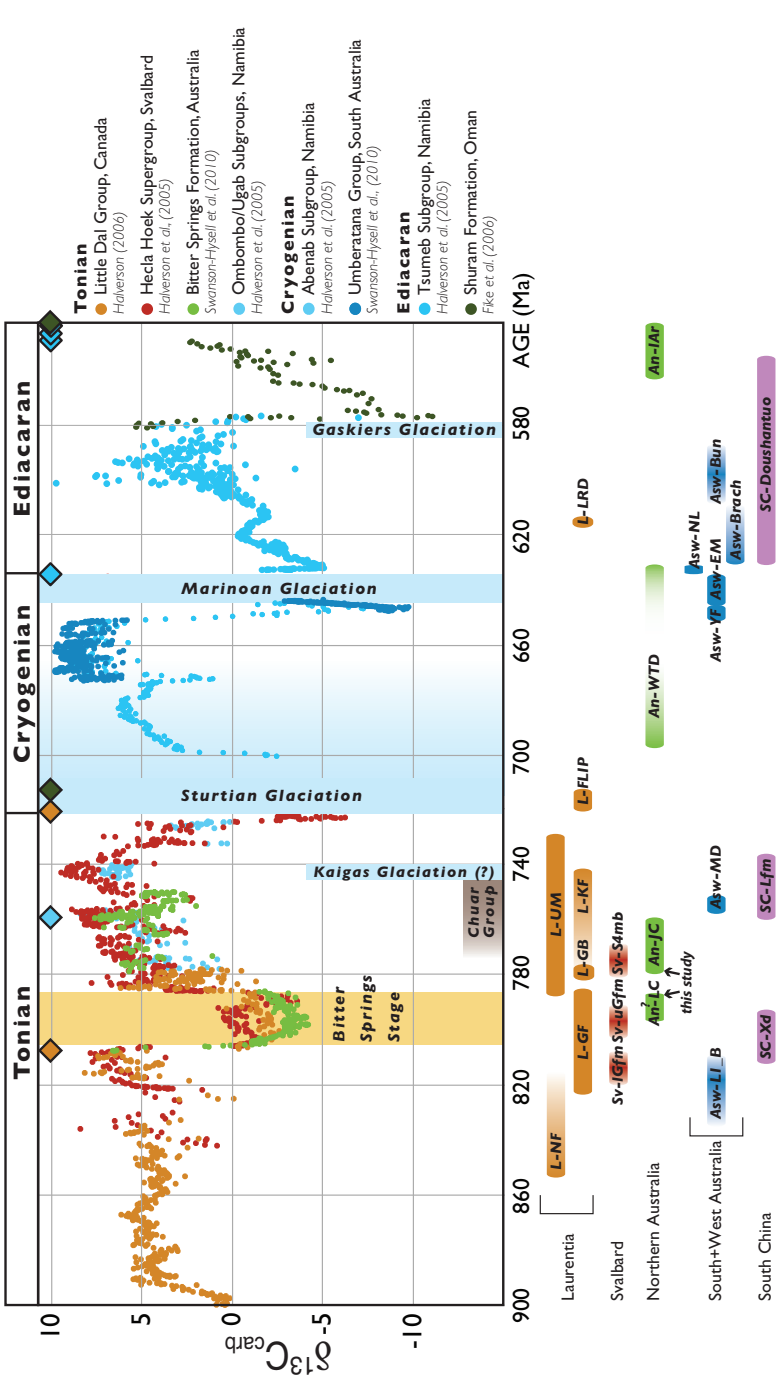

Fig. 1. Neoproterozoic timeline with composite carbonate carbon isotope records compiled from Halverson and others (2005), Fike and others (2006), Halverson (2006), and Swanson-Hysell and others (2010). This compilation is calibrated with U/Pb ages whose positions are indicated with diamonds from the 15-mile Group of NW Canada (Macdonald and others, 2010), the Ombombo Subgroup (Halverson and others, 2005) and Tsumeb Subgroup (Hoffmann and others, 2004) of Namibia and the Huqf Supergroup of Oman (Bowring and others, 2007). The Bitter Springs Stage is constrained to have occurred between 810 and 780 million years ago in this compilation. Although it has yet to be formally defined with a stratotype section, we use the working definition of the Tonian/Cryogenian boundary as being placed at the lowermost robust evidence for Neoproterozoic glaciation (~720 Ma), in concurrence with the 2009 recommendation of the International Commission on Stratigraphy. The ages of Neoproterozoic paleomagnetic poles are shown with their respective codes as keyed out in tables 10, 11, and 12.

base level is punctuated by down-turns in $\delta^{13}C$ that usually are associated with large-scale glacial events. However, prior to the first Neoproterozoic glacial period, and at a time (~800 Ma) when there is no preserved evidence for ice sheets anywhere on the globe, there is a salient interval of low $\delta^{13}C$ that has been identified in the Little Dal Group (Halverson, 2006; Mackenzie Mountains, Canada), the Akademikerbreen Group (Halverson and others, 2007; Svalbard), the Eleonore Bay Supergroup (Halverson and others, unpublished; Greenland), the 15 Mile Group (Macdonald and others, 2010; Ogilvie mountains, Canada), the Tambien Group (Alene and others, 2006; Ethiopia) and the Bitter Springs Formation (Hill and others, 2000; Swanson-Hysell and others, 2010; central Australia). During this interval, known as the Bitter Springs Stage, the $\delta^{13}C$ of carbonate rocks shift from a 250 Myr average of +5 per mil to a ~10 Myr excursion of −4 per mil to −1.5 per mil. Due to its global extent, prolonged duration and the fact that the shift also is recorded in the carbon isotopes of contemporaneous organic matter, the stage likely reflects a steady-state change in the fraction of carbon that was being buried as ^{13}C depleted organic matter in the world's oceans (Swanson-Hysell and others, 2010).

In the carbonate stratigraphy of the Akademikerbreen Group of Svalbard, the Bitter Springs Stage is bracketed by transient changes in sea level and shifts in the directions of paleomagnetic data from the pre–Bitter Springs Stage lower Grusdievbreen Formation to the syn–Bitter Springs Stage upper Grusdievbreen Formation and back to the post–Bitter Springs Stage upper Svanbergfjellet Formation (Maloof and others, 2006). Maloof and others (2006) interpreted the paleomagnetic directions as primary and considered plate tectonics, magnetic excursions, non-geocentric axial-dipole fields (see also Abrajevitch and Van der Voo, 2010), and true polar wander (TPW) as possible explanations for the data. They concluded that the most parsimonious explanation for the coincident changes is that there were rapid shifts in paleogeography resulting from a pair of TPW events that also caused transient changes in local sea level and perturbations to the carbon cycle as tropical sites of organic carbon burial were shifted to higher latitudes (Maloof and others, 2006).

True polar wander occurs on Earth as a result of the tendency for Earth's spin axis to align with the axis of the maximum non-hydrostatic moment of inertia (I_{max}). As a result, perturbations to the distribution of mass, on or inside Earth, can drive rotation of the silicate Earth (crust and the entire mantle) about a single axis (corresponding to the axis of the minimum moment of inertia; I_{min}) relative to Earth's spin axis (that is, the celestial reference frame). These rotations of continents in unison contrast from the differential plate motions of plate tectonics in that the same rotation applies to all continents. Current rates of secular TPW on Earth are ~10 cm/year, and largely are attributed to the redistribution of mass on Earth's surface associated with the demise of Northern Hemisphere ice sheets (Mitrovica and others, 2005; Matsuyama and others, 2010). Over the past 300 Myr, there has been near continuous TPW at rates of 0.1–1°/Myr due to advection of mass heterogeneities in the mantle that has complemented, but not overwhelmed, the apparent polar wander (APW) due to plate tectonics (Steinberger and Torsvik, 2008). The possibility of large-scale TPW, in which there is significant relative motion between the silicate earth and the spin vector at rates that could exceed those of normal plate tectonics, has been discussed as a theoretical possibility for years in the geophysical literature (Gold, 1955; Fisher, 1974; Steinberger and O'Connell, 1997; Evans, 2003; Raub and others, 2007), although the rate at which TPW can progress is an issue of some controversy (Steinberger and O'Connell, 2002; Tsai and Stevenson, 2007). The rate at which true polar wander can occur is a function of the magnitude of the perturbation to Earth's moment of inertia tensor, the timescale on which that perturbation is applied and the timescale for viscoelastic adjustment of Earth's rotational bulge (which is itself largely a function of

mantle viscosity; Tsai and Stevenson, 2007; Steinberger and Torsvik, 2010). The size of a perturbation could be amplified, and its emplacement timescale shortened, if mass advection within the mantle resulted in the deflection of density discontinuity surfaces. The pair of TPW events proposed by Maloof and others (2006) requires ~45 degrees of oscillatory "there-and-back-again" motion. The initial TPW could have been caused by convectively driven inertia perturbations acting on a prolate nonhydrostatic Earth figure (Steinberger and O'Connell, 1998). The "back again" motion may have resulted from TPW-induced elastic stresses in the lithosphere, driving the remnant pre-TPW bulge back to the equator after the initial TPW inducing load was diminished (Creveling and others, 2012).

As TPW moves the solid earth with respect to the rotational bulge, water is able to adjust nearly instantaneously to the newly established gravitational equipotential. In contrast, the solid earth has a response time on the order of 10^4 years and the resulting lag causes a transient relative sea level change (Mound and Mitrovica, 1998). On any rotating body there is a latitudinal dependence of gravitational potential such that: $g_{rot} = g - \omega^2 R_e \cos^2\lambda$, where g_{rot} is the gravity on the rotating spheroid, g is the reference gravity without the effect of rotation, ω is the rotational velocity, R_e is the mean radius of the spheroid, and λ is latitude. As a result of this relationship and the lag in the response time of the solid earth, a continent moving toward the equator during ongoing TPW will experience transient relative sea level rise, while a continent moving to higher latitudes will record transient relative sea level fall. In the 2 km thick succession of platformal carbonates of the Akademikerbreen Group in Svalbard there are only two sequence boundaries that contain evidence for significant relative sea level change. The first of these (termed "G1") is an exposure surface with ~20 meters of karstic relief that coincides with the onset of the Bitter Springs Stage and the observed shift in paleomagnetic directions. The ~45° arc distance between the paleomagnetic poles of the Akademikerbreen group from before and during the Bitter Springs Stage suggest that Svalbard (along with East Greenland and other parts of eastern Laurentia) moved across the equator and then poleward across the G1 boundary. This motion away from the equator would lead to a transient regression and the observed exposure surface. At the end of the Bitter Springs Stage, the proposed second TPW event would have driven Svalbard equatorward and caused the transient rise in sea level responsible for the flooding surface associated with the end of the isotope stage ("S1"). Under the rotation proposed by Maloof and others (2006), east Svalbard would have crossed the equator but would have remained in the tropics. The lack of evidence for significant climate-controlled changes to the sedimentary environment (such as a change in aridity) across G1 and S1 are consistent with this interpretation. However, the true polar wander hypothesis would require certain continents to undergo significant latitudinal changes that would have moved depositional centers into different climatic regimes and resulted in larger transient changes in relative sea level.

A successful stratigraphic test of the TPW hypothesis for the Bitter Springs Stage should recognize identical $\delta^{13}C$ changes that reflect the global carbon cycle, but different changes in relative sea level and local climatic regime that are consistent with the change in paleolatitude implied by the paleomagnetic data. In order to test the TPW hypothesis for the Bitter Springs Stage, we have developed detailed records of the physical, $\delta^{13}C$ and paleomagnetic stratigraphy of the Bitter Springs Formation across the Amadeus Basin of central Australia (fig. 2). As time equivalents to the Akademikerbreen Group of Svalbard, these carbonates should record the same perturbation in $\delta^{13}C$, but have a different record of sea level change, and paleomagnetic direction if TPW shifted Australia's paleoposition with respect to the axis of rotation (I_{min}).

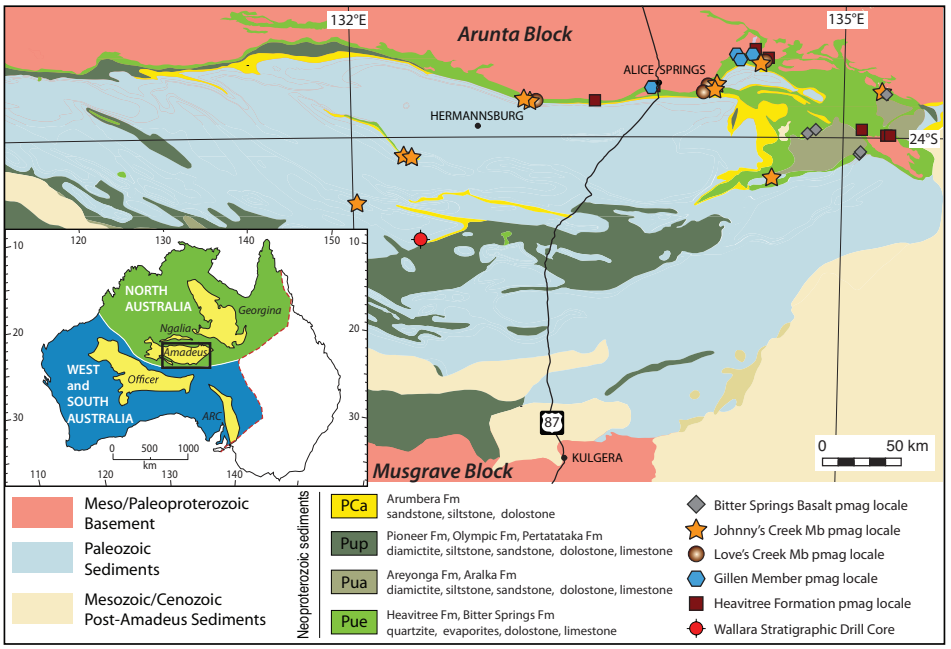

Fig. 2. Geological map of the Amadeus Basin modified from Ahmand and Scrimgeour (2006). Localities for the stratigraphic sections from which paleomagnetic data were obtained are marked and keyed-out by stratigraphic member. Inset map shows basins of Australia that contain Neoproterozoic sediments in yellow (ARC—Adelaide Rift Complex; modified from Raimondo and others, 2009). The black box depicts the extent of the more detailed map of the Amadeus Basin. The red dashed line is the Tasman line, which represents the interpreted eastward extent of pre-Neoproterozoic crust (Li and others, 1995). The division between North Australia and South+West Australia is taken as the Petermann and Paterson Orogenic belt which is the dividing line between the early Proterozoic cratonic blocks of South Australia and West Australia with the North Australian craton. The geometry of this suture is adapted from Myers and others (1996).

The Amadeus Basin and the Bitter Springs Formation

Basin development and nearby orogenesis.—The Amadeus Basin of central Australia is a cratonic basin bounded by Paleozoic uplifts (fig. 2). Sedimentation in the Amadeus basin began in early Neoproterozoic time (at ~850 Ma) and continued into the Late Devonian (360 Ma; Lindsay and Korsch, 1989; Lindsay, 2002; Haines and others, 2001). Deposition in the basin was episodic over this period, and was characterized by various modes of basin development (Lindsay, 2002). Large-scale similarities in the Neoproterozoic stratigraphy of the Amadeus, Officer, Georgina and Ngalia basins have led to the hypothesis that these cratonic basins were once part of a single large subsiding continental platform termed the "Centralian Superbasin" (fig. 2; Walter and others, 1995). The possibility that later orogenic activity and associated sedimentation was associated with post-depositional iron oxide growth/alteration (and thus remagnetization), necessitates an overview of the subsequent history of the basin. Two major orogenic events, the Petermann orogeny (early Cambrian) and the Alice Springs orogeny (Devonian-Carboniferous), led to thick-skinned deformation and the uplift of the basement inliers that fragmented the Centralian Superbasin into its constituent parts (Sandiford and Hand, 1998). In addition to redefining the boundaries of Australian intracratonic basins, these orogenies governed the sediment supply and the subsidence of the post-Neoproterozoic Amadeus Basin and uplifted the deep crustal

rocks that border the Amadeus Basin to the north and to the south (the Arunta and Musgrave blocks respectively; fig. 2).

The Petermann Orogeny resulted in the exhumation of the Musgrave block (fig. 2), a crustal block that currently defines the southern margin of the Amadeus Basin and is composed of Paleoproterozoic to Mesoproterozoic metamorphic rocks that record Grenville-age magmatic and metamorphic events (White and others, 1999; Hand and Sandiford, 1999). The thrusts associated with the orogeny strike east-west, are predominantly north-vergent, and are constrained by $^{40}Ar/^{39}Ar$ ages from micas associated with shear zones to have been active between ~550 to ~520 Ma (Maboko and others, 1992; Camacho and others, 1997). This orogenic belt is effectively the dividing line between the North Australian Craton and the South Australian craton (fig. 2; Myers and others, 1996) and shortening is interpreted to have been restricted to a relatively narrow belt such that there was little deformation within the present day Amadeus Basin (Hand and Sandiford, 1999). U-Pb ages on titanite interpreted to have crystallized during peak upper amphibolite to granulite facies metamorphism in the core of the orogen are ~570 to ~540 Ma (Raimondo and others, 2009). Synorogenic sediments (such as those that outcrop in the famous Ayers Rock–Uluru monolith) were deposited proximal to the mountain belt in the southern Amadeus Basin, and wide-spread sedimentation began throughout the basin at this time and continued into the Ordovician. This period of subsidence has been attributed to thermal subsidence following extension (Korsch and Lindsay, 1989), or due to active extensional processes at the time (Haines and others, 2001). It also is possible that the accommodation space was a result of dynamic subsidence (for example Heine and others, 2008) and/or long-wavelength lithospheric flexure beneath central Australia (as suggested by gravity data; Aitken and others, 2009).

Synorogenic sedimentation in the Amadeus Basin also records the Devonian-Carboniferous Alice Springs orogeny, whose age is constrained by $^{40}Ar/^{39}Ar$ ages on micas from mylonite zones (410-310 Ma; Dunlap and Teyssier, 1995; Haines and others, 2001) and U-Pb dates from synorogenic pegmatites and metamorphic zircon, monazite and titanite (450-310 Ma; Buick and others, 2008 and references therein). This mountain-building event was, in many ways, a mirror image of the Petermann Orogen, as it exhumed the Arunta crustal block that forms the northern margin of the basin along south-vergent faults (fig. 2; Haines and others, 2001). The Alice Springs orogeny was characterized by thick-skinned deformation in the Arunta block, and also caused thin-skinned deformation and the development of a foreland fold-thrust belt within Amadeus Basin sediments. This deformation exposed the basal Neoproterozoic stratigraphy, particularly along the northern margin of the basin in the MacDonnell Ranges (Lindsay, 2002), and caused locally-thick foreland basin sedimentation. The preservation of late Mesoproterozoic $^{40}Ar/^{39}Ar$ cooling ages in K-feldspar from a granite boulder in the Areyonga Formation (the early Cryogenian formation that directly overlies the Bitter Springs Formation; fig. 3) indicates that the Neoproterozoic stratigraphy could not have been heated above 230 °C for any extended period of time (McLaren and others, 2009). This result is indicative of the low-metamorphic grade of the sediments and provides a ~6 km upper limit on the thickness of the sedimentary overburden in the study area.

Neoproterozoic stratigraphy of the Amadeus Basin.—The sedimentary succession in the Amadeus Basin begins with the transgressive sandstone of the Heavitree Formation (also known as the Heavitree Quartzite). This formation has a sheet-like geometry and is interpreted to have been deposited on a high-energy open shelf that was undergoing regional subsidence (Lindsay, 1999). Conformably overlying the Heavitree Formation are >1000 m of shallow marine carbonates and evaporites comprising the Bitter Springs Formation. The age of the basinal sediments are constrained by dikes in the

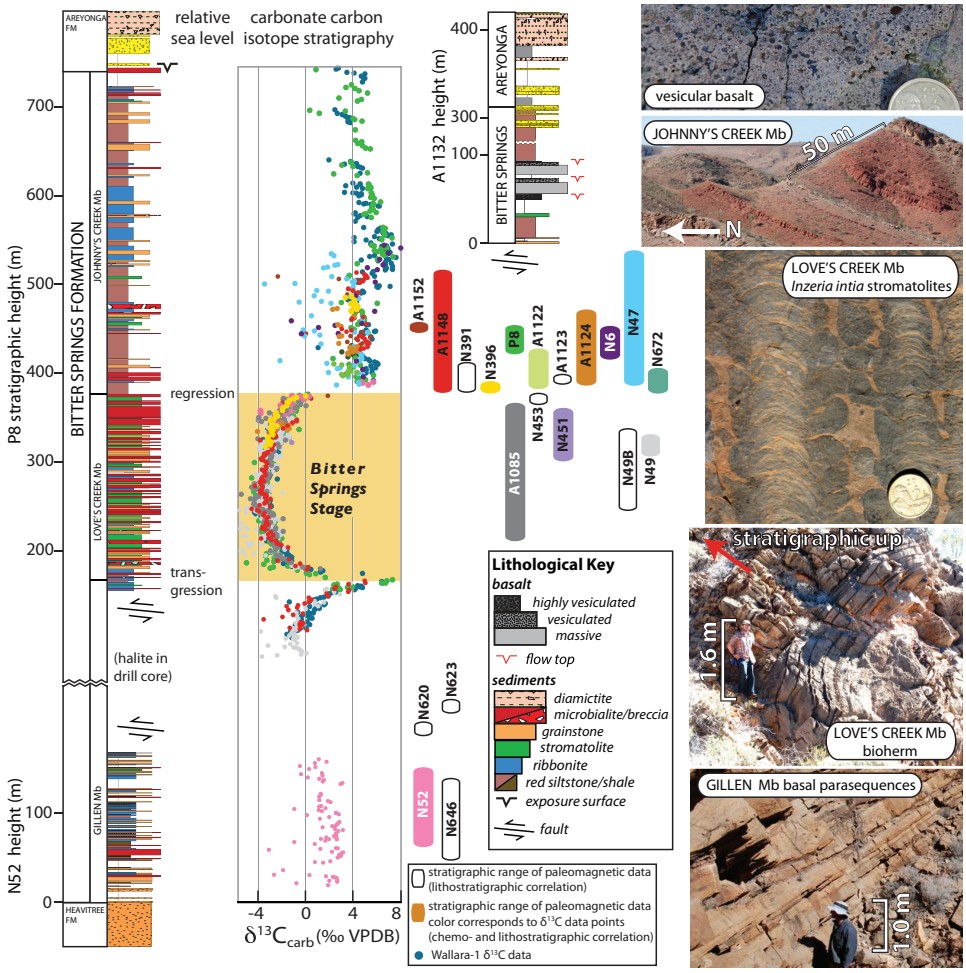

Fig. 3. Representative stratigraphic sections of the Gillen Member from near the Alice Spring's town dump (N52), the Love's Creek Member, Johnny's Creek Member and Areyonga Formation from the Ellery Creek area (P8) and the Johnny's Creek Member, Bitter Springs Volcanics and Areyonga Formation from the section on Love's Creek Station (N1132). Carbonate carbon isotope data are shown for the N52 and P8 sections, as well as for other sections that were targeted for paleomagnetic study. The carbon isotope data from other sections have been scaled to match the P8 carbon isotope record. The stratigraphic range of paleomagnetic samples, that in some cases is a more restricted range than carbon isotope data from the same section, is shown with bars to the right of the composite chemostratigraphy. The carbon isotope record for the Wallara-1 drill-core also is shown as it contextualizes samples used for rock magnetic experiments from the Love's Creek Member and for the N1132 section as it supports the lithostratigraphic correlation shown with the P8 section. The coin for scale in the close-up photos of stromatolites and vesicular basalt has a diameter of 2 cm. The name given for the columnar stromatolites with transversely elongate projections follows the taxonomic classification of Walter (1972).

Arunta block (the ~1070 Ma Stuart dike swarm; Schmidt and others, 2006) and the Musgrave block (the ~1070 Ma Alcurra/Kulgera dike swarm; Schmidt and others, 2006) that do not intrude the basinal sediments and provide a maximum age for the initiation of sedimentation in the Amadeus Basin. Detrital zircon data from the Heavitree Formation contain late Mesoproterozoic zircons (Maidment and others, 2007), but do not provide firmer age constraints than the dikes.

The Bitter Springs Formation can be divided into three members: Gillen, Love's Creek and Johnny's Creek. The Gillen Member consists of dolostone and limestone wavy laminite, as well as grainstone, and commonly contains calcite pseudomorphs after gypsum attesting to arid conditions where evaporation often exceeded precipitation. Massive halite has been encountered in four subsurface cores that penetrate the unit (Lindsay, 1987). The evaporites within the Gillen Member have caused the member to be rheologically weak in comparison to the surrounding units. In contrast to the Heavitree Formation and rest of the Bitter Springs Formation, which are commonly coherently exposed in thrust sheets along the northern basin-bounding monocline, the Gillen Member has been exploited as a structural detachment and often can be seen to be tightly folded and truncated in surface outcrop.

Atop the Gillen Member, the Love's Creek Member (160-260 m thick) is dominated by stromatolite and microbialite facies that are rarely interrupted by thin intraclast breccias and wavy laminites (fig. 3). The base of this unit represents a relative sea level rise (Southgate, 1989). Oolite and intraclast breccia facies mark this transgression and are followed by the largely subtidal microbialite/stromatolite reef facies of the Bitter Springs Stage. This transition also could reflect a decrease in local aridity given the relative paucity of evaporite pseudomorphs in the Love's Creek Member compared to the Gillen Member. However, there are anhydrite nodules present in drill core intersecting the Love's Creek Member (for example in the Wallara-1 and BR05DD01 drill cores) and it is difficult to deconvolve the role of relative sea level change and changing local climatic conditions from this change in evaporite abundance.

There is an abrupt change in sedimentary lithology at the top of the Love's Creek Member, with the sudden appearance of red siltstones that are interbedded with layers of stromatolites, grainstones, and dolostones that contain molar tooth structures and dalmatian (mottled) sedimentary textures of the Johnny's Creek Member (fig. 3). This unit has, in some previous publications, been referred to as the upper Love's Creek Member (or unit 3 of the Love's Creek Member; for example, Southgate, 1989; Hill and others, 2000). We follow the current stratigraphic terminology of the Northern Territory Geological Survey in referring to the unit as the Johnny's Creek Member (Ambrose and others, 2010). In the eastern-most part of the basin, basalt flows are intercalated with siltstone at the top of the Johnny's Creek Member (fig. 2).

In many locations within the Amadeus basin, the top of the Bitter Springs Formation is an unconformity that is overlain by conglomerate, diamictite and sandstone of the glacigenic Areyonga Formation and followed by siltstone of the Aralka Formation. The Areyonga glacial deposits have been correlated (Preiss and others, 1978; Walter and others, 1995) to the ~720 to 660 Ma low-latitude Sturtian glacial event (Macdonald and others, 2010). A Re-Os isochron age of 657.2 ± 5.4 Ma has been obtained from black shales sampled from the Aralka Formation in the Wallara-1 core (Kendall and others, 2006). The Aralka Formation overlies the Areyonga Formation and this result provides a tentative minimum age constraint for the the glacial diamictites, suggesting a pre-Marinoan age while also providing a minimum age constraint for the Bitter Springs Formation.

Chemostratigraphic correlation with stratigraphic successions with direct age constraints provides another means to constrain the age of the Bitter Springs Formation. High-resolution $\delta^{13}C$ data throughout the Bitter Springs Formation, from the basal Gillen Member up to the disconformity with the overlying Areyonga Formation, show values in the Gillen that fluctuate around +3 per mil with small transient negative spikes (fig. 3; Swanson-Hysell and others, 2010). $\delta^{13}C$ values then decrease before rising into a positive $\delta^{13}C$ spike (maximum of >7‰) at the contact with the Love's Creek Member (fig. 3). The $\delta^{13}C$ stratigraphy then enters the period of sustained negative values known as the Bitter Springs Stage that persists over 190 to 270 meters of

stratigraphy, depending on the location within the basin. A gentle rise towards 0 per mil is followed by a step-wise transition back to mean Neoproterozoic $\delta^{13}C$ of +5 to +6 per mil marking the end of the Bitter Springs Stage and the onset of Johnny's Creek Member sedimentation (fig. 3). This extended departure from positive values is similar to the Bitter Springs Stage $\delta^{13}C$ records developed from other stratigraphic successions including the Akademikerbreen Group of Svalbard and the Fifteen Mile Group of NW Canada (fig. 1). If correct, the correlation to the 15 Mile Group lends significant constraints to the age of the Bitter Springs formation, as a volcanic tuff from the stratigraphy immediately preceding the interpreted Bitter Springs Stage has a U-Pb zircon age of 811.5 ± 0.3 Ma (Macdonald and others, 2010)—consistent with thermal subsidence modeling of the Svalbard stratigraphic succession (Maloof and others, 2006). On the basis of the correlation of the Bitter Springs Formation carbon isotope record with the record from the Fifteen Mile Group of NW Canada (Macdonald and others, 2010) as well as the Ombombo Subgroup of Namibia (Halverson and others, 2005), the Bitter Springs Stage, and correspondingly deposition of the Love's Creek Member, is constrained to have been ongoing from ~810 Ma to ~785 Ma (fig. 1). Chemostratigraphic correlation and consideration of the physical stratigraphy suggests that significant time is missing between the top of the Johnny's Creek Member and the onset of Sturtian glaciation at ~720 Ma and leads to an interpretation of the top of the Johnny's Creek Member being ~750 million years old as shown in figure 1.

In the context of the true polar wander hypothesis, the rise in local sea level recorded in the sedimentary succession entering the Bitter Springs Stage at the Gillen/Love's Creek contact and the potential evidence for a decrease in aridity is consistent with rapid motion of Australia from the dry subtropics into the wet tropics (fig. 3). Subsequent rotation at Love's Creek/Johnny's Creek boundary would have returned Australia to the subtropics, a change that is consistent with the demise of the microbialite reefal facies that characterizes the Love's Creek Member, the initial deposition of the mixed siliciclastic/carbonate sediments of the Johnny's Creek Member and the stepwise jump in $\delta^{13}C$ values indicating a temporal gap in the record that is consistent with temporary exposure resulting from a transient fall in local relative sea level. We now seek to use new paleomagnetic data from the Bitter Springs Formation to test the hypothesis that changes in carbon cycling, in local sea level and potentially in local climate are the result of large-scale rapid TPW.

METHODS

Paleomagnetic Methods

Remanent magnetization measurements were made with 2G Enterprises™ DC SQuID magnetometers at the California Institute of Technology and Yale University. These magnetometers have a background noise sensitivity of 5×10^{-12} Am^2 per axis. The magnetometers are equipped with online alternating field (AF) demagnetization coils, an automated pick-and-place vacuum system and a quartz-glass sample holder as described in Kirschvink and others (2008). Samples and instruments were housed in a magnetically shielded room with residual fields <100 nT throughout the demagnetization process.

After measuring the natural remanent magnetization (NRM), but prior to AF and thermal demagnetization, samples were cooled in liquid N_2 in an additionally magnetically shielded space. This procedure brought the samples through the Verwey transition of magnetite (120 K), thereby selectively demagnetizing large multidomain grains whose remanence recovers to a much lesser extent than small single-domain grains upon warming in zero field (Muxworthy and McClelland, 2000).

AF demagnetization proceeded at steps of 2.5, 5, 7.5, and 10 mT for siliciclastic and volcanic lithologies and at steps of 2.0, 4.0, 6.0, and 7.0 mT for the carbonates.

Following these low-field AF demagnetization steps, the samples were thermally demagnetized in a magnetically shielded ASC Scientific™ oven in an N_2 atmosphere. Temperature progressively increased in 2 °C to 50 °C steps for a total of 24 to 30 thermal steps per specimen (see figs. 4 and 5 for the resolution of these steps). Thermal demagnetization usually proceeded to 685 °C for the siltstones of the Johnny's Creek Member, Gillen Member and basalt flows, and proceeded to 550 °C for the carbonates of the Love's Creek and Gillen Members. After each demagnetization step, three-axis measurements were made in both sample-up and sample-down orientation, and samples with a circular standard deviation $>8°$ were reanalyzed. Magnetic components were fit using principal component analysis (Kirschvink, 1980), as implemented in PaleoMag OS X v3.1 (Jones, 2002).

We also discuss paleomagnetic data generated from a locality of the Heavitree Formation at Heavitree Gap with different methods. These samples were measured at the Australian National University in 1976 by JLK using a ScT superconducting magnetometer with background noise sensitivity of $\sim 5 \times 10^{-11}$ Am^2. These samples were thermally demagnetized progressively in air, in magnetic fields held to below ~10 nT by feedback-controlled coil systems, and treated in six steps between 180 and 640 °C. Data were recovered recently from old print-outs through optical scanning and analyzed with modern principal component analysis.

Rock Magnetism Experimental Methods

To characterize the magnetic mineralogy of the Bitter Springs sediments, we conducted a suite of rock magnetic experiments.

Room-temperature remanence experiments.—The same 2G enterprises SQuID magnetometer used for paleomagnetic measurements at Caltech was utilized to conduct room temperature rock magnetic experiments on 18 end chips of paleomagnetic cores from the Love's Creek Member and seven of the Johnny's Creek Member. For isothermal remanent magnetization (IRM) acquisition experiments, the field was increased in a stepwise fashion up to 350 mT (for Love's Creek carbonates) or 900 mT (for Johnny's Creek siltstones) and the samples were subjected to AF demagnetization. Anhysteretic remanent magnetization (ARM) experiments applied a biasing field from 0 to 1 mT in the presence of a 100 mT alternating field before demagnetization. Coercivity spectra (also known as "gradient of acquisition plots") were produced for all analyzed samples by taking the derivative of the stepwise AF and IRM curves with respect to the log of the applied field and smoothing them with a running average (as implemented in Kopp, ms, 2007).

Low-temperature remanence experiments.—A Quantum Design SQuID magnetometer (MPMS-2) was used to perform low-temperature cycling experiments and remanence upon warming experiments at the Institute for Rock Magnetism. In the low-temperature cycling experiments, a 2.5 T isothermal remanent magnetization (IRM) was imparted at room temperature (300 K). The samples were then cooled to 5 to 10 K and then warmed back to room temperature, all in a zero field. In the remanence upon warming experiments, samples were first cooled from 300 K to 10 K in a 2.5 T field and than the remanent magnetization was measured during warming back to 300 K in a zero field (field cooled). Then the samples were cooled again in zero field, pulsed with a 2.5 T IRM at 10 K and warmed back to room temperature in a zero field (zero-field cooled).

These experiments have powerful diagnostic capabilities due to the varying low-temperature behavior of different magnetic mineralogies. For magnetite (Fe_3O_4), at ~120 K there is a conversion from the cubic phase to a low-temperature monocline phase (the Verwey transition; Verwey, 1939). The Verwey transition is expressed upon cooling through ~120 K with significant demagnetization of remanence, some of which recovers upon warming (depending on grain size). Monoclinic pyrrhotite

(Fe_7S_8) has a similar diagnostic magnetic transition at ~35 K that results in loss of remanence (the Besnus transition; Besnus and Meyer, 1964). Some minerals that lack crystallographic transitions at low temperature nevertheless have characteristic remanence behavior. For example, the remanence of the iron oxyhydroxide goethite (αFeOOH) is greatly enhanced upon cooling in a zero field (Maher and others, 2004; Liu and others, 2006).

Hysteresis experiments.—Hysteresis loops were acquired for 30 to 150 mg rock chips on a Princeton Measurements Corporation alternating gradient magnetometer in acoustic shielding at the Princeton Measurements Corporation headquarters. The sensitivity of the instrument is ~1 nAm^2 with an accuracy of ±2 percent versus the calibration that was made using the National Institute of Standards and Technology yttrium iron garnet sphere standard. Loops were acquired from +500 mT to −500 mT (+1 T to −1 T if necessary) at steps of 1 mT. Values of saturation magnetization (Ms), saturation remanence (Mr) and coercivity (Hc) were determined from the hysteresis loops. Remanent moments were measured with increasing magnitude of a demagnetizing "backfield" following a saturating IRM on the same magnetometer in order to determine the coercivity of remanence (H_{cr}).

PALEOMAGNETIC RESULTS

Given the clarity of recognizable components in the results from the Love's Creek Member and Johnny's Creek Member of the Bitter Springs Formation, we begin by presenting those results, followed by the results in stratigraphic order from the Heavitree Formation, the Gillen Member of the Bitter Springs Formation and the Bitter Springs basalt flows.

Paleomagnetic Results for the Love's Creek Member

The paleomagnetic components that were determined through principal component analysis (Kirschvink, 1980) are illustrated in figure 4, summarized in the text below and reported in tables 1, 2, and 3.

The magnetization of the stromatolitic carbonates of the Love's Creek Member consists of three components:

Component A. This component is removed during low-field AF (0-8 mT) and low-temperature thermal demagnetization (up to 150 °C). The least-square fits to component A fail the McElhinny (1964) fold test at 99 percent confidence. A bootstrap fold test on the fits (Tauxe and Watson, 1994; Tauxe, 2010) indicates that this component was acquired while the beds were in their current tilted orientation as the 95 percent confidence bounds on the degree of untilting required for maximizing the principle eigenvalue of the orientation matrix include 0 percent unfolding (with a range of −2% to 3%; fig. 6). When uncorrected for bedding tilt (*in situ* coordinates), the component's direction corresponds to the direction of the present local field (PLF) of central Australia (north and up; IAGA-Working-Group and others, 2010). The mean calculated from all samples (Dec of 000.8, Inc of −51.7, α_{95} of 1.2) is quite close both to the axial dipole for the localities (Dec 000, Inc ~ −41.5) and the current IGRF2011 modeled field (IAGA-Working-Group and others, 2010; Dec of 004.7, Inc of −55.7).

Component B. Between 150 °C and 320 °C, a component is removed from the samples that fails the McElhinny (1964) fold test at 99 percent confidence (fig. 6). A bootstrap fold test on component B gives the result that maximum concentration of the data results in the range of 4 to 8 percent unfolding, indicating that the component was acquired when the beds were very near their current orientation. The *in situ* mean of this component is steeply inclined. This steep inclination corresponds to an early Carboniferous paleolatitude of Australia (fig. 7; table 4) suggesting that the remanence was acquired during the late phases of the Alice Springs orogeny.

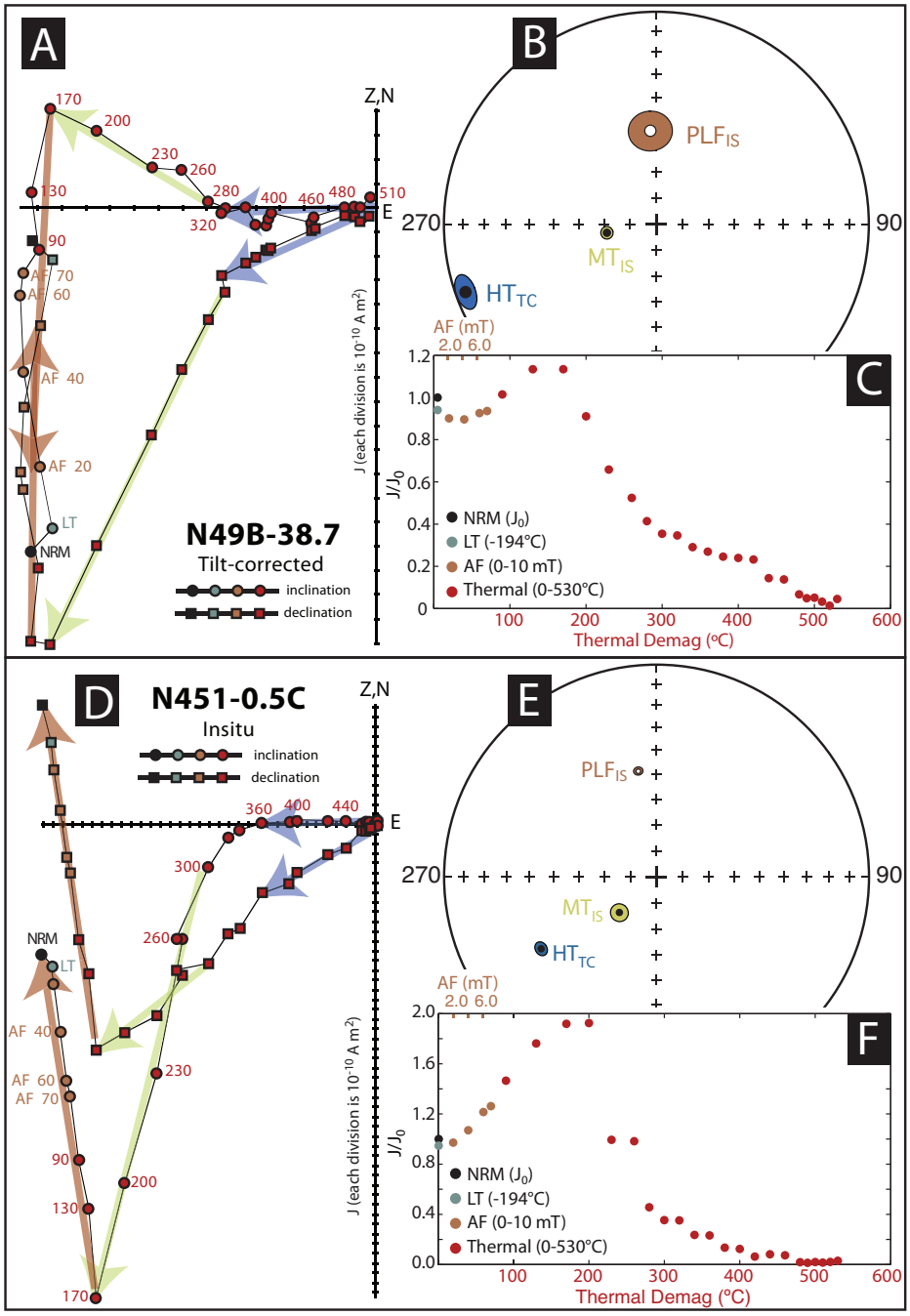

Fig. 4. (A, D, G, J) Representative vector component diagrams (Zijderveld, 1967), (B, E, H, K) least-squares fits of vector components and (C, F, I, L) magnetic intensity (J/J_0) plots showing demagnetization behavior for carbonates of the Love's Creek Member. In the vector component diagrams, the primary, high-temperature component that decays to the origin is traced with a blue arrow, a mid-temperature component is traced with a green arrow and the present local field overprint is traced with a red-orange arrow. Least-squares fits of these components from the principle component analysis are summarized in an adjacent equal area projections, and are labeled HT_{TC}, MT_{IS}, and PLF_{IS}, (caption continued on next page)

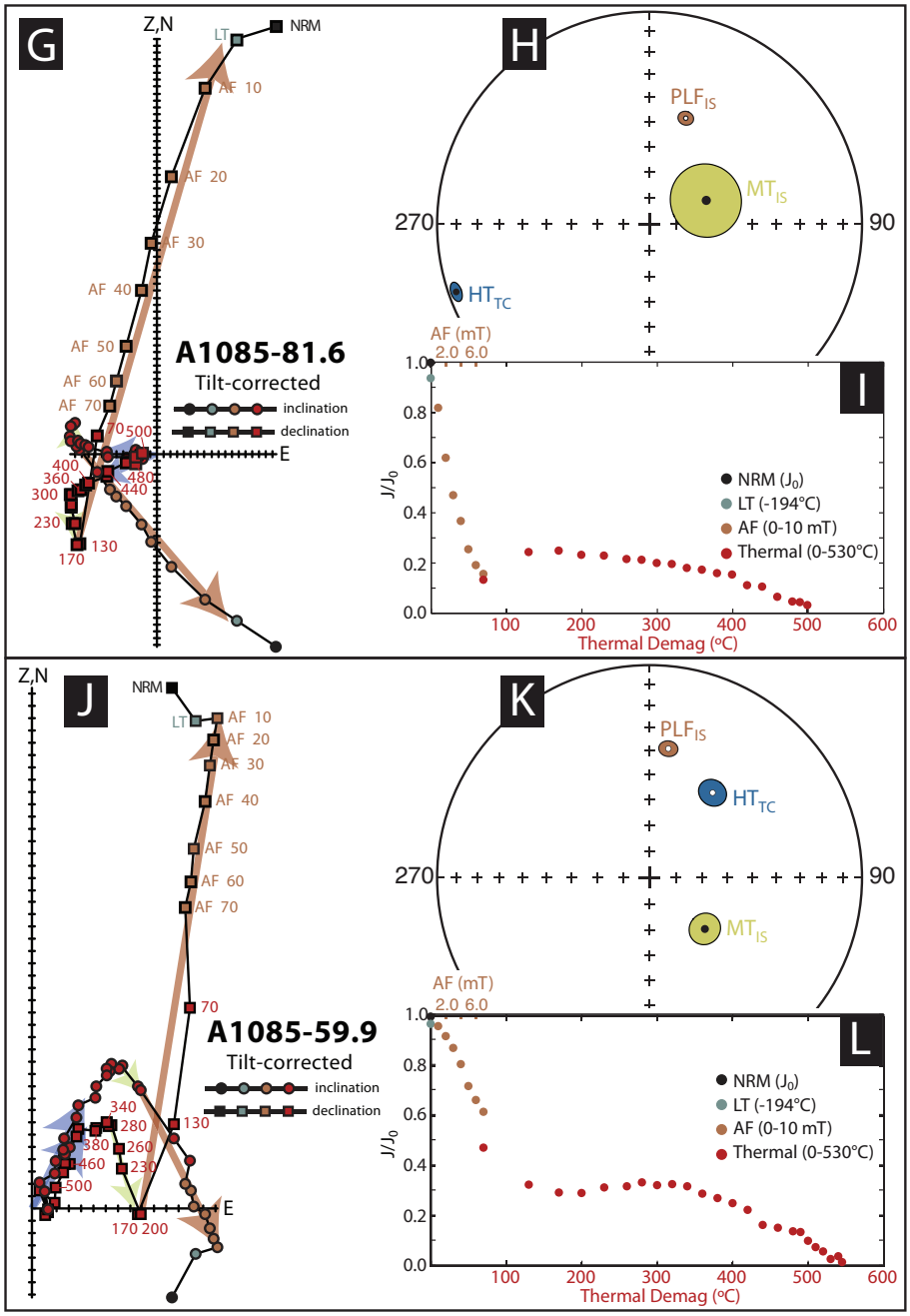

Fig. 4 (continued) respectively, where TC refers to tilt-corrected and IS refers to *in situ* coordinates. In these equal area projections, error ellipses represent circular maximum angular deviation (MAD) angles of the fits, closed circles are vectors intersecting the lower hemisphere and open circles are vectors intersecting the upper hemisphere. In the vector component diagrams and J/J_0 plots, black-filled shapes are natural remanent magnetization (NRM), blue-filled shapes are the low-temperature (LT) step, brown-filled shapes are the alternating field (AF) demagnetization steps and red-filled shapes represent thermal demagnetization. In the vector component diagrams, squares represent declination while circles represent inclination.

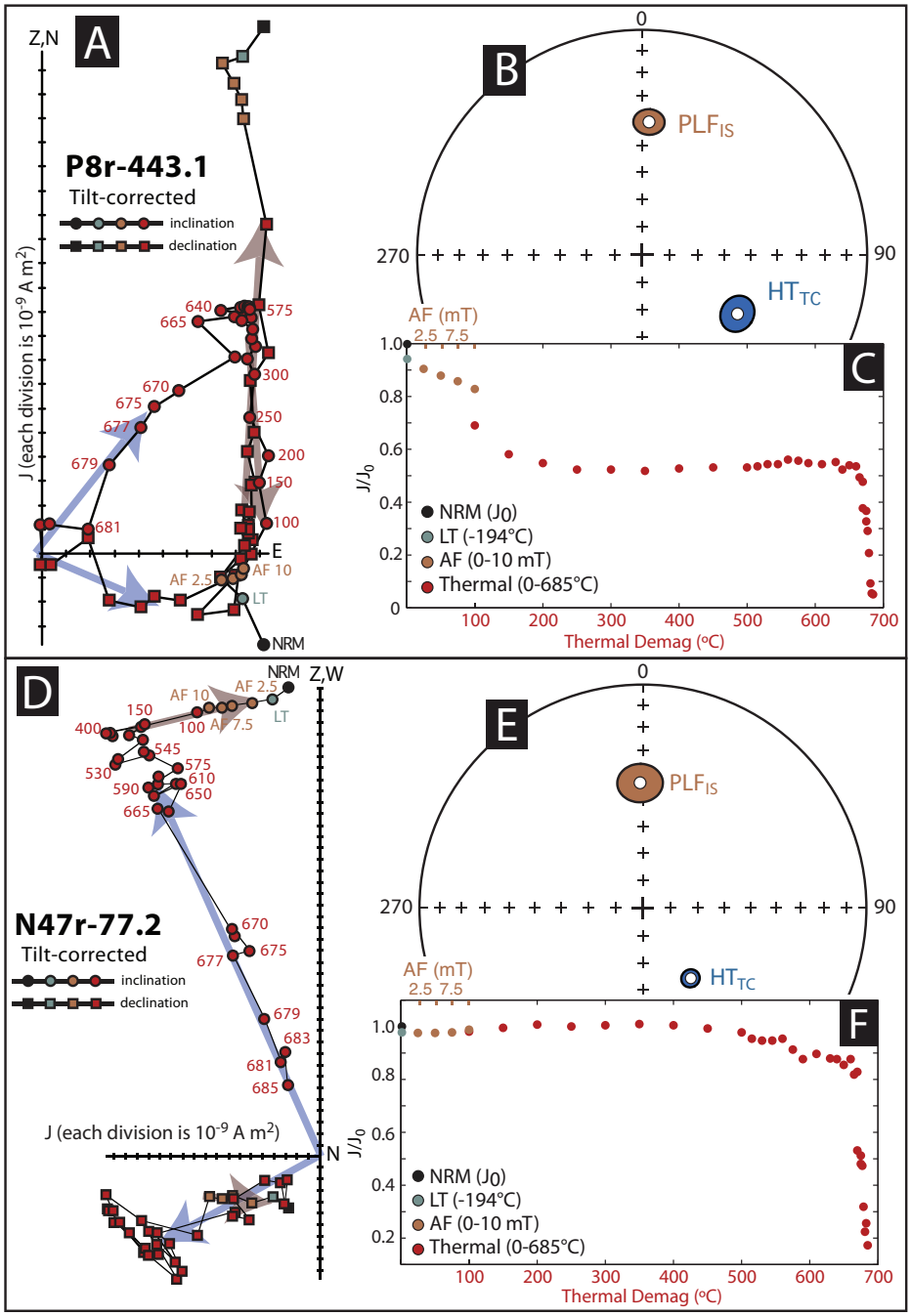

Fig. 5. (A, D, G, J) Representative vector component diagrams (Zijderveld, 1967), (B, E, H, K) least-squares fits of vector components and (C, F, I, L) magnetic intensity (J/J_0) plots showing demagnetization behavior for siltstones of the Johnny's Creek member. The primary, high-temperature component that decays to the origin is traced with a blue arrow, and the present local field overprint is traced with a brown arrow. Least-squares fits of these components from the principle component analysis are summarized in an adjacent equal area projections, and are labeled HT_{TC} and PLF_{IS}, respectively, where TC refers to tilt-corrected and IS refers to *in situ* coordinates. In these equal area projections, error ellipses represent circular maximum angular deviation (MAD) angles of the fits and open circles (caption continued on next page)

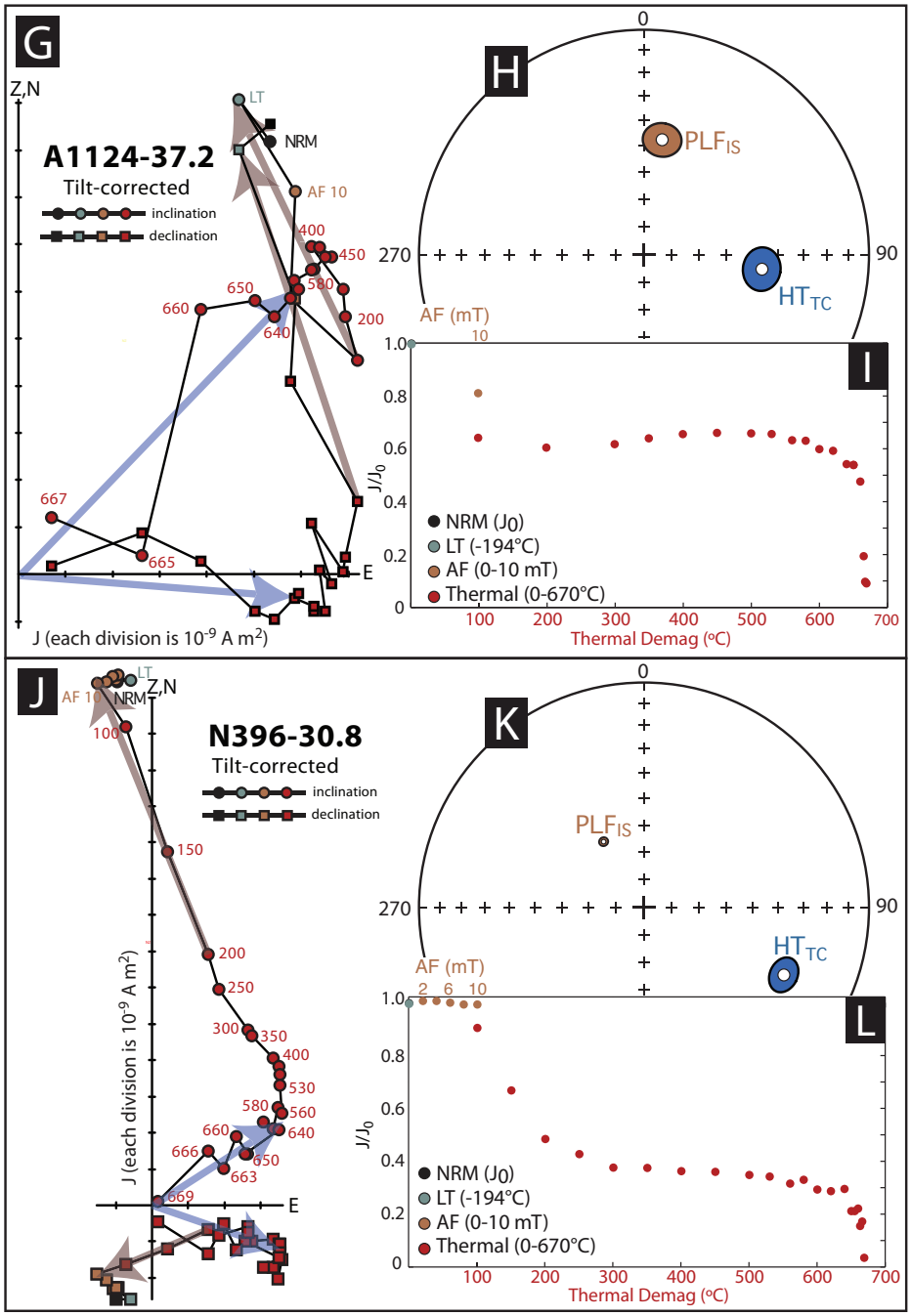

Fig. 5 (continued) are vectors intersecting the upper hemisphere. In the vector component diagrams and J/J_0 plots, black-filled shapes are natural remanent magnetization (NRM), blue-filled shapes are the low-temperature (LT) step, brown-filled shapes are the alternating field (AF) demagnetization steps and red-filled shapes represent thermal demagnetization. In the vector component diagrams, squares represent declination while circles represent inclination.

TABLE 1

Paleomagnetic data from Love's Creek Mb of the Bitter Springs Fm, Amadeus Basin (Component A)

Stratigraphic section	Location N00° 00', E00° 00'	n/N	*In situ*									Tilt-corrected			
			D_m (°)	I_m (°)	k_1	α_{95} (°)	λ (°E)	ϕ (°N)	A_{95} (°)	Plat (°)		D_m (°)	I_m (°)	k_2	α_{95} (°)
Ross River (N49B)	S23° 4.7', E134° 30.3'	75/98	359.1	-52.7	72.4	1.9						0.9	43.8	63.9	2.1
U. Ross River (N49)	S23° 4.8', E134° 30.5'	24/26	002.3	-52.8	45.6	4.4						2.9	44.1	45.1	4.4
Undoolya Station (N451)	S23° 40.5', E134° 14.6'	26/28	358.7	-50.1	62.2	3.6						309.9	-53.2	59.1	3.7
Undoolya Station (N453)	S23° 40.5', E134° 14.7'	16/16	358.8	-53.9	178.6	2.8						308.7	-54.9	178.6	2.8
East Ellery Creek (A1085)	S23° 47.2', E133° 6.6'	107/107	002.4	-50.8	51.1	1.9						004.2	9.2	45.7	2.0
TOTAL Component A (samples)		248/275	000.8	-51.7	59.1	1.2	81.3	309.7	1.4	-32.3	-31.2 -33.5	357.1	15.0	4.7	4.6

n—number of samples used (samples that are not overprinted through lightening remagnetization). Component A fits were made to low-field AF (0-8 mT) and initial thermal demagnetization steps (up to 150 °C). N—total number of samples collected; D_m and I_m—mean declination and inclination of N stratigraphic horizons or samples; k—Fisher's (1953) precision parameter; α_{95}—radius of confidence circle for the mean direction; λ and ϕ—latitude and longitude of paleopole for mean direction in present-day Australia coordinates; A_{95}—radius of 95% cone of confidence; Plat—paleolatitude. The latitude and longitude of the locations are in WGS84 coordinates.

TABLE 2

Paleomagnetic data from Love's Creek Mb of the Bitter Springs Fm, Amadeus Basin (Component B)

Stratigraphic section	Location N00° 00', E00° 00'	n/N	*In situ*									Tilt-corrected			
			D_m (°)	I_m (°)	k_1	α_{95} (°)	λ (°E)	ϕ (°N)	A_{95} (°)	Plat (°)		D_m (°)	I_m (°)	k_2	α_{95} (°)
Ross River (N49B)	S23° 4.7', E134° 30.3'	74/98	260.8	70.4	31.0	3.0	-24.3	95.6	4.8			207.0	-12.4	32.8	2.9
U. Ross River (N49)	S23° 4.8', E134° 30.5'	24/26	274.4	70.6	46.4	4.4	-16.7	97.7	7.1			205.5	-7.0	46.4	4.4
Undoolya Station (N451)	S23° 40.5', E134° 14.6'	26/28	237.3	70.8	85.8	3.1	-37.8	96.7	5.0			61.3	72.9	85.8	3.1
Undoolya Station (N453)	S23° 40.5', E134° 14.7'	16/16	236.2	71.8	199.7	2.6	-38.0	98.8	4.3			68.6	74.0	199.7	2.6
East Ellery Creek (A1085)	S23° 47.2', E133° 6.6'	83/107	124.7	75.0	8.7	5.6	-37.0	162.2	9.8			173.2	22.4	8.7	5.6
TOTAL Component B (samples)		223/275	231.8	80.2	11.1	3.0	-34.4	116.1	5.6	70.9	76.6 65.6	189.0	18.5	3.3	6.2
TOTAL Component B (w/o A1085) (samples)		140/168	256.1	71.1	38.4	1.9	-27.1	96.2	3.1	55.6	58.6 52.8	14.3	2.6	9.4	14.3

Component B fits were made to some of the thermal demagnetization steps between 150 °C and 320 °C. n—number of samples used (samples that are not overprinted through lightening remagnetization and have stable behavior at high temperatures). N—total number of samples collected; D_m and I_m—mean declination and inclination; k—Fisher's (1953) precision parameter; α_{95}—radius of confidence circle for the mean direction; λ and ϕ—latitude and longitude of paleopole for mean direction in present-day Australia coordinates; A_{95}—radius of 95% cone of confidence; Plat—paleolatitude. The latitude and longitude of the locations are in WGS84 coordinates.

TABLE 3

Paleomagnetic data from Love's Creek Mb of the Bitter Springs Fm, Amadeus Basin (Component C)

Stratigraphic section	Location N00° 00', E00° 00'	n/N	*In situ* coordinates				Tilt-corrected coordinates								
			D_m (°E)	I_m (°N)	k_1	α_{95} (°)	D_m (°E)	I_m (°N)	k_2	α_{95} (°)	λ (°N)	ϕ (°E)	A_{95} (°)	Plat (°)	
Ross River (N49B)	S23° 4.7', E134° 30.3'	61/98	284.2	28.4	15.5	4.8	248.2	2.5	15.5	4.8					
U. Ross River (N49)	S23° 4.8', E134° 30.5'	20/26	279.0	30.5	52.0	4.6	245.4	-1.0	52.0	4.6					
Undoolya Station (N451)	S23° 40.5', E134° 14.6'	26/28	239.4	-4.7	50.9	4.0	239.4	31.8	52.9	3.9					
Undoolya Station (N453)	S23° 40.5', E134° 14.7'	16/16	241.5	-3.3	62.4	4.7	241.4	30.7	62.4	4.7					
East Ellery Creek *normal* (A1085)	S23° 47.2', E133° 6.6'	64/115	265.3	30.5	15.7	4.6	245.7	4.5	14.4	4.8					
East Ellery Creek *reversed* (A1085)	S23° 47.2', E133° 6.6'	34/115	117.3	-55.5	24.9	5.0	048.3	-37.2	22.8	5.3					
East Ellery Creek *all* (A1085)	S23° 47.2', E133° 6.6'	98/115	273.6	40.1	10.8	4.6	240.5	16.1	9.7	4.8					
TOTAL Component C with reversed (samples)		221/275	269.6	28.4	7.7	3.7	243.2	13.8	11.5	2.9	-27.3	39.8	2.1	7.0	8.5 5.5
TOTAL Component C w/o reversed (samples)		187/275	266.3	22.9	8.9	3.7	245.4	9.4	13.7	2.9	-24.4	38.5	2.1	4.7	6.6 3.3
TOTAL Component C (sections)		5/5	261.9	19.5	7.9	28.9	243.1	15.8	25.6	15.4	**-28.1**	**41.1**	**8.7**	8.1	17.1 0.08

Component B fits were made to some of the thermal demagnetization steps between 150 °C and 320 °C. n—number of samples used (samples that are not overprinted through lightening remagnetization and have stable behavior at high temperatures). N—total number of samples collected. D_m and I_m—mean declination and inclination; k—Fisher's (1953) precision parameter; α_{95}—radius of confidence circle for the mean direction; λ and ϕ—latitude and longitude of paleopole for mean direction in present-day Australia coordinates; A_{95}—radius of 95% cone of confidence; Plat—paleolatitude. The "sections" pole in bold was calculated as the Fisher mean of the poles from each section (using A1085-all). The latitude and longitude of the locations are in WGS84 coordinates.

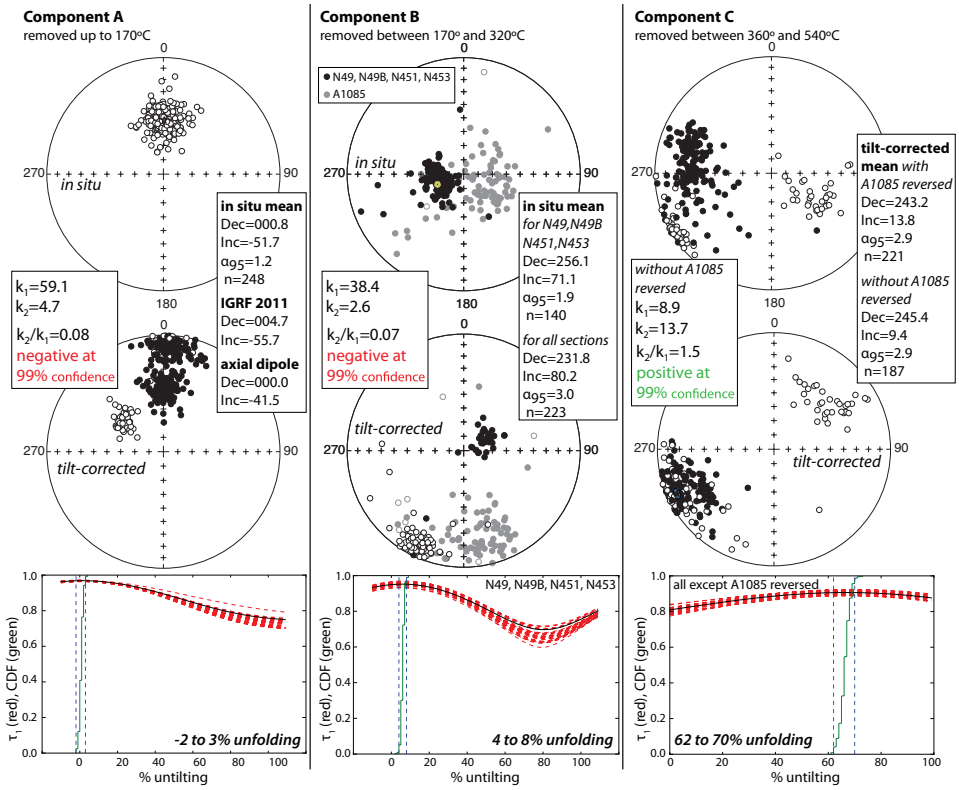

Fig. 6. Equal area plots of the paleomagnetic directions from the syn–Bitter Springs Stage Love's Creek Member carbonates. Directions are shown in *in situ* and tilt-corrected coordinates for the least-square fits to the low-temperature direction, the mid-temperature direction and the high-temperature direction. Estimates of the concentration parameter are shown for directions in *in situ* coordinates (k_1) and tilt-corrected coordinates (k_2) along with the results from the associated fold tests (McElhinny, 1964) to the side of the respective equal area plots. The low- and mid-temperature fits have the highest concentration parameters prior to unfolding suggesting that those magnetizations were acquired after regional-scale folding. The mean direction, calculated with Fisher statistics (Fisher, 1953), is displayed for the directions as they are in *in situ* coordinates for the component removed at low temperatures and at mid-temperatures while the mean for the high-temperature direction is given in 100% tilt-corrected coordinates. The lowermost plots are the results of bootstrap fold tests (Tauxe and Watson, 1994; Tauxe, 2010) where τ_1 is the major eigenvalue of the orientation matrix shown as a function of unfolding percentage. The red dashed lines are representatives of the 500 bootstrapped data sets while the green lines are the cumulative density function of the maxima in τ_1 for all of the bootstraps. The bounds that enclose 95% of the maximum τ_1 values from the pseudo-sample sets are shown with the blue dashed lines and written on the plots. Results are reported for each stratigraphic section in tables 1, 2, and 3.

Component C. Between thermal demagnetization steps of 370 °C and 510 °C, a component is removed that decays to the origin in vector component diagrams (fig. 4). This component C passes the McElhinny (1964) fold test at 99 percent confidence (fig. 6), suggesting that it was acquired prior to Devonian-Carboniferous folding. A bootstrap fold test on the component C least-squares fits gives the result that the principle eigenvalue of the orientation matrix is maximized between 62 and 70 percent unfolding thereby indicating that both the *in situ* and tilt-corrected coordinate systems are excluded at the 95 percent confidence level. While this result could indicate that the remanence was acquired during folding, the direction does not overlap with the Devonian-Carboniferous poles from the time of deformation. Therefore, it is likely that the maximized concentration of directions between 62 and 70 percent unfolding

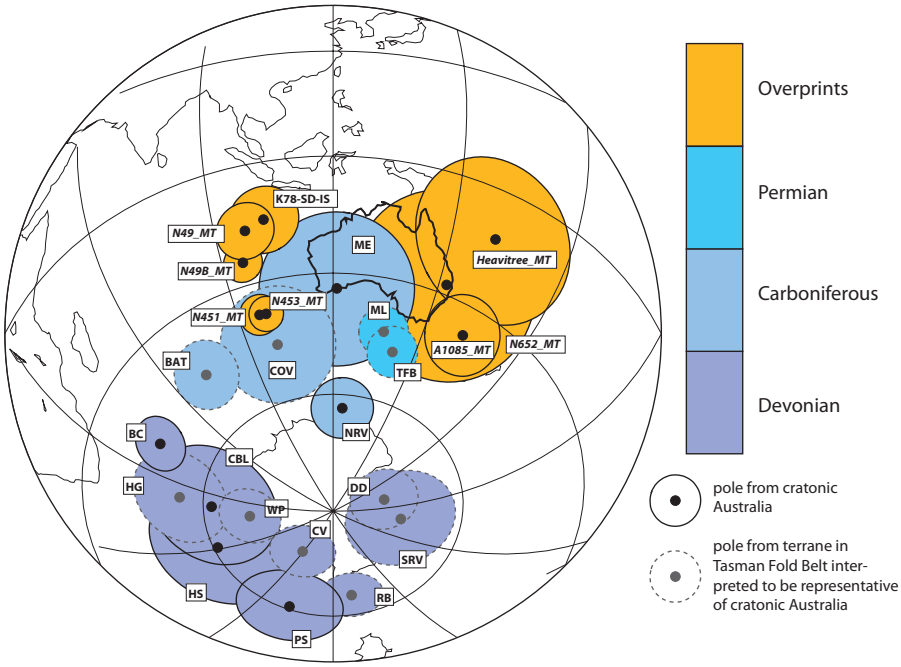

Fig. 7. Equal area projection of Devonian to Permian paleomagnetic poles from Australia (details in table 4) with overprint directions from Amadeus Basin sediments. K78-SD-IS is the pole calculated for the *in situ* directions of an overprint documented in Ediacaran to Cambrian sedimentary lithologies in the Ross River area of the Amadeus Basin by Kirschvink (1978). The rest of the overprint poles are from *in situ* means of fits to component B of Love's Creek Member carbonates reported in table 2 and of Heavitree Formation sandstones reported in table 7.

is an artifact of structural complications such as vertical axis rotations that are not fully represented in the simple untilting of the individual dip panels (for example Tauxe and Watson, 1994). Samples from the A1085 section revealed dual polarities with the southwest and down directions being significantly shallower in absolute inclination than the northeast and up inclinations such that the two populations fail the reversal test of McFadden and McElhinny (1990).

Lightning remagnetization can be a significant concern when working on rocks that outcrop in central Australia. Despite efforts to collect samples in topographic lows, some analyzed samples appear to have been remagnetized by lightning. Samples that we interpret as having undergone lightning remagnetization have single-component magnetizations, in contrast to the majority of samples, which have three components, and have higher magnetic moments by up to an order of magnitude. Such remagnetization was not observed in the N453 or A1085 sections. Lightning remagnetized samples were identified in the N49B, N49 and N451 sections (19%, 8%, and 4% of analyzed specimens respectively).

Paleomagnetic Results for the Johnny's Creek Member

The magnetization of the siltstones of the Johnny's Creek Member consists of two components (figs. 5 and 8; tables 5 and 6).

Component A. This component is removed during low field AF and initial thermal demagnetization steps (usually up to 150 °C, but sometimes continuing to be removed up to 350 °C). This component fails a fold test at 99 percent confidence

TABLE 4

Phanerozoic paleomagnetic poles from Australia

pole	abbr	Pole (°N)	Pole (°E)	A_{95}(°)	Age (Ma)	Pmag ref	Terrane
Arumbera sandstone (Upper)	A-uAr	46.6	157.4	3.5	542-525	Kirschvink (1978)	cratonic Australia
Todd River dolomite,Allua Fm., Eninta Fm.	A-Todd	43.2	159.9	5.9	525-510	Kirschvink (1978)	cratonic Australia
Billy Creek/ Wirre-alpa/Arona Creek Limestone	A-Flin-Billy	37.4	200.1	9.0	522-517	Klootwijk (1980)	cratonic Australia
Kangaroo Island RedvBeds	A-Flin-KangI	33.8	195.1	8.7	517-513	Klootwijk (1980)	cratonic Australia
Lower Lake Frome Group	A-Flin-Frome	29.3	206.1	9.3	510-505	Klootwijk (1980)	cratonic Australia
Hugh River Shale	A-HR	22.3	203.1	13.2	515-508	Mitchell and others (2010)	cratonic Australia
Jay Creek Limestone	A-JCa	20.2	227.9	9.4	508-500	Mitchell and others (2010)	cratonic Australia
Hugh River shale, Jay Creek limestone	A-HR-JC	19.3	219.1	10.0	515-500	Mitchell and others (2010)	cratonic Australia
Georgina Basin Cambrian Limestones	A-GBL	48.6	186.0	2.9	500-480	Anderson and others (2004b)	cratonic Australia
Black Hill Norite	A-BHN	37.5	214.4	3.2	501-495	Schmidt and others (1993)	cratonic Australia
Walli and Mount Pleasant Andesites	A-WMP	12.2	183.3	12.5	468-456	Goleby (1980)	Tasman Fold-Thrust Belt (Molomg-Monaro terrane) [1]
Theresa Creek Volcanics	A-TCV	4.1	188.9	18.2	470-400	Anderson and others (2004a)	Tasman Fold-Thrust Belt (Lolworth-Ravenswood Terrane)[2]
Mereenie Sandstone	A-MS	-15.7	242.7	23.7	440-400	Li and others (1991)	cratonic Australia
Ravenswood Batholith	A-RVB	-17.5	232.7	5.3	428-422	Clark (1996)	Tasman Fold-Thrust Belt (Lolworth-Ravenswood Terrane)[2]
Mount Leyshon Silurian Dikes	A-SD	-21.7	231.9	6.3	428-422	Clark (1996)	Tasman Fold-Thrust Belt (Lolworth-Ravenswood Terrane)[1]
Snowy River Volcanics	A-SRV	-74.3	222.7	12.6	410-384	Schmidt and others (1987)	Tasman Fold-Thrust Belt (Molomg-Monaro terrane[1]≈cratonic Australia)
Mount Leyshon Devonian Dikes	A-DD -	78.0	198.8	7.9	415-382	Clark (1996)	Tasman Fold-Thrust Belt (Lolworth-Ravenswood Terrane[2]≈cratonic Australia)
Retreat Batholith	A-RB	-66.0	290.7	6.5	390-370	Anderson and others (2004a)	Tasman Fold-Thrust Belt (Lolworth-Ravenswood Terrane[2]≈cratonic Australia)
Parke Siltstone	A-PS	-60.9	318.1	10.7	400-385	Li and others (1991)	cratonic Australia
Comerong Volcanics	A-CV	-76.9	330.7	7.2	380-360	Schmidt and others (1986)	Tasman Fold-Thrust Belt (Molomg-Monaro terrane[1]≈cratonic Australia)
Hermannsburg Sandstone	A-HS	-61.0	0.9	15.6	385-375	Li and others (1991)	cratonic Australia
Brewer Conglomerate	A-BC	-47.1	41.0	6.4	375-360	Chen and others (1993)	cratonic Australia
Worange Point Formation	A-WP	-70.8	19.7	7.1	365-354	Thrupp and others (1991)	Tasman Fold-Thrust Belt (Molomg-Monaro terrane[1]≈cratonic Australia)
Canning Basin Limestone	A-CBL	-62.0	23.2	15.2	385-359	Chen and others (1995)	cratonic Australia
Hervey Group	A-HG	-54.4	24.1	11.3	374-359	Li and others (1988)	Tasman Fold-Thrust Belt (Molomg-Monaro terrane[1]≈cratonic Australia)
Connors Volcanics	A-COV	-46.0	100.0	14.4	357-343	Clark (1994)	Tasman Fold-Thrust Belt (New England Fold belt)
Bathurst Batholith	A-BAT	-45.3	71.9	8.3	340-310	Wahyono (1992)	Tasman Fold-Thrust Belt (Molomg-Monaro terrane[1]≈cratonic Australia)
Newcastle Range Volcanics	A-NRV	-63.4	125.0	7.6	329-310	Anderson and others (2003)	Cratonic Australia (Georgetown Inlier)
Mount Leyshon Intrusive Complex	A-ML	-43.2	137.3	6.2	296-278	Clark and Lackie (2003)	Tasman Fold-Thrust Belt (Lolworth-Ravenswood Terrane[2]≈cratonic Australia)
Tuckers Igneous Complex	A-TIC	-47.5	142.0	6.3	295-270	Clark and Lackie (2003)	Tasman Fold-Thrust Belt (Lolworth-Ravenswood Terrane[2]≈cratonic Australia)

[1] While the rough proximity of the A-WMP pole to cratonic poles of similar early Silurian age lends support to the Molomg-Monaro terrane being close to the Gondwana cratonic margin during the Ordovician, the terrane may not have been docked yet. McElhinny and others (2003) interpret the Molomg-Monaro terrane to be docked prior to 400 Ma.

[2] McElhinny and others (2003) argue that the Lolworth-Ravenswood terrane underwent a significant end Silurian rotation and that pre-400 Ma poles cannot be taken as representative of cratonic Australia. McElhinny and others (2003) argue that the correspondence between the A-DD pole and the A-SRV pole provide evidence that both the Lolworth-Ravenswood terrane and the Molomg-Monaro terrane were docked with cratonic Australia by the middle Devonian.

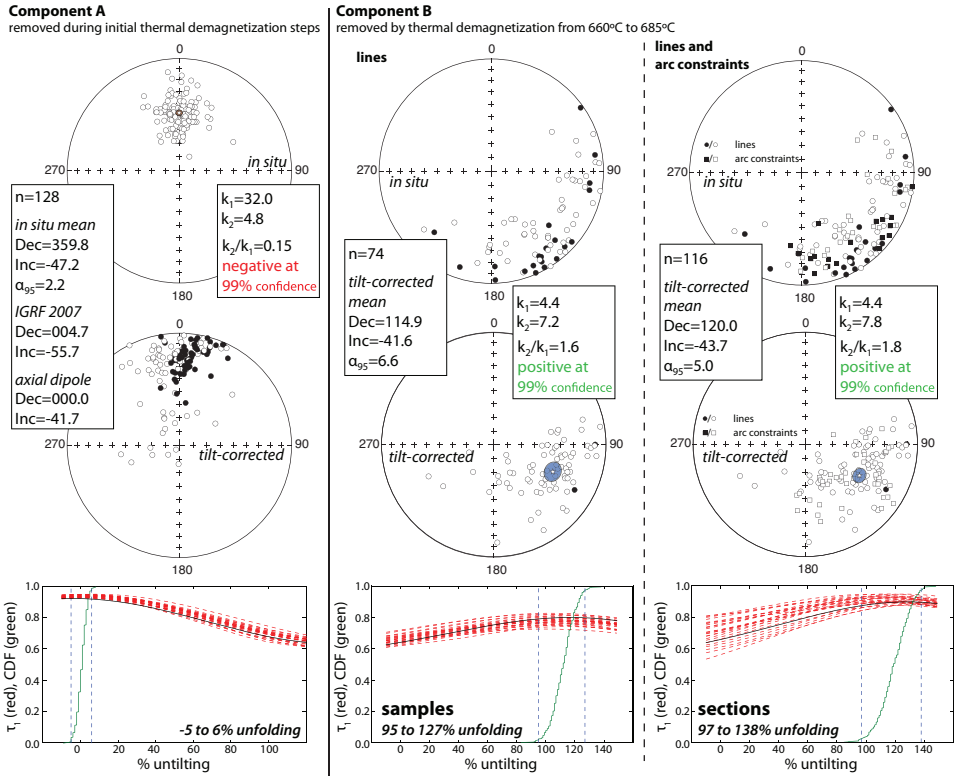

Fig. 8. Equal area plots of the paleomagnetic directions from the post–Bitter Springs Stage siltstones of the Johnny's Creek Member. Directions are shown in *in situ* and tilt-corrected coordinates. Estimates of the concentration parameter are shown for directions in *in situ* coordinates (k_1) and tilt-corrected coordinates (k_2) along with the results from the associated fold tests (McElhinny, 1964) to the right side of the respective equal area plots. Arc constraints in the right-most panel were determined from best-fit demagnetization planes using the method of McFadden and McElhinny (1988) as implemented in Jones (2002). The mean direction, calculated with Fisher statistics (Fisher, 1953), is displayed for the directions as they are in *in situ* coordinates for the component removed at low temperatures while the mean for the ChRM is the mean in tilt-corrected coordinates. The lowermost plots are the results of bootstrap fold tests (Tauxe and Watson, 1994; Tauxe, 2010) where τ_1 is the major eigenvalue of the orientation matrix shown as a function of unfolding percentage. The red dashed lines are representatives of the 500 bootstrapped data sets while the green lines are the cumulative density function of the maxima in τ_1 for all of the bootstraps. The 95% bounds for the maximum of τ_1 are shown with the blue dashed lines and written on the plots.

(McElhinny, 1964) indicating that it was acquired when the rocks were in their current orientation (fig. 8). The results of the bootstrap fold test on this component are that the 95 percent confidence interval on the corrections of the data for the best grouping are from −5 to 6 percent, encompassing a completely uncorrected *in situ* value and indicating that the magnetization was acquired when the rocks were in their present-day structural orientation (fig. 8). When the data are uncorrected for bedding the mean direction corresponds to the present local field (PLF) of central Australia (fig. 8; IAGA-Working-Group and others, 2010). The mean calculated from all samples (Dec of 359.8, Inc of −47.2, α_{95} of 2.2) is quite close both to the axial dipole for the localities (Dec 000, Inc ~41.5) and and the current IGRF2011 modeled field (IAGA-Working-Group and others, 2010; Dec of 004.7, Inc of −55.7).

Component B. After thermal demagnetization of component A some samples become unstable (~15 of 139 specimens), but in many samples a component is

TABLE 5

Paleomagnetic data from the Johnny's Creek Mb of the Bitter Springs Fm, Amadeus Basin (Component A)

Stratigraphic section	Location N00° 00', E00° 00'	n/N	*In situ*									Tilt-corrected			
			D_m (°)	I_m (°)	k_1	α_{95} (°)	λ (°E)	ϕ (°N)	A_{95} (°)	Plat (°)		D_m (°)	I_m (°)	k_2	α_{95} (°)
Ross River (N47)	S23°34.9', E134°30.6'	23/26	0.0	-48.8	29.4	5.8						359.8	-49.5	22.1	6.8
Ellery Creek (N6)	S23°47.0', E133°4.0'	11/11	358.2	-51.7	44.1	6.6						359.8	33.3	31.9	7.8
Ellery Creek (P8)	S23°47.1', E133°5.1'	18/18	001.9	-47.0	50.0	4.9						003.6	29.2	53.5	4.8
Gairdner Range (N391)	S24°6.8', E132°21.3'	5/5	342.3	-54.3	15.0	20.4						262.8	-67.2	13.9	21.3
Gairdner Range (N396)	S24°7.2', E132°22.2'	6/6	353.1	-51.1	26.4	12.1						299.2	-78.9	26.3	12.1
Allambi Station (N672)	S24°13.2', E134°34.2'	6/6	357.6	-45.9	24.1	12.7						008.8	-70.1	24.0	12.7
Love's Creek Station (N1132)	S23°45.5', E135_15.6'	6/6	000.0	-47.4	101.5	7.6						350.0	-20.8	100.4	7.7
S of Benstead Creek (A1122-3)	S23°41.2', E134°14.1'	10/11	358.6	-34.9	20.7	10.3						353.6	-8.7	18.0	11.1
S of Benstead Creek (A1124)	S23°40.8', E134°14.7'	14/16	2.8	-44.0	25.9	7.7						341.5	-30.8	24.4	7.9
Gairdner Range (A1148)	S24°0.6', E132°19.2'	21/25	359.3	-49.8	48.5	4.6						010.3	10.8	54.2	4.4
Petermann Hills (A1152)	S24°22.8', E132°1.2'	9/9	8.9	-44.2	34.3	8.9						017.9	01.6	34.3	8.9
TOTAL Component A (samples)		129/139	359.8	-47.2	32.0	2.2	85.4	315.3	2.3	-28.4	-26.6 -30.3	359.4	-8.1	4.8	6.4
TOTAL Component A (sections)		11/11	001.4	-45.8	174	4.6	86.4	293.1	4.7	-27.2	-23.6 -31.1	001.4	-01.6	6.5	25.7

Component A fits were made to low-field AF (0-10 mT) and initial thermal demagnetization steps (generally up to 150 °C and sometimes continuing to 350 °C). n(p)—number of samples used (samples that are not overprinted through lightening remagnetization and have stable behavior at high temperatures); (p)—number of fits that are planes instead of lines; N—total number of samples collected; D_m and I_m—mean declination and inclination; k—Fisher's (1953) precision parameter; α_{95}—radius of confidence circle for the mean direction; λ and ϕ—latitude and longitude of paleopole for mean direction in present-day Australia coordinates; A_{95}—radius of 95% cone of confidence; Plat—paleolatitude "Sections" poles were calculated as the Fisher mean of the poles from each section. The latitude and longitude of the locations are in WGS84 coordinates.

TABLE 6

Paleomagnetic data from Johnny's Creek Mb of the Bitter Springs Fm, Amadeus Basin (Component B)

Stratigraphic section	Location N00° 00', E00° 00'	n/N	*In situ* coordinates				Tilt-corrected coordinates								
			D_m (°E)	I_m (°N)	k_1	α_{95} (°)	D_m (°E)	I_m (°N)	k_2	α_{95} (°)	λ (°N)	ϕ (°E)	A_{95} (°)	Plat (°)	
Ross River (N47)	S23°34.9', E134°30.6'	24(6)/26	162.7	-27.5	13.0	6.9	153.1	-56.1	12.4	7.5					
Ellery Creek (N6)	S23°47.0', E133°4.0'	11(6)/11	158.1	24.5	12.2	16.6	143.8	-52.8	13.4	15.7					
Ellery Creek (P8)	S23°47.1', E133°5.1'	17(6)/18	146.0	4.5	8.1	14.9	120.2	-42.7	8.4	14.6					
Gairdner Range (N391)	S24°6.8', E132°21.3'	5(1)/5	78.1	-15.0	12.2	24.8	94.5	-33.8	17.0	20.8					
Gairdner Range (N396)	S24°7.2', E132°22.2'	5(0)/6	84.8	-11.9	19.2	15.9	94.0	-18.3	19.2	15.9					
Allambi Station (N672)	S24°13.2', E134°34.2'	4(2)/6	63.3	-30.7	49.6	17.7	79.2	-33.4	49.6	17.7					
Love's Creek Station (N1132)	S23°45.5', E135_15.6'	4(2)/6	109.1	-18.4	25.4	25.0	97.1	-40.6	25.4	25.0					
S of Benstead Creek (A1122-3)	S23°41.2', E134°14.1'	8(6)/11	125.5	-12.8	41.0	12.1	124.6	-41.3	27.5	14.8					
S of Benstead Creek (A1124)	S23°40.8', E134°14.7'	11(6)/16	103.0	-14.6	16.8	13.0	101.1	-44.4	17.0	12.9					
Gairdner Range (A1148)	S24°0.6', E132°19.2'	18(4)/25	143.9	-9.9	7.9	14.1	119.7	-28.4	8.4	13.5					
Petermann Hills (A1152)	S24°22.8', E132°1.2'	9(3)/9	152.0	-36.4	20.8	13.0	110.0	-38.7	20.8	13.0					
TOTAL Component B (all line fits)		74/139	133.7	-16.2	4.4	8.9	114.9	-41.6	6.6	7.2	10.9	075.5	5.6	-23.9	-19.3 -29.2
TOTAL Component B (all lines and arc constraints)		116/139	135.8	-13.4	4.4	7.1	120.0	-43.7	7.8	5.0	13.8	079.5	4.9	-25.7	-21.8 -29.6
TOTAL Component B (all sections)		11/11	120.9	-16.1	5.1	22.6	110.0	-40.9	17.7	11.2	**7.9**	**74.3**	**12.5**	-23.4	-15.9 -32.7
TOTAL Component B (sections with n≥6)		7/11	141.3	-11.1	8.3	22.2	122.8	-44.6	28.3	11.5	**15.8**	**83.0**	**13.5**	-26.2	-18.2 -36.3

Component B fits were made to high temperature thermal demagnetization steps above 600 °C. n—number of samples used (samples that are not overprinted through lightening remagnetization and have stable behavior at high temperatures); (p)—number of fits that are planes instead of lines; N—total number of stratigraphic horizons or samples collected, where great-circle-fits are weighted as 1/2 and line-fits are weighted as 1; D_m and I_m—mean declination and inclination; k—Fisher's (1953) precision parameter; α_{95}—radius of confidence circle for the mean direction; λ and ϕ—latitude and longitude of paleopole for mean direction in present-day coordinates; A_{95}—radius of 95% cone of confidence; Plat—paleolatitude. "All line fits" and "all lines and arc constraints" poles were calculated using D_m and I_m with the latitude and longitude of Ellery Creek. "Sections" poles in bold were calculated as the Fisher mean of the poles from each section. The latitude and longitude of the locations are in WGS84 coordinates.

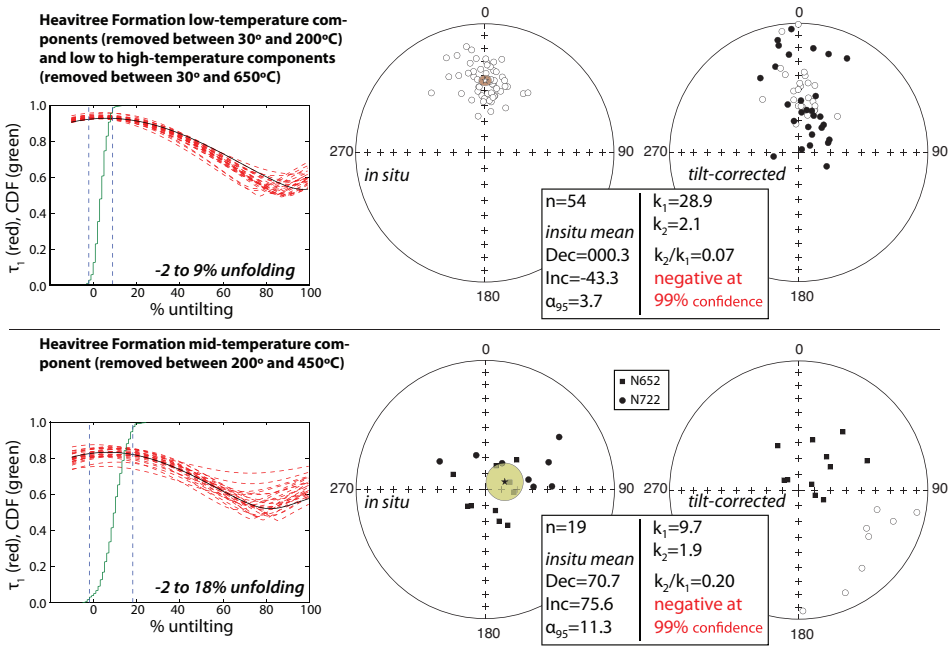

Fig. 9. Equal area plots of the least-square fits to paleomagnetic components from fine-grained Heavitree Formation. These fits are shown in *in situ* and tilt-corrected coordinates and the mean direction, calculated with Fisher statistics (Fisher, 1953), is displayed for the directions as they are in *in situ* coordinates as both components fail the McElhinny (1964) fold test. The results of bootstrap fold tests (Tauxe and Watson, 1994; Tauxe, 2010) are shown where τ_1 is the major eigenvalue of the orientation matrix shown as a function of unfolding percentage. The red dashed lines are representatives of the 500 bootstrapped data sets while the green lines are the cumulative density function of the maxima in τ_1 for all of the bootstraps. The 95% bounds for the maximum of τ_1 are shown with the blue dashed lines and written on the plot. Results for each stratigraphic section are reported in table 7.

removed between thermal demagnetization steps of 650 °C and 685 °C that decays to the origin in vector component diagrams (see fig. 5) and was either fit with lines or planes during the principal component analysis. Arc constraints were determined from the best-fit demagnetization planes using the method of McFadden and McElhinny (1988) as implemented in (Jones, 2002). This component passes the McElhinny (1964) fold test at 99 percent confidence (fig. 8). A bootstrap fold test on line fits to the component constrains the 95 percent confidence interval of the unfolding to between 95 to 127 percent. Given that this range encompasses the complete structural correction of 100 percent the data "passes" the bootstrap fold test. A bootstrap fold test on section means (N = 11) also encompasses 100 percent unfolding providing further evidence that component B was acquired prior to structural tilting.

Paleomagnetic Results for the Other Amadeus Basin Units

Heavitree Formation.—Samples recently were collected from six stratigraphic sections of the Heavitree Formation (fig. 2). Within these sections, fine-grained red sandstones (quartzite) were targeted for collection and 79 such samples were analyzed. In addition to these sections, one of us (JLK) collected 76 oriented block samples in 1975 that were stratigraphically dispersed through the Heavitree Formation at the type section at Heavitree Gap, near Alice Springs. Results from these analyses are summarized in figure 9 and table 7. These samples behaved in one of six ways: (1) completely

TABLE 7

Paleomagnetic data from Heavitree Fm, Amadeus Basin

Stratigraphic section	Location N00° 00', E00° 00'	n/N	*In situ*									Tilt-corrected			
			D_m (°)	I_m (°)	k_1	α_{95} (°)	λ (°E)	ϕ (°N)	A_{95} (°)	Plat (°)		D_m (°)	I_m (°)	k_2	α_{95} (°)
Heavitree Formation LT-LHT fits															
Limbla Cliffs (N480)	S23°59.3', E135°17.7'	6/6	000.2	-41.9	60.3	7.9						001.1	-50.8	59.1	8.1
Limbla Cliffs (N481)	S23°59.3', 135°17.3'	9/16	000.8	-42.4	45.2	7.3						006.4	-52.1	45.3	7.3
Gypsum Creek (N483)	S23°57.5', E135°7.6'	7/13	000.2	-38.4	22.9	11.9						355.2	13.1	22.9	11.9
Jay Creek road cut (N490)	S23°47.9', E133°29.5'	4/9	000.6	-42.8	8.4	28.8						002.5	23.7	8.3	28.9
Ross Hwy E of Bitter Sp. Creek (N652)	S23°32.8', E134°28.3'	9/11	005.5	-40.1	20.0	11.1						003.3	-57.9	21.6	10.9
Ross River Tourist Camp (N722)	S23°34.2', E134°31.1'	19/24	357.3	-47.4	28.2	6.4						023.5	71.8	28.2	6.4
TOTAL LT (recent samples)		54/79	000.3	-43.3	28.9	3.7						005.6	3.1	2.1	18.1
Heavitree Gap (HHG-1975)	S23°43.6', E133°51.9'	25/76	358.9	-55.0	20.1	6.6						002.1	-8.9	19.8	6.7
Heavitree Formation MT fits															
Ross Hwy E of Bitter Sp. Creek (N652)	S23°32.8', E134°28.3'	11/11	108.8	81.7	13.6	12.2						037.6	71.4	12.4	12.8
Ross River Tourist Camp (N722)	S23°34.2', E134°31.1'	8/24	054.0	63.3	7.2	20.5						129.4	-25.8	7.2	20.5
TOTAL MT(samples)		19/79	70.7	75.6	9.7	11.3	-12.5	160.7	19.9	62.8	83.8 46.1	102.1	-42.8	1.9	34.1
Heavitree Formation HT fits															
Heavitree Gap (HHG-1975)	S28°43.6',E138°51.9'	30/76	245.7	46.8	10.3	8.6						223.8	13.4	10.5	8.5

LT fits were to a component in the first thermal demagnetization steps up to 200 °C. LHT indicates a fit from initial thermal demagnetization steps to thermal demagnetization steps above 600 °C. MT indicates a fit to a component removed between 200 and 475 °C. HT indicates a fit to a component that continued unblocking to temperature steps of 550 °C. n—number of samples used (samples that are not overprinted through lightening remagnetization and have stable behavior); N—total number of stratigraphic horizons or samples collected; D_m and I_m—mean declination and inclination; k—Fisher's (1953) precision parameter; α_{95}—radius of confidence circle for the mean direction; λ and ϕ—latitude and longitude of paleopole for mean direction in present-day Australia coordinates; A_{95}—radius of 95% cone of confidence; Plat—paleolatitude. The latitude and longitude of the locations are in WGS84 coordinates.

unstable from the first demagnetization steps with a NRM that is usually in the vicinity of the present local field (17% of the recently collected samples); (2) present local field overprint removed during the first thermal demagnetization steps (up to ~200 °C) followed by instability (23% of the recently collected samples); (3) present local field overprint that continues to be removed with thermal demagnetization up into the mid to high 600 °C steps (28% of the recently collected samples); (4) present local field overprint removed during the first thermal demagnetization steps, followed by a variably well-defined mid-temperature component removed between 200 °C to 475 °C, followed either by instability or a high-temperature remanence holding the present local field direction (28% of the recently collected samples); (5) lightning remagnetization (4% of the recently collected samples); (6) 30 of the 76 samples from the Heavitree Gap sample set reveal a component that unblocks between 180 °C and 550 °C and after tilt-correction has a shallow, two-polarity NE/SW direction (tilt-corrected declination, inclination of ~224°, 13°), broadly similar to component C from the Love's Creek Member described above. This component direction was cited as evidence (by way of personal communication) for a low-latitude position of Australia during deposition of the basal Amadeus Basin stratigraphy by Vanyo and Awramik (1982, 1985).

The mid-temperature component was present in most samples from two sections to the north of Ross River Tourist camp in the East MacDonnell Ranges that have significantly contrasting bedding orientation (fig. 9). This component fails the McElhinny (1964) fold test at 99 percent confidence and a bootstrap fold test on the component gives the result that maximum concentration of the data results in the range of −2 to 18 percent unfolding, indicating that the component was acquired when the beds were at or very near their current orientation (fig. 9). The *in situ* mean of this component is steeply inclined and corresponds to an early Carboniferous paleolatitude of Australia (fig. 7), suggesting that the remanence was acquired during the late phases of the Alice Springs orogeny. With the possible exception of the previously developed data from Heavitree Gap near Alice Springs, the sections studied of the Heavitree Formation have not yielded any paleomagnetic component predating the Alice Springs Orogeny that could help constrain paleogeography at the time of Heavitree Formation deposition prior to the Bitter Springs Stage. Further study of the Heavitree Gap section with modern methods is warranted and its remanence suggests that there may be other localities in the formation not identified in this study that could yield useful data. At present, the dual polarity component isolated from that section is intriguing, but given its occurrence in only one locality it is difficult to constrain the timing of its acquisition and the direction will not be used in the following discussion of paleogeography.

Gillen Member of the Bitter Springs Formation.—The basal Gillen Member outcrops atop the Heavitree Formation along the northern basin-bounding monocline of the Amadeus Basin (fig. 3). The lower 100 to 300 meters of the Gillen Member typically is preserved in a coherent dip panel with the underlying Heavitree Formation. Above the basal Gillen Member stratigraphy are chaotic exposure patterns, evaporite-detachment faulting and dramatic non-cylindrical folding. Due to this structural complexity, the Gillen Member was not a major target of this study's paleomagnetic sampling. However, given the importance of any constraint on pre–Bitter Springs Stage paleogeography, paleomagnetic samples were collected and analyzed from: two stratigraphic sections from the basal carbonate parasequences within coherent dip panels of the lower Gillen Member directly overlying the Heavitree Formation (N52, N646; fig. 3), one site within a unit of the member that is dominated by dolostone grainstone with abundant gypsum pseudomorphs (N623) and includes a tight chevron fold (N623f),

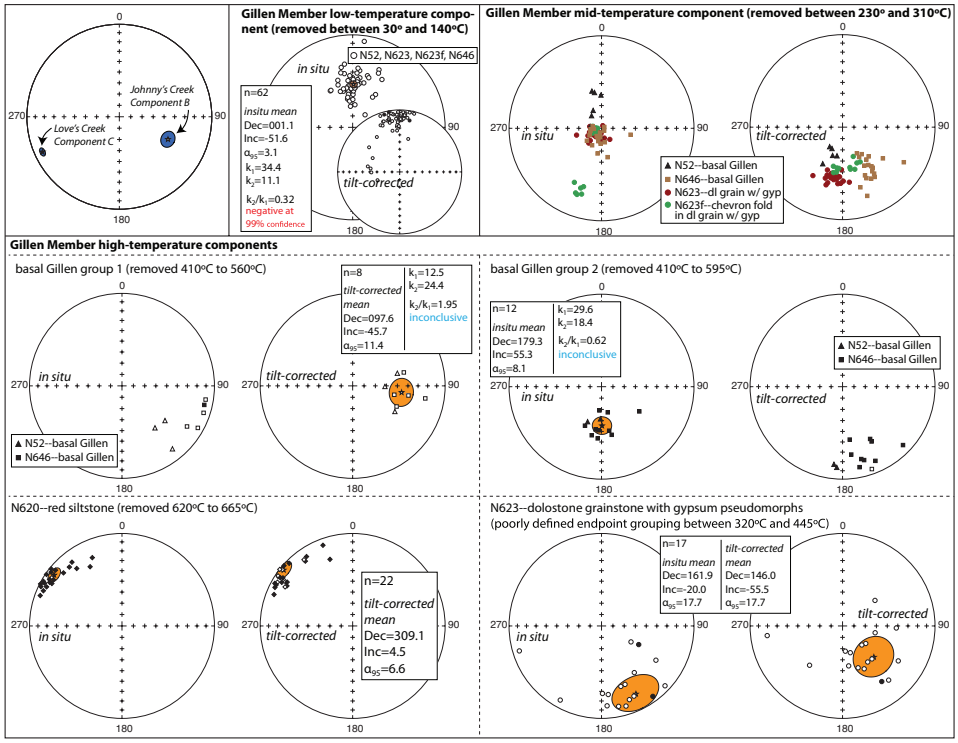

Fig. 10. Equal area plots of the least-square fits to paleomagnetic components from lithologies of the Gillen Member of the Bitter Springs Formation. These fits are shown in *in situ* and tilt-corrected coordinates and the mean direction, calculated with Fisher statistics (Fisher, 1953), is displayed for the directions either in *in situ* or tilt-corrected coordinates. Results for each stratigraphic section are reported in table 8. For reference, the mean of component C of the Love's Creek Member and the mean of component B of the Johnny's Creek Member are shown in the upper left panel.

and one stratigraphic section through red siltstone from within the member (N620). Results are summarized in figure 10 and table 8.

Component A. The carbonates analyzed from the Gillen Member have a component removed during the first steps of thermal demagnetization, homologous to Component A from the Love's Creek Member. This component is removed up to 130 °C, sometimes continuing up to 170 °C, and fits to it are grouped much tighter when uncorrected for bedding tilt failing the McElhinny (1964) fold test at the 99 percent confidence level (fig. 10). In uncorrected *in situ* coordinates, the mean of fits to this component (Dec of 001.1, Inc of −51.6, α_{95} of 3.1) is quite close both to the axial dipole for the localities (Dec of 000, Inc of ~41.5) and and the current IGRF2011 modeled field (IAGA-Working-Group and others, 2010; Dec of 004.7, Inc of −55.7).

Component B. Similarity between the analyzed Gillen Member carbonates and Love's Creek Member carbonates continues with the removal of a component between 230 °C and 310 °C homologous to component B from the Love's Creek Member. A boot-strap fold test on a small-scale chevron fold in the dolostone grainstone with gypsum pseudomorph facies (N623f) gives the result that the tightest clustering of fit directions occurs with 74 to 88 percent unfolding. A regional boot-strap fold-test between all sections gives the result that 95 percent of the peaks in concentration of the pseudo-sample sets occur between 27 to 71 percent unfolding. A regional fold-test

TABLE 8

Paleomagnetic data from Gillen Mb of the Bitter Springs Fm, Amadeus Basin

Stratigraphic section/ fit type	Location N00° 00',E00° 00'	n(p)/N	*In situ* coordinates				Tilt-corrected coordinates							
			D_m (°E)	I_m (°N)	k_1	α_{95} (°)	D_m (°E)	I_m (°N)	k_2	α_{95} (°)	λ (°N)	ϕ (°E)	A_{95} (°)	Plat (°)
Alice Springs Dump Basal Gillen (N52)/ LT	S23°43.4', E133°50.3'	9/9	356.4	-53.2	112.1	4.6	358.2	-6.2	121.0	4.4				
Alice Springs Dump Basal Gillen (N52)/ MT	S23°43.4', E133°50.3'	5/9	345.4	64.9	47.0	10.1	203.6	64.0	90.6	7.2				
Alice Springs Dump Basal Gillen (N52)/ HT1	S23°43.4', E133°50.3'	3/9	137.6	-32.1	15.6	26.1	96.3	-53.6	14.5	27.1				
Alice Springs Dump Basal Gillen (N52)/ HT2	S23°43.4', E133°50.3'	2/9	192.5	59.4			185.2	15.2						
Gillen red siltstone (N620)/ LHT-HT	S23°32.6', E134°27.5'	22/26	306.9	9.1	32.5	5.5	309.1	4.5	23.2	6.6				
Gillen Dolostone Grainstone (N623)/ LT	S23°34.2', E134°22.9'	23/25	357.6	-53.3	63.2	3.8	359.8	-13.4	63.2	3.8				
Gillen Dolostone Grainstone (N623)/ MT	S23°34.2', E134°22.9'	25/25	215	80.7	138.6	2.5	189.9	41.9	138.1	2.5				
Gillen Dolostone Grainstone (N623)/ HT	S23°34.2', E134°22.9'	17/25	161.9	-20.0	4.9	17.7	146.0	-55.5	4.9	17.7				
N of Benstead Crk Basal Gillen (N646)/ AF-LT	S23°32.4', E134°21.4'	18/20	008.4	-44.5	21.2	7.7	351.8	-14.5	15.6	9.0				
N of Benstead Crk Basal Gillen (N646)/ MT	S23°32.4', E134°21.4'	19/20	193.3	80.0	52.0	4.7	147.9	43.1	34.3	5.8				
N of Benstead Crk Basal Gillen (N646)/ HT1	S23°32.4', E134°21.4'	5/20	110.2	-6.6	33.8	13.4	98.2	-40.9	26.7	15.1				
N of Benstead Crk Basal Gillen (N646)/ HT2	S23°32.4', E134°21.4'	10/20	177.0	54.3	24.0	9.5	159.5	21.0	18.4	10.9				
TOTAL LT			001.1	-51.6	34.4	3.1	353.1	-17.0	11.1	5.7				
TOTAL HT1			119.4	-16.5	12.5	16.3	97.6	97.6	24.4	11.4				
TOTAL HT2			179.3	55.3	29.6	8.1	164.0	20.3	18.4	10.4				

LT fits were made to the initial thermal demagnetization steps up to 140 °C. MT fits were made to a component removed between 230 and 310 °C. HT fits are to components that persisted to higher thermal demagnetization steps upwards of 400 °C. n—number of samples used (samples that are not overprinted through lightening remagnetization and have stable behavior); N—total number of samples collected; D_m and I_m—mean declination and inclination of N stratigraphic horizons or samples; k—Fisher's (1953) precision parameter; α_{95}—radius of confidence circle for the mean direction; λ and ϕ—latitude and longitude of paleopole for mean direction in present-day coordinates; A_{95}—radius of 95% cone of confidence; Plat—paleolatitude. The latitude and longitude of the locations are in WGS84 coordinates.

between data from the N623 and N646 stratigraphic sections give the result that the 95 percent confidence interval for the degree of unfolding required to produce the tightest group is −10 to 10 percent—encompassing no unfolding and failing a fold test. Taken together, these results suggest that the acquisition of this component was associated with Alice Springs Orogeny deformation and largely formed after regional folding. The direction of the majority of the component B fits are steeply down to the SE in *in situ* coordinates (fig. 10). As with Love's Creek Member component B, this steep inclination corresponds to an early Carboniferous paleolatitude of Australia (fig. 7) suggesting that the remanence was acquired during the late phases of the Alice Springs orogeny.

High-temperature components. The components isolated at high-temperature from the Gillen Member cannot be described as forming a single population, as would be expected if all remanences isolated at high temperature were primary (fig. 10). Samples collected from the basal Gillen Member (sections N52 and N646) reveal high temperature components that decay towards the origin in two distinct populations, both removed from 410 °C to 560 °C or up to 595 °C for group 1 and group 2 respectively (fig. 10). Basal Gillen group 1 was isolated primarily from samples of dark gray dolostone wavy laminite, while basal Gillen group 2 directions were isolated from gray stromatolitic dolostone and gray to tan dolostone wavy laminites that were sometimes slightly pink. Since the number of samples from which these components could confidently be isolated were few, fold tests on each population were inconclusive. Nevertheless, a tighter grouping is achieved for basal Gillen group 1 after correction for tilting (tilt-corrected mean with Dec of 97.6, Inc of −45.7, α_{95} of 11.4) and a tighter grouping is achieved for basal Gillen group 2 prior to untilting (*in situ* mean with Dec of 179.3, Inc of 55.3, α_{95} of 8.1). Of potential significance is the correspondence of basal Gillen group 2 with the antipode of the present local field. However, this similarity to the present field could be coincidental and associated with an overprint at another time. The mean direction of basal Gillen group 1 is similar to that isolated from some sections of Johnny's Creek siltstone such that the α_{95} error ellipses overlap (figs. 8 and 10).

Between 320 °C and 450 °C, samples from the N623 section of dolostone grainstone with gypsum pseudomorphs achieve a quasi-stable endpoint with some movement toward the origin prior to instability. As with the remanence direction isolated at high-temperature for basal Gillen group 1, the α_{95} error ellipse for the mean overlaps with that of component B from the post–Bitter Springs Johnny's Creek Member.

Between 620 °C and 665 °C in samples from the N620 section of red siltstone, a component is removed that decays to the origin. This component is directed to the northeast with a quite shallow inclination and does not correspond to any remanence direction isolated for other studied units in the Bitter Springs Formation. With only one stratigraphic section through a unit that rarely is exposed within the heavily deformed Gillen Member, we do not have additional context with which to evaluate the age of this remanence.

The similarity in directions from the basal Gillen group 1 directions and the N623 directions may provide additional support for the more robustly constrained direction of Johnny's Creek component B. However, given the poor constraints on the high-temperature remanences, the Gillen Member data do not feature prominently in the discussion below.

Bitter Springs basalt flows.—Basalt flows occur at the top of the Bitter Springs Formation in the easternmost Amadeus Basin (fig. 2). Generally, the basalts are deeply weathered and outcrop poorly, but in rare localities the flows crop out coherently and can be sampled for paleomagnetic analysis. The presence of vesiculated flow tops and thin interflow siltstones support the interpretation that the basalts are extrusive lava

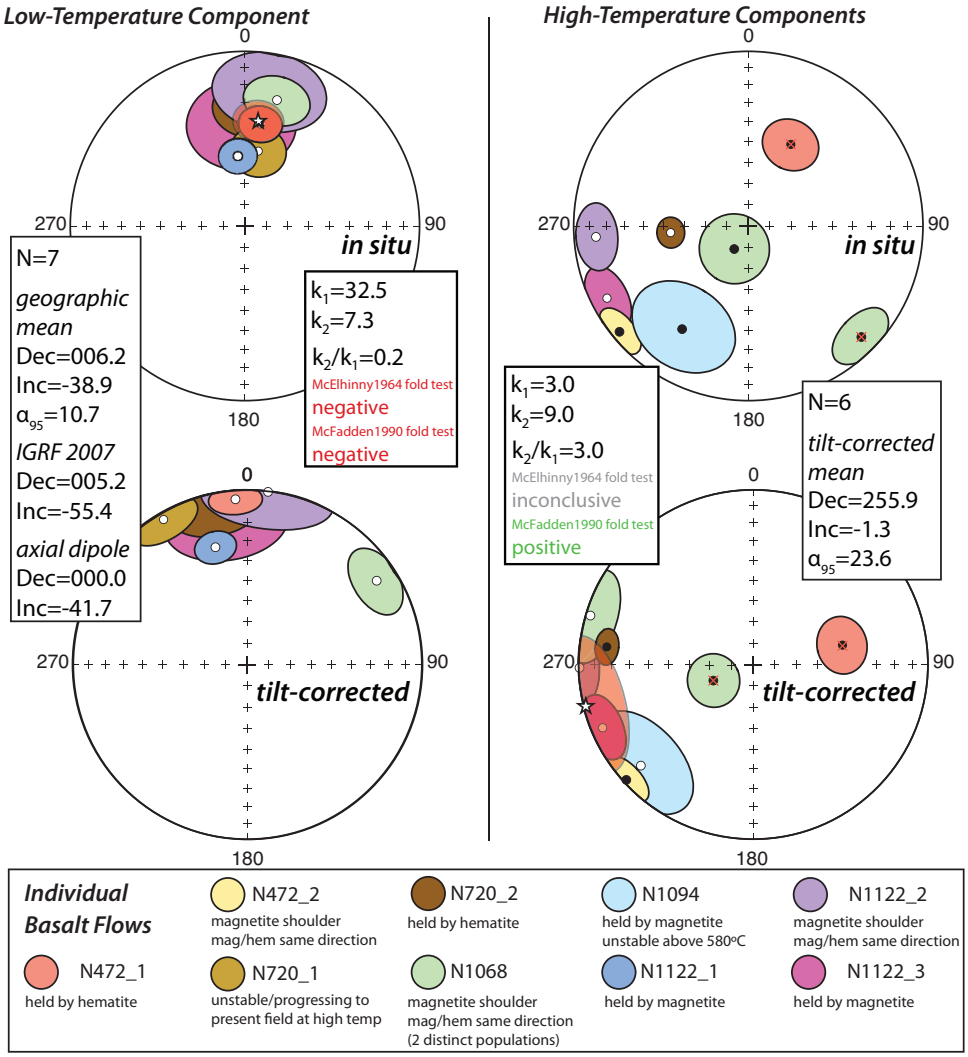

Fig. 11. Equal area plots of the paleomagnetic directions from the post–Bitter Springs Stage Amadeus Basin basalts. Directions are shown as the α_{95} ellipses of individual flows. The mean directions are marked with a star and shown with an associated translucent light red α_{95} ellipse (calculated with Fisher statistics; Fisher, 1953). The mean direction is displayed in *in situ* coordinates for the component removed at low temperatures. For the high temperature components, the high inclination directions marked with a red "x" were excluded from the calculated mean. The resulting mean from the six low inclination directions is shown in tilt-corrected coordinates.

flows (fig. 3). Figure 11 shows results from 7 analyzed flows of the Bitter Springs basalt that revealed two components of magnetization (table 9):

1. Component A. Between the measurement of natural remanence and the thermal demagnetization step at 200 °C, a component is removed from the basalt flows that corresponds to the present local field in *in situ* coordinates (fig. 11). This component is more tightly clustered when the Fisher mean is calculated without correction for bedding tilt, and fails a fold test at 99 percent confidence

TABLE 9

Paleomagnetic data from basalt flows in the uppermost Bitter Springs Fm, Amadeus Basin

Stratigraphic section and flow number/fit type	Location	n(p)/N	*In situ* coordinates				Tilt-corrected coordinates							
	N00° 00',E00° 00'		D_m (°E)	I_m (°N)	k_1	α_{95} (°)	D_m (°E)	I_m (°N)	k_2	α_{95} (°)	λ (°N)	ϕ (°E)	A_{95} (°)	Plat (°)
N472 Flow 1/ LT	S23°59.0', E134°47.6'	5/5	008.6	-40.6	55.2	9.3	359.8	-1.8	55.8	9.2				
N472 Flow 1/ HT (hematite)	S23°59.0', E134°47.6'	5/5	008.8	50.1	21.3	15.1	087.6	67.1	21.3	15.1				
N472 inter flow siltstone/ LT	S23°59.0', E134°47.6'	5/5	355.9	-45.3	39.4	11.0	355.6	-5.6	39.4	11.0				
N472 inter flow siltstone/ HT (hem)	S23°59.0', E134°47.6'	5/5	235.9	3.7	14.2	18.7	232.4	4.7	14.2	18.7				
N472 Flow 2/ HT (magnetite)	S23°59.0', E134°47.6'	5/6	230.6	5.1	53.9	9.4	231.0	-6.0	53.6	9.4				
N720 Flow 1/ LT	S23°57.6', E134°50.4'	3/3	009.9	-53.8	65.3	12.5	330.2	-4.1	65.3	12.5				
N720 Flow 2/ LT	S23°57.6', E134°50.4'	4/6	003.4	-31.6	24.8	16.2	348.3	9.8	24.8	16.2				
N720 Flow 2/ HT (hematite)	S23°57.6', E134°50.4'	6/6	265.2	-52.7	81.4	6.8	276.9	16.5	81.4	6.8				
N1068 Flow 1/ LT	S24°5.7', E135°7.0'	8/10	014.3	-26.5	15.9	13.4	057.1	-12.7	15.7	13.4				
N1068 Flow 1/ HT Group 1 (magnetite)	S24°5.7', E135°7.0'	5/10	213.8	77.7	14.8	16.4	287.1	-2.9	14.8	16.3				
N1068 Flow 1/ HT Group 1 (mag/hem)	S24°5.7', E135°7.0'	6/10	134.3	10.5	25.7	12.3	249.9	70.6	25.7	12.3				
N1094 Flow 1/ HT (magnetite)	S24°5.4', E135°7.2'	9/9	212.7	30.5	10.1	22.4	228.4	-14.1	10.1	22.4				
N1122 Flow 1/ LHT (hematite)	S23°45.6', E133°15.7'	6/6	354.1	-56.5	63.6	8.6	345.0	-31.1	63.6	8.6				
N1122 Flow 2/ LT	S23°45.6', E133°15.7'	6/6	10.4	-21.6	8.3	22.3	006.9	-0.5	8.3	22.3				
N1122 Flow 2/ HT (mag/hem)	S23°45.6', E133°15.7'	4/6	256.9	-13.6	41.7	12.4	269.0	-0.7	41.7	12.44				
N1122 Flow 3/ LT	S23°45.6', E133°15.7'	5/8	358.0	-40.5	9.4	23.3	351.7	-16.0	9.4	23.3				
N1122 Flow 3/ HT (magnetite)	S23°45.6', E133°15.7'	6/8	242.8	-10.4	27.0	11.9	247.2	-7.8	26.7	12.0				
TOTAL LT (flow mean)			006.2	-38.9	32.5	10.7	358.2	-9.6	7.3	23.3				
TOTAL HT (N472-2, N720-2, N1068a, N1094, N1122-2, N1122-3)			241.0	4.8	3.0	46.3	255.9	-1.3	9.0	23.6	**12.6**	**218.7**	**22.2**	-0.7	11.6 -13.1

LT indicates fits made to the initial thermal demagnetization steps. HT indicates fits made to higher thermal demagnetization steps either corresponding to unblocking temperatures characteristic for magnetite or hematite as indicated parenthetically. n—number of samples used (samples that are not overprinted through lightening remagnetization and have stable behavior); N—total number of samples collected; D_m and I_m—mean declination and inclination; k—Fisher's (1953) precision parameter; α_{95}—radius of confidence circle for the mean direction; λ and ϕ—latitude and longitude of paleopole for mean direction in present-day coordinates; A_{95}—radius of 95% cone of confidence; Plat—paleolatitude. "HT" pole in bold was calculated as the Fisher mean of the poles from each flow indicated. The latitude and longitude of the locations are in WGS84 coordinates.

(McElhinny, 1964). The mean calculated from the flow means for this component (Dec of 006.2, Inc of −37.3, α_{95} of 10.7) is quite close both to the axial dipole for the localities (Dec 000, Inc ~41.5) and and the current IGRF2011 modeled field (IAGA-Working-Group and others, 2010; Dec of 004.7, Inc of −55.7).

2. High-Temperature Components. There is not uniform thermal demagnetization behavior between the various sampled flows, and flows behaved in the following ways during paleomagnetic analysis:
   (a) Removal of present local field component up into the highest thermal demagnetization steps (N720 flow 1; N1122 flow 1).
   (b) Removal of a component up to 580 °C, followed by instability or remanence with present local field direction (N1068 Group 1; N1094; N1122 flow 3).
   (c) Removal of remanence up to 580 °C with a prominent "shoulder" in the demagnetization spectra. This inflection is followed by removal of a similarly directed component at subsequent thermal demagnetization steps up to 670 °C (N1122 flow 2; N472 flow 2; N1068 group 2).
   (d) No resolvable "shoulder" in demagnetization spectra at 580 °C with the majority of remanence lost during thermal demagnetization steps above 600 °C (N472 flow 1; N720 flow 2).

Of the seven flows that yielded high temperature remanence directions distinct from the present local field, six are loosely grouped in a single population in tilt-corrected coordinates (fig. 11). The McElhinny (1964) fold test is inconclusive on these directions, but a McFadden and McElhinny (1990) fold test is positive at the 95 percent confidence level with k_{max} at 85 percent unfolding (statistically indistinguishable from 100%). This result suggests that these remanence directions were acquired prior to tilting associated with the Alice Springs Orogeny. The α_{95} error ellipse of the tilt-corrected mean (Dec of 255.9, Inc of −1.3, α_{95} of 23.6) encompasses component C of the Love's Creek Member rendering the directions statistically indistinguishable from one another.

ROCK MAGNETIC DATA

Love's Creek Member Carbonates

Coercivity spectra and IRM/ARM acquisition curves.—The coercivity spectra of Love's Creek Member carbonates show a distinct peak centered at ~50 to 70 mT (fig. 12). The coercivity of stochiometric magnetite is strongly controlled by grain shape. Coercivities start at ~15 mT for equidimensional grains where the coercivity is dominated solely by multiaxial magnetocrystalline anisotropy, and can be as high as ~150 mT for an infinitely long magnetite rod with uniaxial anisotropy (Kopp and Kirschvink, 2008). A coercivity of ~50 mT could arise from a 50 nm long magnetite particle that is twice as long as it is wide. The main peak of the coercivity spectra is consistent with a population of magnetite. The width of the coercivity spectra peak is narrower than that observed from detrital magnetite populations where broad spectra arise from a range of particle sizes and shapes, is wider than that obtained from magnetofossil cultures where biogenically precipitated magnetosomes have tightly controlled size and shape distributions, and is similar to, but slightly wider than, data obtained for recent carbonate muds on Andros Island on the Great Bahama Bank (fig. 12; Maloof and others, 2007). Fitting the main peak with a log-Gaussian distribution does not achieve a tight fit at low coercivity, indicating that either the main magnetite population is skewed to lower coercivities, or that there is another population with a smaller contribution and a peak near that expected for magnetocrystalline anisotropy.

If this primary coercivity peak was the only coercivity distribution, df_{IRM}/dB should return to zero at the high-field end of the displayed spectra (fig. 12). Instead,

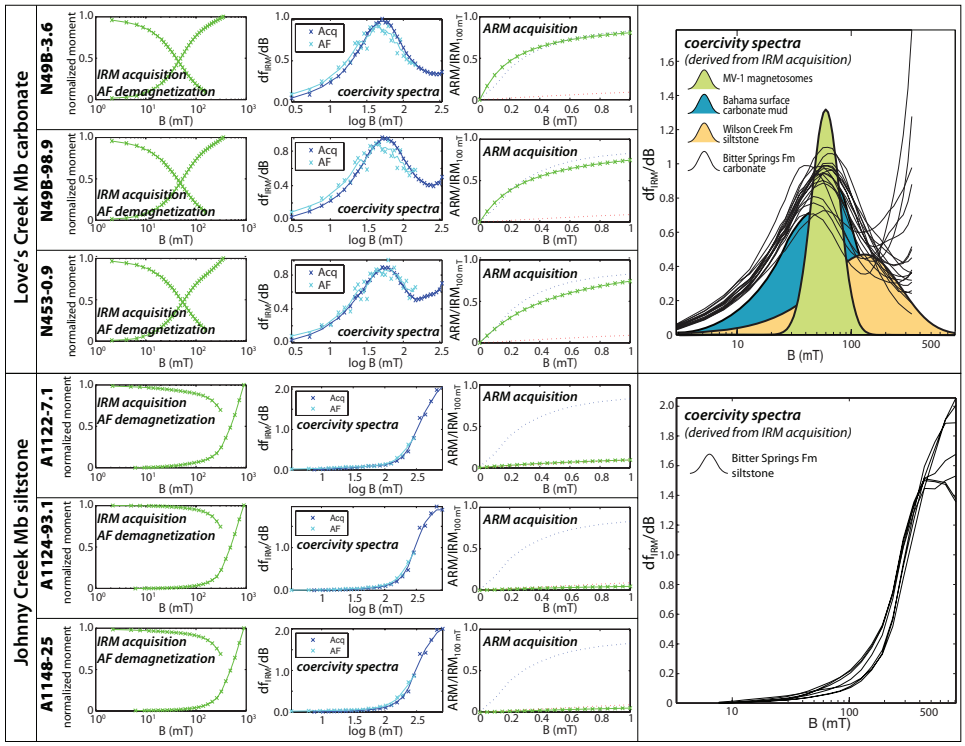

Fig. 12. IRM acquisition, AF demagnetization and ARM acquisition examples of samples of stromatolitic carbonate from the Love's Creek Member and red siltstones from the Johnny's Creek Member. The y-axis of the IRM acquisition plot is normalized to the moment at the peak applied field. The blue dotted line in the ARM acquisition plots represents a sample of weakly to non-interacting intact AMB-1 magnetotactic bacteria while the red dotted line is a sample of tightly packed, and highly interacting, chiton teeth (Cisowski, 1981). The rightmost coercivity spectra show all 18 Love's Creek Member samples analyzed overlain on the coercivity spectra for a culture of elongate magnetosomes in chains (MV-1; Kopp and Kirschvink, 2008), a surface sample of carbonate mud from the Great Bahama Bank and detrital magnetic particles from the Wilson Creek Formation (Kopp and Kirschvink, 2008), and all 7 Johnny's Creek Member samples analyzed. These plots were generated and summary parameters obtained using the routines of Kopp (ms, 2007).

df_{IRM}/dB begins to rise above applied fields of 250 mT and does not come close to peaking at saturation before the maximum applied field of 350 mT. This result demonstrates that there are additional magnetic minerals present in the samples with coercivities higher than 300 mT.

The crossover values (Cisowski R parameter) for the 18 room-temperature IRM acquisition and AF demagnetization curves acquired for Love's Creek Member carbonates are quite close to 0.5 (average of 0.447 with 1σ of 0.017) indicating that the ferromagnetic grains are weakly interacting (Cisowski, 1981). The ARM acquisition curves of the carbonates have high anhysteretic susceptibility plotting very near the AMB-1 standard of non-interacting single domain magnetite (fig. 12). Since interparticle magnetostatic interactions significantly reduce ARM susceptibility, this result provides further evidence that the magnetic material in the carbonates is well-separated such that it is non-interacting, or very weakly interacting (Cisowski, 1981).

Mineral identification through low-temperature remanence behavior.—The low-temperature remanence experiments shown in figure 13 elucidate the magnetic mineralogy of the Love's Creek Member carbonates. The outcrop samples show dramatic increases in

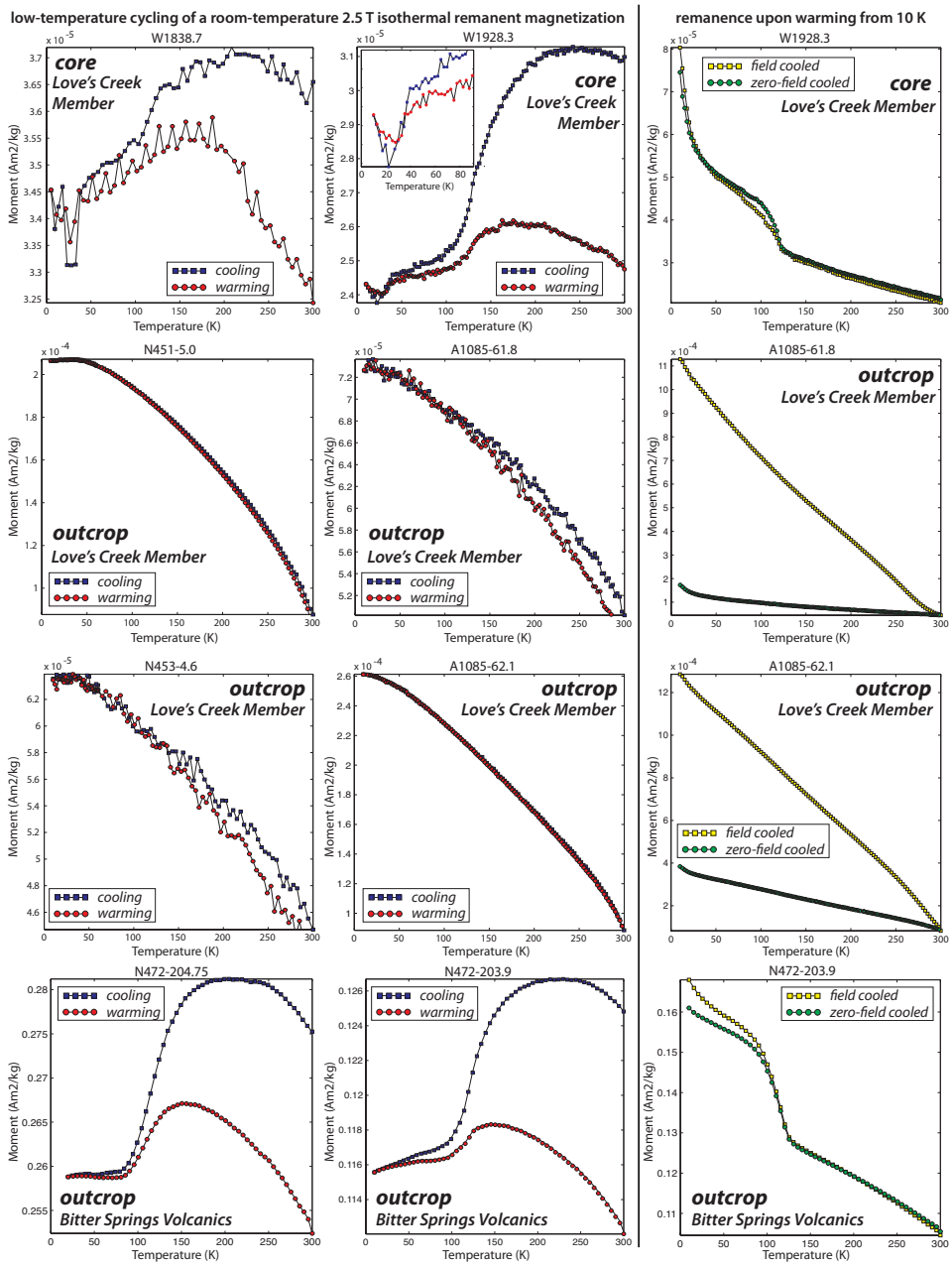

Fig. 13. Results from low temperature rock magnetic remanence experiments on Love's Creek carbonates and Bitter Springs Volcanics. Shown in columns 1 and 2 are the moments during low-temperature cycling experiments after exposure to a 2.5 T field at room temperature. Shown in column 3 is the moment during warming in a near zero field after cooling in a 2.5 T field (field cooled; yellow squares) and during warming after being cooled in zero field with a brief 2.5 T pulse at 10 K (zero-field cooled; green circles).

remanence upon cooling in the low-temperature cycling experiments that swamp all other signals. Warming of the low-temperature IRM for these samples leads to a large drop in remanence with a significant difference between the field cooled and zero-

field cooled runs with the field cooled protocol leading to a much stronger sample magnetization. Both the large difference between the ZFC and FC curves and the large increase of the 30 K remanence upon cooling are diagnostic of the presence of goethite (αFeOOH) within a sample, as is the tight correspondence between the cooling and warming curves during low-temperature cycling (Rochette and Fillion, 1989; Dekkers, 1989; Maher and others, 2004; Liu and others, 2006; Berquó and others, 2007). The presence of goethite in the outcrop samples also can explain the high coercivity component that is inferred from the IRM acquisition coercivity spectra (fig. 12). Goethite can not be the only magnetic mineralogy in these carbonates as it has a Curie point of ~120 °C (Özdemir and Dunlop, 1996) and there is significant remanence beyond those temperatures in these carbonates. However, in outcrop samples, the presence of the goethite masks the low-temperature behavior of other contributors to the magnetic mineralogy and no other components can be recognized.

In order to get around the overwhelming influence of goethite on the low-temperature behavior of the remanence, experiments were run on samples of Love's Creek Member carbonates from the Wallara-1 stratigraphic drill core (figs. 2 and 3). The drill core is not oriented azimuthally and therefore was not targeted for study of remanence direction. However, these samples of the same lithology give the opportunity to probe the magnetic mineralogy of these carbonates where they have not been subjected to surface weathering and associated goethite formation. Two significant transitions are observed in the low-temperature remanence experiments of these drill core samples (fig. 13): (1) the ~120 K Verwey transition is evident both in the low-temperature cycling experiments and the FC/ZFC warming experiments and indicates the presence of near stoichiometric magnetite (Fe_3O_4) and (2) the ~35 K Besnus transition is evident by the significant remanence loss between 39 and 27 K during low-temperature cycling that is diagnostic of the the iron sulphide pyrrhotite (Fe_7S_8; Fillion and Rochette, 1988; Dekkers and others, 1989; Rochette and others, 1990).

"Wasp-waisted" hysteresis loops.—Hysteresis experiments on both outcrop and subsurface core specimens demonstrate "wasp-waisted" behavior that occurs when there are multiple fractions of magnetic minerals with strongly contrasting coercivity (fig. 14; Tauxe and others, 1996). Much emphasis has been placed on the hysteresis parameters of carbonates as being diagnostic of primary versus secondary magnetization (for example Jackson and others, 1992; McCabe and Channell, 1994; Tarduno and Myers, 1994; Channell and McCabe, 1994; Dunlop, 2002b; Weil and Van der Voo, 2002; Elmore and others, 2006; Jackson and Swanson-Hysell, 2012). Originally proposed on the basis of the hysteresis behavior of early Paleozoic Appalachian carbonates that are interpreted to have undergone late Paleozoic remagnetization, high-values for the ratio of the coercivity of remanence to the coercivity (H_{cr}/H_c) and "wasp-waisted" behavior where the hysteresis loops are constricted about their middle have been interpreted as indicative of remagnetization (Jackson, 1990; McCabe and Channell, 1994). It has been proposed that this behavior in remagnetized carbonates arises from the presence of both stable single-domain and superparamagnetic magnetite, and that the presence of magnetite grain populations that span the superparamagnetic to single-domain size range boundary is a signature of chemical remagnetization (Jackson, 1990; Channell and McCabe, 1994; Dunlop, 2002b; Jackson and Swanson-Hysell, 2012). A bimodal coercivity distribution also can arise from multiple magnetic mineralogies that produces similar hysteresis behavior such as in Triassic carbonates from northern Italy that contain both magnetite and pyrrhotite (Muttoni, 1995). Therefore, the power of hysteresis loop parameters as a unique "fingerprint" for identifying magnetite spanning the superparamagnetic to single-domain size range boundary is

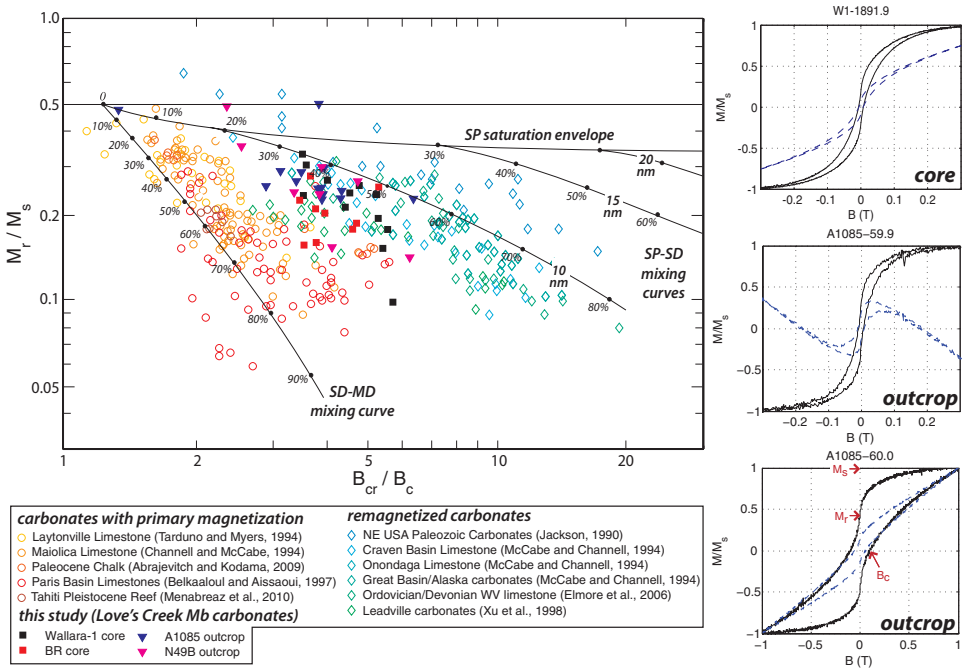

Fig. 14. (A) Summary of hysteresis parameters for carbonates of the present study and a compilation of hysteresis parameters of carbonates from the literature (Jackson, 1990; McCabe and Channell, 1994; Tarduno and Myers, 1994; Channell and McCabe, 1994; Belkaaloul and Aissaoui, 1997; Xu and others, 1998; Abrajevitch and Kodama, 2009; Ménabréaz and others, 2010) on a log-log Day plot where the ratio of saturation remanence to saturation magnetization (M_{rs}/M_s) is plotted against the ratio of the coercivity of remanence to the coercivity (B_{cr}/B_c) (Day and others, 1977). Also shown are the mixing curves between single-domain and multidomain magnetite and single-domain and superparamagnetic magnetite developed by Dunlop (2002a).

reserved for instances where there is a largely mono-mineralic population of magnetic grains (Jackson and Swanson-Hysell, 2012).

In the case of the Bitter Springs Formation carbonates analyzed from subsurface stratigraphic drill-core, the wasp-waisted behavior could be a result of the presence of both pyrrhotite and magnetite in the samples and/or indicative of the presence of significant superparamagnetic magnetite. The interpretation of multiple mineralogies with contrasting coercivities (such as magnetite and pyrrhotite) contributing significantly to this behavior is supported by non-linear demagnetization during backfield demagnetization experiments. The large decrease in remanence from 10 to 30 K during remanence upon warming experiments (fig. 13) indicates the presence of a significant population of superparamagnetic grains whose remanence is unblocking upon warming. It could be that these superparamagnetic grains are a significant contributor to the constriction of the hysteresis loops and the resulting location of the hysteresis parameters on the Day plot (fig. 14). For outcrop samples, the wasp-waisted behavior could be a result of the presence of single-domain magnetite, superparamagnetic magnetite, goethite and pyrrhotite. Some outcrop specimens have quite similar hysteresis loops to core specimens (see A1085-59.9 in fig. 14), while others have a distinct wider shape that do not approach saturation until close to 1 T as a result of the presence of goethite that as a result significantly alters the hysteresis parameters (see A1085-60.0 in fig. 14).

Johnny's Creek Member Siltstones

Coercivity spectra and IRM/ARM acquisition curves.—At the peak applied IRM of 900 mT, saturation of the magnetization of Johnny's Creek Member siltstones had not been achieved, indicating the presence of a high-coercivity component. Component analysis through cumulative log-Gaussian modeling of the IRM acquisition curves (Kruiver and others, 2001) reveals that the curves cannot be fit simply with one high-coercivity component with a log-Gaussian distribution. Rather, low residual fits to the curves are achieved by including a component with a coercivity of ~50 mT in addition to a component with a coercivity of ~1 to 2 T. However, this lower coercivity contribution (likely magnetite) to the overall IRM is quite small—between 1 to 2 percent for the 7 samples modeled. This result shows that the high-coercivity component (hematite as revealed through thermal demagnetization) dominates the samples magnetic mineralogy.

ORIGIN OF THE OBSERVED MAGNETIZATIONS

Love's Creek Member Component A

The component of the Love's Creek Member that is removed in the first steps of thermal demagnetization corresponds quite closely to the present local geomagnetic field in the study region (see the *Paleomagnetic Results for the Love's Creek Member* section). Given that IRM acquisition experiments demonstrate the presence of a high coercivity component, and that low-temperature remanence experiments of outcrop samples display the characteristic behavior of goethite, this component most likely is held by the iron oxyhydroxide mineral goethite. Goethite has coercivities that often are many hundreds of mT, but it is efficiently removed by thermal demagnetization due to its low Néel temperature of ~120 °C (Dunlop and Özdemir, 1997). Given that goethite forms through oxidative surface weathering, it follows that this goethite component would hold a recent magnetization corresponding to the present local field in the study area. However, in addition to the remanence removed at low-temperatures, there is a present local field direction that is removed by low-field AF demagnetization steps (0-7 mT). It is likely that the portion of the component that is readily removed by low-field AF demagnetization is a viscous remanent magnetization of magnetite acquired during the Brunhes epoch (the last 780 kyr). The interpretation of goethite as the primary carrier of this remanence can be extended to the remanence removed by 120 °C in the Gillen Member carbonates.

Love's Creek Member Component B

The least-square fits to the mid-temperature component of the Love's Creek Member carbonates are best clustered at 5 percent unfolding—a statistically indistinguishable result from 0 percent unfolding (see the *Paleomagnetic Results for the Love's Creek Member* section). This result indicates that the mid-temperature component was acquired when the sites were at their current structural attitude. As can be seen in figure 7, all of these overprint poles (except for those at A1085) are quite similar to Carboniferous poles for Australia. In particular, many of the overprint poles plot within error of the Carboniferous (constrained to 350 ± 7 by a U-Pb SHRIMP age on a rhyolitic ignimbrite; Hutton and others, 1999) Connors Volcanics pole from the New England Fold belt [argued to be representative of cratonic Australia at the time of eruption by McElhinny and others (2003)]. The poles also plot within error to the Mount Eclipse sandstone of the Amadeus Basin that was deposited in the latest Devonian to early Carboniferous, but whose magnetization is interpreted to be a syn-deformational remanence associated with the Alice Springs orogeny (Li and others, 1989).

Given that the rock magnetic experiments have indicated the presence of pyrrhotite in the Love's Creek Member and that this mid-temperature component unblocks up to temperatures of 300 to 320 °C, the component B direction most likely is held by pyrrhotite (the Curie temperature for pyrrhotite is 320 °C). The similarity of this direction to the Carboniferous poles for Australia suggests that it was acquired during the late stages of the Alice Springs Orogeny. Numerous studies have recognized the presence of secondary pyrrhotite as a syn- to post-folding magnetization in carbonate lithologies, and have attributed the pyrrhotite formation to the tectonically-driven migration of reducing fluids through porous sedimentary rock (Dinarès-Turell and Dekkers, 1999; Weaver and others, 2002; Otofuji and others, 2003; Zegers and others, 2003). In such a scenario, pyrrhotite can form at the expense of already present magnetite or pyrite, or can precipitate directly from fluid.

The presence of this post-folding pyrrhotite provides two temporal constraints for the Alice Springs Orogeny: (1) in the eastern MacDonnell Ranges, structural tilting effectively was complete by the early Carboniferous and (2) there was significant tectonic activity in the Early to Late Carboniferous that could have lead to orogenic fluid flow (or associated thermal activity). The timing of this paleomagnetically inferred tectonism in the eastern MacDonnell Ranges is consistent with ~330 to 310 Ma Ar/Ar ages of white micas from mylonite zones in the Arltunga Nappe Complex ~30 km to the northeast of the Ross River Region (Dunlap and others, 1991, 1995). In addition to recording active tectonism in the region at the time of the pyrrhotite formation, the trend of ages within the thrust sheet indicates a migration of tectonic activity into the hinterland (northward). This result is consistent with the cessation of structural tilting at the studied paleomagnetic localities prior to the pyrrhotite formation. The remagnetization associated with Alice Springs Orogeny tectonic activity is limited to the pyrrhotite component in the carbonates, as it appears that both magnetite and hematite paleomagnetic directions survived unaltered and record directions that are distinct from Alice Springs Orogeny overprints.

Love's Creek Member Component C

Low-temperature remanence experiments indicate the presence of magnetite within the Love's Creek carbonates (fig. 13). The high unblocking temperatures of component C (400 °C to 530 °C) combined with the coercivity spectra and hysteresis data demonstrate that component C largely resides in a population of single-domain magnetite.

The regional fold test demonstrates that the data are significantly better grouped in tilt-corrected coordinates than *in situ* coordinates, so this population of magnetite can be constrained to have acquired its remanence prior to the Alice Springs Orogeny. We are left to evaluate the question: Does component C of the Love's Creek Member represent a primary remanence from the time of the deposition of the carbonate, or was its origin associated with the growth of a population of authigenic magnetite at some other time prior to the Alice Springs Orogeny? We address this question by considering the dual polarity directions of component C, the apparent polar wander path for Australia prior to the Alice Springs Orogeny and the mechanisms through which a carbonate rock can acquire a magnetization held by magnetite.

Dual polarity directions.—High-resolution sampling from the A1085 section revealed that the high-temperature remanence is of dual polarity (component C of fig. 6); (fig. 15). The presence of reversals is taken as a reliability criteria in the evaluation of paleomagnetic data (Van der Voo, 1990), so these two populations could, at first glance, be considered to support an interpretation of the component C remanence as a primary magnetization. However, there are a number of puzzling features related to the reversed directions from the A1085 section. A McFadden and McElhinny (1990) reversal test conducted on the A1085 directions is negative (with an angle between the

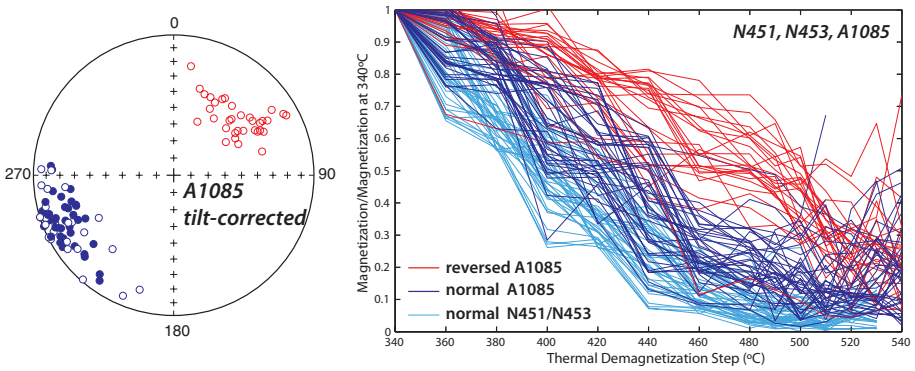

Fig. 15. High-temperature thermal demagnetization spectra for Love's Creek Member carbonates normalized to the magnetization at the 340 °C demagnetization step (a temperature by which the MT component is removed). The spectra for samples with a reversed magnetization (NE declination and upper hemisphere inclination) from A1085 are colored red while the spectra for normal samples from A1085, N451 and N453 are colored blue.

two means of 40.3°) indicating that the null hypothesis of a common mean direction for the normal and reversed directions is rejected with 95 percent confidence. The reversed intervals are often quite thin (<0.5 m) in the A1085 section, but do not have a clear relationship with lithofacies.

The N49B section covers the same stratigraphic range as part of the A1085 section with multiple reversals, but is of single "normal" polarity. In order to evaluate whether there is a dependence of polarity on magnetic mineralogy, the high-temperature demagnetization behavior of specimens from the A1085 section are plotted in figure 15. The temperature at which a population of magnetic minerals unblocks is controlled by changes in both chemical composition and grain size. Given that there is no expected correlation between chemical composition or grain size of the magnetic minerals holding the high-temperature remanence with the polarity of the geomagnetic field, the expectation is that, if both of these polarities are a primary remanence, there should be no notable difference in their thermal demagnetization spectrum. However, a distinct spectra of thermal demagnetization is present in the A1085 samples with "reversed" component C magnetization (NE declination and upper hemisphere inclination) compared to those with a "normal" magnetization (WSW declination and shallow inclination). In "reversed" specimens, the high-temperature component is removed at higher temperatures leading to a more "blocky" demagnetization curve where there is a narrower range of temperatures over which the component is unblocked. This result suggests that there are two populations of magnetite with different size distributions/stoichiometry that hold similar directions, but of dual polarity. At least one of these populations must not be the primary remanence.

Comparison to the APWP.—The reliability of a given paleomagnetic pole is increased if that pole does not fall on younger portions of the apparent polar wander path (APWP) for that continent (Van der Voo, 1990). This reliability criteria becomes more difficult to fulfill with older and older poles, as the likelihood increases of an overlap with younger paleomagnetic poles that is not due to remagnetization. One prominent example of such of overlap, that is largely accepted as a primary feature of the record, is the proximity of mid-Neoproterozoic poles of the Laurentian APWP to 300 million year older late-Mesoproterozoic poles forming the so-called "Grenville Loop." Nevertheless, pole overlap in general is a cause for skepticism of primary remanence, particularly if the portion of the APWP that the older remanence overlaps

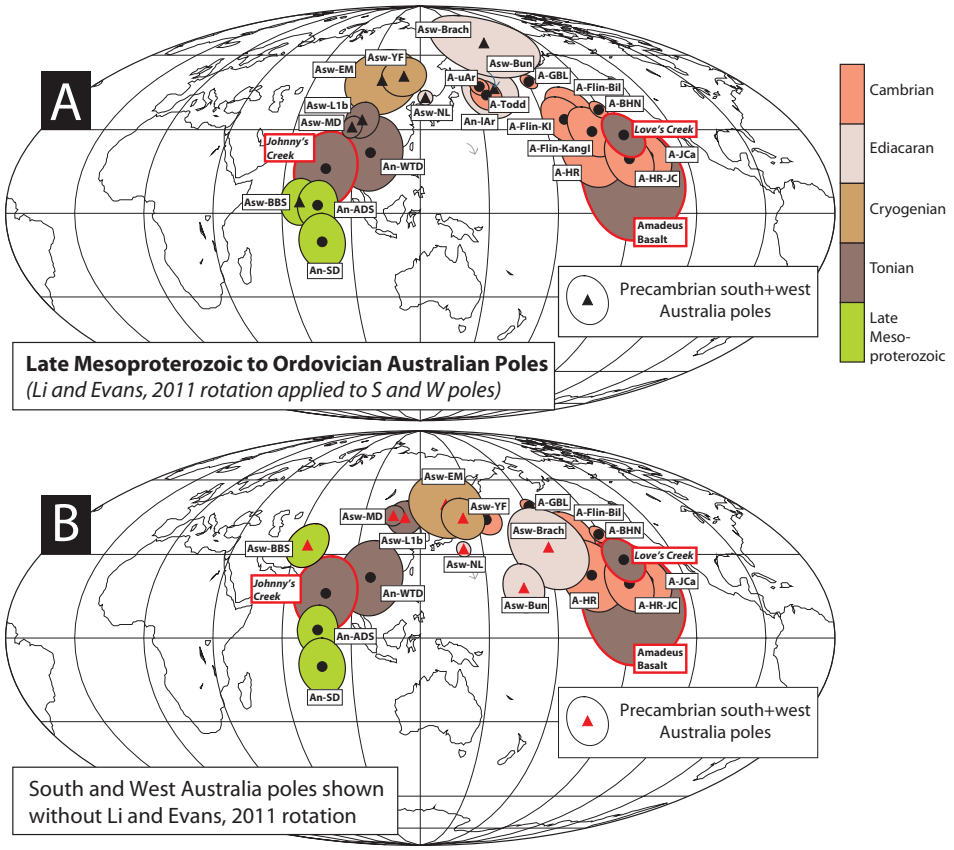

Fig. 16. Mollweide projection of Late Mesoproterozoic to Ordovician paleomagnetic poles from cratonic Australia. In (A) Proterozoic South and West Australia poles have been rotated with the hypothesized 40° rotation of (Li and Evans, 2011) into North Australia coordinates. The unrotated positions of those poles are shown in (B). The abbreviations for the paleomagnetic poles are keyed out in tables 4 and 10. Paleomagnetic poles from this study are accentuated with red lines around their A_{95} ellipses and labels. The Johnny's Creek and Love's Creek poles displayed are those calculated as the Fisher mean of section (with >6 samples) mean VGPs. The Amadeus Basalt pole is calculated as the Fisher mean of individual flow VGPs.

with is a time period associated with orogenesis or burial. In the case of the pole for the Love's Creek Member carbonates, the pole falls directly on the pole obtained for the Hugh River Shale and Jay Creek Limestone (Cambrian sediments from the Amadeus basin; fig. 16; Mitchell and others, 2010). While the timing of remanence acquisition of these middle Cambrian sediments are not constrained by a field test, the tight correspondence between the Love's Creek pole and the Hugh River/Jay Creek poles suggests that either the Love's Creek Member was undergoing remagnetization at the time of Hugh River/Jay Creek Formation deposition, or that both the Love's Creek Member and the Hugh River/Jay Creek were remagnetized in the late Cambrian. The Hugh River/Jay Creek poles, and correspondingly the Love's Creek member pole, are quite close to the late Cambrian Black Hill Norite pole of south Australia (A-BHN) and Cambrian poles from south Australia sediments such as the Kangaroo Island red beds (A-Flin-KangI). This correspondence provides further evidence that this pole position corresponds with the late Cambrian/early Ordovician APWP (fig. 16).

Primary magnetite in carbonates.—Primary magnetite in carbonates could be introduced through a detrital flux or through the biogenic production of magnetite by

magnetotactic bacteria (Blakemore, 1975; Maloof and others, 2007; Kopp and Kirschvink, 2008) and/or extracellular production through microbial Fe reduction (Li and others, 2004a). However, within the sediment column, there frequently is a tendency for reductive dissolution of magnetite followed by the production of magnetic iron sulfides associated with sulfate reduction (Hilgenfeldt, 2000; Housen and Moskowitz, 2006; Maloof and others, 2007). With less sulfate in Proterozoic waters and the potential for less organic matter without the presence of terrestrial organics (such as sea grasses and mangrove roots), reductive dissolution of magnetite may have been less aggressive in Precambrian shallow-water carbonates. More pervasive microbial binding in the Proterozoic would have led to more facies with early cementation and an increased potential for primary magnetite preservation. There are numerous examples of ancient carbonate magnetizations held by magnetite that are of convincingly primary origin including: the Mesoproterozoic Riphean carbonates of the Uchar-Maya Region (Pavlov and Gallet, 2010); the Neoproterozoic Svanbergfjellet Member of East Svalbard (Maloof and others, 2006); and Cretaceous Chalks of southern England (Montgomery and others, 1998). These considerations and examples demonstrate that the possibility of the magnetite remanence being primary exists and should not be rejected without careful consideration.

However, given the peculiar correspondence between magnetic mineralogy and polarity in the A1085 section, the failure of a reversal test in the A1085 section, the lack of reproducible reversal stratigraphy across the Love's Creek Member, and the overlap with the Cambrian APWP, it appears likely that the Love's Creek component C is a remagnetization. Nevertheless, given the potential for spurious APWP overlap and the positive fold test result, we will briefly consider the implications of a syn-depositional origin for component C in the discussion.

Authigenic magnetite formation.—Remagnetization of carbonates with remanences carried by magnetite have been identified in numerous studies, both in fold and thrust belts and in cratonic interiors (for example Jackson, 1990; McCabe and Channell, 1994; Xu and others, 1998; Elmore and others, 2006). There are two main mechanisms that have been invoked to explain authigenic magnetite formation in carbonates:

(1) precipitation of authigenic magnetite during the migration of orogenic fluids (for example Miller and Kent, 1988; McCabe and Elmore, 1989) and (2) the formation of magnetite associated with the smectite to illite conversion during burial diagenesis of clay (Katz and others, 1998; Tohver and others, 2008). In either scenario, the authigenic growth of magnetite could lead to grains too small to stably hold a remanence (superparamagnetic) as well as grains that grew large enough to be in the single domain size range where they would be thermally stable and acquire a secondary remanence. A magnetite population spanning the superparamagnetic to single domain size range could explain the rock magnetic behavior of some remagnetized carbonates such as the hysteresis parameters discussed above. A mix of superparamagnetic and single-domain magnetite within the Love's Creek Member carbonates is consistent with the rock magnetic data, although this size distribution, while characteristic of remagnetization, is not necessarily indicative of it (see discussion in Jackson and Swanson-Hysell, 2012).

The orogenic fluid hypothesis arose due to the observation that the origin of carbonate remagnetization in many instances had close temporal association with nearby mountain-building. The most well-studied example of such remagnetization is that of early Paleozoic carbonates in eastern north America that were remagnetized during the late Paleozoic Alleghanian orogeny (Miller and Kent, 1988; McCabe and Elmore, 1989). This remagnetization is well-constrained both by APWP comparison and fold tests on the Alleghanian fold-thrust belt that in some cases indicate a post-folding acquisition of magnetite remanence, while in other cases suggest that

magnetite remanence was acquired while folding was active (McCabe and others, 1983; Elmore and others, 2001). Some authors have critiqued the orogenic fluid hypothesis for magnetite formation on the basis of the spatial pervasiveness of chemical remanent magnetizations held by secondary magnetite and, in some cases, the lack of evidence for geochemical alteration by such fluids (Katz and others, 1998; Elmore and others, 2001).

Regarding the clay alteration burial diagenesis hypothesis, compilations of the illitization of smectite in shales show that the conversion begins at temperatures of ~60 to 70 °C and is effectively complete upon burial to temperatures of 100 to 120 °C (Srodon and Eberl, 1984). As a result, the transformation of smectite to illite is effectively complete by depths of ~3 to 4 kilometers depending on the local geothermal gradient as well as the concentration of potassium (Cuadros, 2006). The hypothesis that smectite alters to illite+magnetite is predicated on the fact that there are cations in the crystal structure of smectite (Ca, Fe and Mg) that do not become incorporated into the resulting illite and therefore form other minerals (Chamley, 1989).

There are currently two positive presence-absence tests in the literature for the hypothesis that illitization can be accompanied by the production of significant populations of authigenic magnetite. These tests demonstrate the presence of secondary magnetite in portions of basins without smectite, but not in portions of the basin where original smectite clays have gone unaltered (Katz and others, 2000; Woods and others, 2002). Similarly, a transect of the Devonian Onondaga Limestone across New York State found a correlation between the degree of illitization and the amount of magnetite (Jackson and others, 1988; McCabe and Elmore, 1989). $^{40}Ar/^{39}Ar$ dating of fine-grained illite fractions from Ediacaran carbonates of the São Francisco Craton and Devonian carbonates of Iberia have given ages that roughly coincide with the predicted ages of remagnetization on the basis of pole comparison to the respective APWP (Tohver and others, 2008; D'Agrella-Filho and others, 2008). This illitization mechanism provides a means for authigenic magnetite formation at relatively low-temperatures and predicts that the origin of the magnetite's CRM should date to a time of increased burial. Interpreting the similarity of Love's Creek Member component C to the Cambrian portion of the APWP for Australia as a result of magnetite formation from the smectite-to-illite alteration would require significant subsidence and sediment accumulation at this time in the Amadeus Basin.

In the late Ediacaran, the Love's Creek Member of the Bitter Springs Formation of the northern outcrop region where the paleomagnetic data samples were collected (fig. 2), was shallowly buried under ~1.2 km of Cryogenian and Ediacaran sediments. By the end of the Ordovician (taking the stratigraphy at Ellery Creek as an example), the Love's Creek Member was buried under ~3.9 km of sediments. For an average geothermal gradient of 30 °C/km and an average surface temperature of 15 °C, the Love's Creek Member would have been outside the illitization window at the Precambrian-Cambrian boundary (~51 °C) and would have moved through it during the early Paleozoic (~99 °C at the Cambrian-Ordovician boundary; ~132 °C at the end of the Ordovician). The timing of the potential remagnetization as inferred by APWP comparison is consistent with burial diagenesis and authigenic magnetite formation through transformation of smectite to illite during the late Cambrian.

Johnny's Creek Member component A.—Component A in the Johnny's Creek siltstones corresponds quite closely with the present local geomagnetic field (see the PALEOMAGNETIC RESULTS section). The component is predominantly removed at low temperatures (up to 200 °C), but can continue to be removed during thermal demagnetization steps up to ~400 °C. This thermal demagnetization behavior indicates that the component is not held solely by goethite. Instead, this component in these hematite-

rich sediments is most likely a viscous overprint of hematite acquired during the Bruhnes epoch.

Johnny's Creek Member component B.—The high-temperature component of magnetization of the siltstones of the Johnny's Creek Member is dominated by hematite (αFe_2O_3). After removal of the present local field overprint very little remanence is lost until thermal steps above 665 °C (fig. 5). This high unblocking temperature indicates that the magnetic mineral responsible for the ChRM in these samples is hematite, which has a Néel temperature of 675 °C (Dunlop and Özdemir, 1997). Given that this component passes a regional fold test (indicating that the magnetization was acquired prior to Paleozoic folding), that its pole position can reasonably connect to the other poles of the Neoproterozoic Australian APWP, and that it does not lie directly on the APWP prior to the timing of tilting, we interpret this remanence direction as a primary/early diagenetic magnetization.

Bitter Springs volcanics high-temperature component.—The high-temperature components isolated in the Bitter Springs volcanics form a poorly defined cluster in a similar direction to Love's Creek Member component C (fig. 11). Like the pole calculated for that component, the pole for the Amadeus Basalts (calculated as the Fisher mean of individual flow VGPs) falls on the late Cambrian portion of the Australia APWP path (fig. 16). This result indicates that the volcanics may have been remagnetized in the time period associated with the Petermann Orogeny and further subsidence in the basin. The volcanics are spilitic such that the original plagioclase is now albite (Wells and others, 1970). It is possible that either burial alteration or metamorphic fluids resulted in a late Cambrian overprint. The basalts contain significant magnetite (as evidenced through the expression of the Verwey transition in low-temperature remanence experiments; fig. 13) and often are characterized by a component that unblocks up to the Curie temperature of magnetite. These results suggest that remagnetization would involve the growth of secondary magnetite, although thermal viscous overprints can have anomalously high unblocking temperatures approaching the Curie temperature of magnetite if the grain assemblage is dominated by multidomain grains (Dunlop and others, 1997). If the cluster of these directions does represent a primary magnetization, the paleopole would imply oscillatory motion, off of and then back to the currently defined APWP, subsequent to that inferred in Svalbard for the Bitter Springs Stage.

PAELOGEOGRAPHY DISCUSSION

The "Grenville Loop" and Quantitatively Constraining Paleogeography with Paleomagnetic Data

The paleomagnetic database between 1050 and 700 Ma in Australia currently is quite limited with the 755 Ma pole from the Mundine Well dike swarm serving as the only robust paleomagnetic pole (fig. 1; table 10). The new paleomagnetic pole from the Johnny's Creek Member siltstones dates to ~780 to 760 Ma on the basis of the lithostratigraphic correlation of the Areyonga formation to the Sturtian glaciation and the correlation of the composite carbon isotope record to the global database (green bar labeled "An-JC" in fig. 1). These correlations lead to U/Pb age constraints from NW Canada (811 Ma; Macdonald and others, 2010) and Namibia (760 Ma; Halverson and others, 2005) that bracket the portion of the stratigraphy from which the Johnny's Creek Member data are obtained. With this approximate age of 770 Ma, the Johnny's Creek Member pole becomes the only result between the Alcurra dike Swarm pole (~1065 Ma) and the Walsh Tillite cap (~635 Ma) for north Australia and can be used to test paleogeographic models.

In contrast to the Australian record, the APWP from North America (Laurentia) is much better developed and defines a path known as the "Grenville Loop" (McWilliams

TABLE 10

Proterozoic paleomagnetic poles from Australia

pole	abbr	Pole (°N)	Pole (°E)	A_{95}(°)	Age (Ma)	Reference
South+West Australia						
Marnda Morn mean	Asw-MM	-48	148	15.5	~1200	Evans (2009)
Bangemall Basin Sills	Asw-BBS	33.8	95	8.3	1070±6	Wingate and others (2002)
Lancer Browne Formation	Asw-L1b	44.5	141.7	6.8	~820 Ma	Pisarevsky and others (2007)
Mundine Well Dykes	Asw-MD	45.3	135.4	4.1	755±3	Wingate and Giddings (2000)
Yaltipena Formation	Asw-YF	44.2	172.7	8.2	~640	Sohl and others (1999)
Elatina Formation Mean	Asw-EM	49.9	164.4	13.5	~636	as compiled in Li and Evans (2011)
Nuccaleena Formation	Asw-NL	32.3	170.8	2.9	~635	Schmidt and others (2009)
Brachina Formation	Asw-Brach	33.0	212.0	15.5	~630	Schmidt and others (2009)
Bunyeroo Formation	Asw-Bun	18.1	196.3	8.8	~600	Schmidt and Williams (1996)
North Australia						
Lakeview Dolerite	An-LD	-9.5	131.1	17.4	1141±6	Tanaka and Idnurm (1994)
Alcurra Dykes and Sills	An-ADS	2.8	80.4	8.8	1066-1087	Schmidt and others (2006)
Stuart Dykes	An-SD	-10.0	82.0	10.0	1057-1069	Idnurm and Giddings (1988)
Bitter Springs Formation Johnny's Creek Member	An-JC	15.8	83.0	13.5	780-760	preliminary result this study
Walsh Tillite Cap Dolomite	An-WTD	21.5	102.4	13.7	~635	Li (2000)
upper Pertatataka Fm and lower Arumbera Fm	An-lAr	44.3	161.9	10.2	~560-545	Kirschvink (1978)

and Dunlop, 1975; Weil and others, 1998; fig. 17). Efforts to quantitatively constrain early Neoproterozoic paleogeography with paleomagnetic data have been focused on comparing the poles from other cratons to these Laurentian data. The hypothesis of a cohesive Rodinia supercontinent leads to the testable hypothesis that the APWP of other continents should trace out similar loops during this time interval. Similarity of the paleomagnetic database of Baltica (the so-called "Sveconorwegian loop") with the "Grenville Loop" has been presented as evidence for a position of Baltica off of NE Laurentia throughout the Meso- to Neoproterozoic transition (Morris and Roy, 1977; Weil and others, 1998; Pisarevsky and others, 2003a)—a connection that is supported through geological correlation (Cawood and Pisarevsky, 2006). This approach of comparisons to the Laurentian APWP was applied to all continents in an effort to develop an all-inclusive and paleomagnetically viable Rodinia reconstruction by Weil and others (1998), by Li and others (2008), and again by Evans (2009) whose approach with an updated paleomagnetic database led to a radically revised reconstruction.

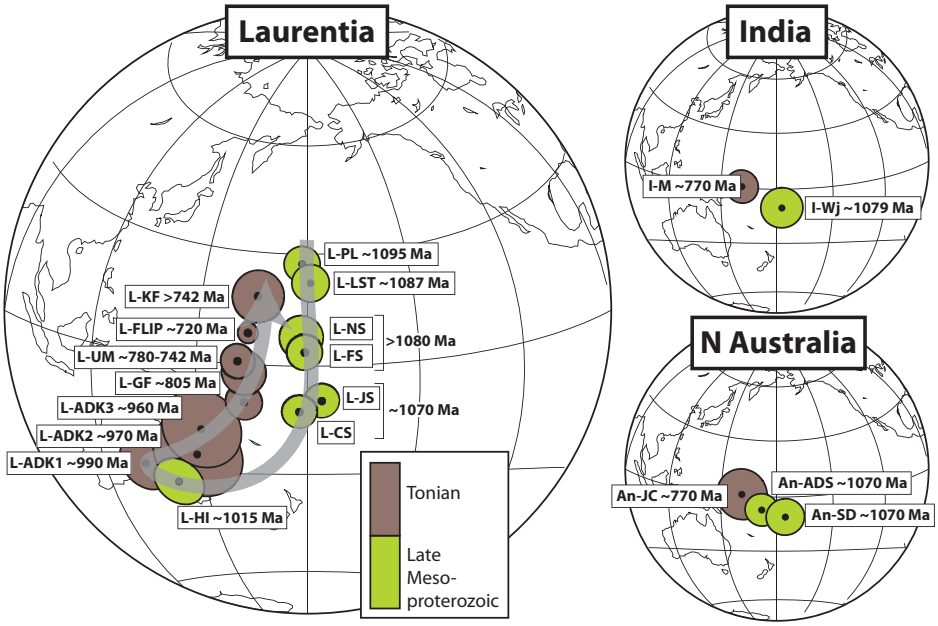

Fig. 17. The late Mesoproterozoic to early Neoproterozoic "Grenville Loop" apparent polar wander path of North America and poles of similar age from India and north Australia are shown in equal area projections. The poles for India and north Australia have been rotated so that they correspond to the Laurentia path (as was done for the reconstruction in fig. 18) and are shown in Laurentia coordinates for the purpose of comparison. The abbreviations for the paleomagnetic poles are keyed out in table 11 except for poles of the Grenville Province from Brown and McEnroe (2012) that are Adirondack fayalite granite (L-ADK1), Adirondack metamorphic anorthosites (L-ADK2) and Adirondack microcline gneisses (L-ADK3). The ages of these poles are derived from cooling age calculations (Brown and McEnroe, 2012). The age assignment for the Keweenawan sedimentary poles is approximate and is detailed in the discussion. Other poles that have been obtained from the Grenville Province are of similar direction to the L-ADK poles and, as discussed in the text, the difficulty in obtaining robust age estimates has led to debate as to whether the "Grenville Loop" is of clockwise or counter-clockwise vorticity. Regardless, the APWP moves to dramatically different latitude from the sedimentary poles of the Keweenawan Rift (L-NS, L-FS, L-JS and L-CS) before returning to a similar pole position as those poles at ~780 Ma thereby closing the loop. This proximity between poles of ~1080 to 1070 Ma and ~770 Ma is a feature of the Australian record (similar positions between the Asw-BBS, An-ADS and An-SD poles and the new Johnny's Creek Member pole) and the Indian record (similar positions of the I-Wj and the I-M poles).

While some of the specifics concerning the direction of pole progression in the "Grenville Loop" are debated (see summary in Weil and others, 2006), a principal pattern that emerges from the database is that high quality paleomagnetic poles of late Mesoproterozoic age (~1070 Ma) and early-mid-Neoproterozoic age (~750 Ma) are of similar geographic position (fig. 17). This feature of the record sets up a prediction that any continent that was conjoined to Laurentia during its early Neoproterozoic wandering should also have tight spatial correspondence between 1070 Ma and 770 Ma paleomagnetic poles as well as a similar loop away from this position in the intervening time period (fig. 17); (table 11).

A Tale of Two Australias

In an effort to reconcile coeval, but disparate, paleomagnetic poles of Paleoproterozoic, Mesoproterozoic and Neoproterozoic age between northern and south+western Australia, Li and Evans (2011) proposed a large-scale rotation between those portions of the continent. The timing of this relative rotation is proposed to

TABLE 11

Proterozoic paleomagnetic poles from Laurentia

pole	abbr	Pole (°N)	Pole (°E)	A_{95} (°)	Age (Ma)	Reference
Mackenzie Dykes	L-MD	4	190	5	1267±2	Buchan and Halls (1990)
Sudbury Dykes	L-SD	-3	192	3	1235+7/-3	Palmer and others (1977)
Abitibi Dykes	L-AD	43	209	14	1141±1	Ernst and Buchan (1993)
Logan sills	L-LS	49	220	4	1109±3	Buchan and others (2000)
Osler Volcanics	L-OV	43.7	196.3	7.6	1105±2	Halls (1974)
North Shore Volcanic Group (upper)	L-NSVG	36.7	182.3	3.6	1098.4±1.9, 1096.6±1.7	Tauxe and Kodama (2009)
Portage Lake Volcanics	L-PL	27.3	178.3	4.8	1095±3	Hnat and others (2006)
Lake Shore Traps	L-LST	22.2	180.8	5	1087±2	Diehl and Haig (1994)
Nonesuch Shale	L-NS	7.7	178.2	5.9	<1087	Henry and others (1977)
Freda Sandstone	L-FS	3.7	179.1	4.8	<L-NS (deposited during active rift volcanism)	Henry and others (1977)
Jacobsville Sandstone	L-JS	-9.3	183.6	4.7	< L-FS	Roy and Robertson (1978)
Chequamegon Sandstone	L-CS	-12.3	177.7	4.6	< L-FS,~upper L-JS	McCabe and Van der Voo (1983)
Haliburton Intrusives	L-HI	-32.6	141.9	6.3	1015±15	Warnock and others (2000)
Nankoweap Formation	L-NF	-10	163	4.9	<942 Ma	Weil and others (2003)
Gunbarrel dykes and sills	L-GB	9.2	138.7	9.0	782-776	Harlan and others (2008)
Uinta Mountain Group	L-UM	0.8	161.3	4.6	780-742	Weil and others (2006)
Galeros Formation	L-GF	-2.1	163	6.0	804±20	Weil and others (2004)
Kwagunt Formation	L-KF	18.2	166	7.0	older than 742±6	Weil and others (2004)
Franklin Event Grand Mean	L-FLIP	8.4	163.8	2.8	721-712	Denyszyn and others (2009)
Long Range Dykes	L-LRD	19.0	355.3	17.4	615±2	Murthy and others (1992)

correspond with the end-Neoproterozoic Petermann orogeny when there was large-scale shortening in central Australia whose structural geometry, metamorphic fabrics and inferred kinematic history have been compared to that of the Himalayan orogen (Raimondo and others, 2010). Relative rotation between N and SW Australia is an elegant and feasible paleogeographic solution that brings three sets of key paleomagnetic poles into closer alignment (fig. 16): ~1800 Ma Elgee-Pentecost (northern Australia) to ~1800 Ma Frere Formation (western Australia); 1066 to 1087 Ma Alcurra dike Swarm (An-ADS; northern Australia) to 1070 ± 6 Ma Bangemall Basin Sills (Asw-BBS; western Australia); 755 ± 3 Ma Mundine Well dikes (Asw-MD; western Australia) to ~710 to 635 Ma Walsh Tillite cap dolomite (An-WTD; northern Australia).

However, such a rotation has the effect of putting an additional degree of freedom into the exercise of generating an Australian APWP to compare to the Laurentian "Grenville Loop." While Li and Evans (2011) favor a 40° rotation, slight differences in the age of the poles as well as the A_{95} confidence ellipses on the poles themselves mean that there is a range of rotation values that would fit the hypothesis. This complexity adds uncertainty to using poles from between the two sub-cratons to develop a single

APWP. As a result, we lose some degree of confidence in applying the 755 Ma Asw-MD pole to constrain the relative position between the northern Australian craton and Laurentia. Intriguingly, the proposed relative rotation of Li and Evans (2011) has the effect of bringing the 755 Ma Asw-MD into much better agreement with the ~770 Ma Johnny's Creek Member pole (An-JC; northern Australia) developed herein from the Bitter Springs Formation. Without the rotation, the minimum arc distance between the poles is >50°, while with the rotation the A_{95} error ellipses slightly overlap (fig. 16). Thus, this result constitutes a positive test of the relative rotation hypothesis. The importance of this test is amplified by the realization that the Asw-MD/An-WTD is the weakest of the pole pairings utilized by Li and Evans (2011) because of the likely Marinoan age (~635 Ma) of the Walsh Tillite cap carbonate (An-WTD)—as opposed to Sturtian age (~700 Ma) as has been previously argued (Li, 2000). A Marinoan age assignment for the Walsh Tillite cap carbonate is supported by a high-degree of lithological and carbon isotopic similarity between it and other ~635 Ma cap dolostones (Corkeron, 2007). The proposed Li and Evans (2011) rotation does bring the An-WTD pole closer towards agreement with the correlative Nuccaleena Formation pole from south Australia (Asw-NL; fig. 16). Given that the Asw-MD and An-JC poles are much closer to time-equivalents, their reconciliation through the proposed rotation from their otherwise disparate positions can be considered a more robust positive test of the rotation from a set of mid-Neoproterozoic poles.

Implications of the Johnny's Creek Pole for an Australia–West Laurentia Connection

Comparisons of Neoproterozoic stratigraphy, timing of conjugate rift-drift margins and proposed alignments of Grenville-aged orogenic belts originally spawned the proposed late Mesoproterozoic connection between Australia and West Laurentia (Bond and others, 1984; Hoffman, 1991; Dalziel, 1991; Moores, 1991) at a time when there were few paleomagnetic data to test the configuration. An important feature of paleogeographic models in the time of Rodinia and Gondwana is that they maintain a connection between southern Australia and East Antarctica (Mawsonland). The connection of Mawsonland to southern Australia gains supporting evidence from the marked similarities between the Grenville-age orogenic Albany-Fraser belt of southwest Australia and the Bunger Hills region of East Antarctica (Duebendorfer, 2002), and a continuous connection between these two continents is thought to have been maintained until they rifted apart at ~95 Ma (Veevers and Eittreim, 1988). Recently, the geological basis for a SouthWest North America East Antarctica (SWEAT) style connection has been argued to be reinforced by the finding that ~1.4 Ga rapakivi granites of East Antarctica have very similar neodymium and hafnium isotopic signatures to coeval granites from southern Laurentia (Goodge and others, 2008). New data from East Antarctica also have revealed the presence of orthogneiss with a 1.1 Ga igneous age, which may represent a continuation of the Laurentian Grenville belt (Goodge and Fanning, 2010). This interpretation resolves the problem of some SWEAT-style reconstructions that had the Grenville province abruptly terminating at the SW Laurentia rift margin with no known equivalents in East Antarctica. A discovery of Grenville-age magmatic rocks on the South Tasman rise were argued by Fioretti and others (2005) to be a correlative of the Llano uplift granite suite in Texas and thus a more northerly piercing point for a continuation of the Laurentian Grenville province—a connection that would be consistent with the AUSWUS connection that has Australia (rather than Antarctica) aligned with southwest Laurentia.

Paleomagnetic data from the 1070 ± 6 Ma Bangemall Basin sills (Asw-BBS) were compared to the Laurentia APWP by Wingate and others (2002) and used to argue that neither SWEAT nor AUSWUS were paleomagnetically feasible in the late Mesoproterozoic. Their favored reconstruction had Australia so that the northernmost margin of eastern Australia was aligned with the southernmost margin of west Laurentia. How-

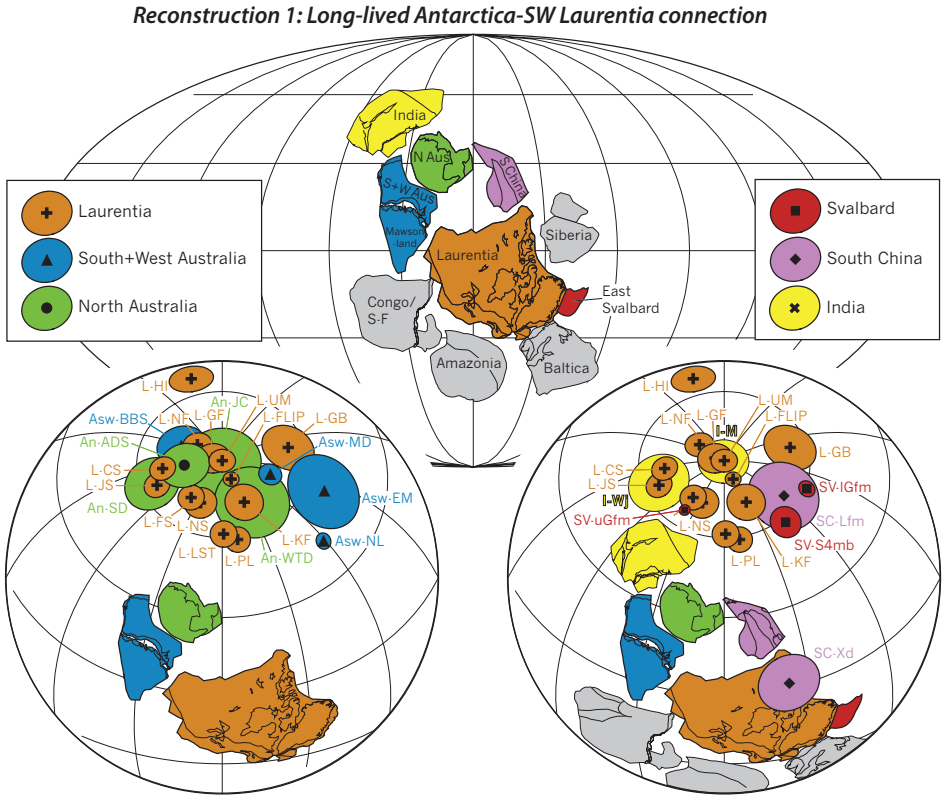

Fig. 18. Paleogeographic reconstruction discussed in section titled *Implications of the Johnny's Creek Pole for an Australia–West Laurentia Connection* that constrains the relative paleolongitude of Australia, Laurentia and India on the basis of supercontinent coherency and the direct comparison between late Mesoproterozoic (~1070 Ma) and mid Neoproterozoic (~770 Ma) poles (fig. 17). The left equal-area projection displays poles from Laurentia, northern Australia and south+west Australia. The right equal-area projection displays poles from Laurentia (including Svalbard), India and south China while the center Mollweide projection shows the resultant paleogeography resulting from this pole comparison. The abbreviations for the paleomagnetic poles are keyed out in tables 10, 11, and 12.

ever, with the position of the Bangemall basin to the south of the Paterson orogeny (a time-equivalent and probable extension of the Petermann Orogeny; Bagas, 2004), the Bangemall sill pole becomes part of the S+W Australia block in the Li and Evans (2011) model and the resulting rotation of the pole allows for a more northerly position for Australia relative to Laurentia (in present-day coordinates) as in Li and Evans (2011) and figure 18.

The most striking characteristic of the new ~770 Ma Johnny's Creek pole is its similarity to the late Mesoproterozoic Alcurra dike swarm (An-ADS) pole (figs. 16, 17, and 18). This close proximity between a latest Mesoproterozoic pole (An-ADS) and mid-Neoproterozoic poles (the Johnny's Creek pole) is quite similar to the Laurentian APWP (fig. 17). This result thus constitutes a successful test from north Australia of a continual connection of Australia with Laurentia across the Meso- to Neoproterozoic transition as it is consistent with the closure of the APWP as predicted by the Grenville loop (fig. 17).

The Johnny's Creek pole can be used to constrain the relative position between north Australia and Laurentia within Rodinia using the now reinforced hypothesis that

there was a continuous connection between the two continents between 1070 Ma and 770 Ma with minimal relative motion. With that working hypothesis, time-equivalent paleomagnetic poles from north Australia and Laurentia can be aligned to determine relative longitudinal as well as latitudinal positioning (fig. 18).

Li and Evans (2011) recently argued that such a connection between Australia and Laurentia must have been established post-1070 Ma as they considered the An-ADS pole (along with the rotated Bangemall Sill pole) to be incompatible with Laurentian APWP path at the time (the "Keweenawan Track"). They argued that the An-ADS pole would be expected to correspond with a gap between the youngest Keweenawan volcanics pole (the 1087 Ma Lake Shore Trap pole from lava flows within the Copper Harbor Conglomerate; Diehl and Haig, 1994) and the poles from Keweenawan sediments which they assign to be 1050 Ma (an age that was originally assigned to the units prior to precise geochronological control within the rift; Henry and others, 1977). However, given that the youngest Keweenawan volcanic pole is 1087 Ma, and that the Keweenawan record of volcanism shows continued rapid equatorward motion (Davis and Green, 1997; Swanson-Hysell and others, 2009), there is no reason to infer a 35 million year age gap between the eruption of the Lake Shore Traps (1087 ± 2 Ma) and the deposition of early Keweenawan Rift sediments such as Nonesuch Shale (L-NS) and Freda Sandstone (L-FS). This interpretation of a short temporal gap is supported by the fact that Nonesuch Shale and Freda Sandstone are conformable with the Copper Harbor Conglomerate, with the lower Nonesuch Shale interfingering with the conglomerate representing the more distal facies to time-equivelant alluvial fan facies (Elmore and others, 1989). Furthermore, the Freda sandstone itself is intruded by a volcanic plug ("the Bear Lake body"; Nicholson and others, 1997). Although this intrusion has not been dated, it is unlikely to be significantly (that is 10s of millions of years) younger than the youngest dated igneous activity in the Keweenawan rift (the 1086.5 + 1.3/−3.0 Ma Michipicoten Island Formation quartz-feldspar porphyry; Palmer and Davis, 1987). As a result, the Nonesuch Shale and Freda Sandstone poles likely date to be older than the ~1070 Ma An-ADS and Asw-BBS poles in contrast with the interpretation used by Li and Evans (2011). We instead consider the poles of the stratigraphically-higher Jacobsville Sandstone (L-JS) and Chequamegon Sandstone (L-CS), and the gap between these poles and the Freda-Nonesuch poles, to be likely time-equivalents to the ~1070 Ma An-ADS, An-SD and Asw-BBS poles and thus ripe for comparative analysis.

For this comparative pole analysis (fig. 18), the Johnny's Creek pole is aligned with the time-equivalent Uinta Mountain pole to constrain the paleolatitudes of both Australia and Laurentia. The southwestern Laurentia poles are utilized as opposed to the pole calculated from 6 VGPs of the contemporaneous Gunbarrel Magmatic event of northwestern Laurentia as their closeness to the Mesoproterozoic Laurentia poles forms the tight closure of the Grenville Loop that is paralleled in the Australian data. Following alignment of the Neoproterozoic poles, the relative longitudinal position of the two continents is then constrained through rotation until the ~1070 Ma Australian poles are aligned with the Jacobsville/Chequamegon poles. The result of this analysis is a positioning between Laurentia and Australia in which there is a tight connection between Mawsonland and southern Laurentia, but a significant gap between Australia and Laurentia. This relative positioning is quite similar to reconstruction of Laurentia and Australia in the "missing-link" model of Li and others (2008), but as in Li and Evans (2011), there is a tighter fit between Mawsonland and SW Laurentia due to the relative "tale of two Australias" rotation. This relative rotation of S+W Australia works well with this reconstruction in that there is no overlap between S+W Australia/Mawsonland and SW Laurentia although there is a tight fit.

TABLE 12

Proterozoic paleomagnetic poles from other cratons used in this study

pole	abbr	Pole (°N)	Pole (°E)	A_{95} (°)	Age (Ma)	Reference
Svalbard						
Lower Grusdievbreen Formation	Sv-lGfm	19.6	211.3	3.0	~815	Maloof and others (2006)
Upper Grusdievbreen Formation	Sv-uGfm	2.6	71.9	2.0	~800	Maloof and others (2006)
Svanbergfjellet Member	Sv-S4mb	25.9	226.8	5.8	~780	Maloof and others (2006)
South China						
Xiaofeng dikes	SC-Xd	14	91	11	802±10	Li and others (2004b)
Liantuo Formation	SC-Lfm	4	161	13	760-722	Evans and others (2000)
India						
Wajrakarur kimberlite	I-Wj	45	59	11	~1079	Miller and Hargraves (1994)
Malani Igneous Suite	I-M	67.8	72.5	8.8	771±5	Gregory and others (2009)
Congo						
Luakela Volcanics	C-Lk	40	302	14	765±5	Wingate and others (2010)
Mbozi Complex	C-Mb	46	325	9	748±6	Meert and others (1995)

This result allows for a long-lasting, tight-fitting connection between the continents. In light of the Goodge and others' (2008) evidence for a Antarctica-Laurentia connection at ~1400 Ma, it is worth discussing whether such a close connection could have been maintained for a significant period prior to 1070 Ma. The current paleomagnetic database suggests that continuous connection throughout the Mesoproterozoic is not tenable as data from a 1212 ± 10 Ma dike from the Fraser dike swarm of SW Australia (Pisarevsky and others, 2003b) indicates a high latitude position for Australia during a time period where robust coeval data from the "Logan Loop" for Laurentia indicate a low-latitude position. At present the Fraser direction remains a single virtual paleomagnetic pole emphasizing the need to reinforce that direction with additional data. If the high-latitude result stands with future work, it may imply that the 1.4 Ga granite tie-point has more bearing on reconstructions of Nuna (the supercontinent preceding Rodinia, see Evans and Mitchell, 2011) than it does on Rodinia. Regardless of their pre-1100 Ma relative positioning, the 1070 Ma and 760 Ma Australia-Laurentia pole pairs suggest a continuous connection between Antarctica and Laurentia across the Meso-Neoproterozoic boundary.

India also has a pairing of a late Mesoproterozoic pole (from the Wajrakarur kimberlite at ~1079 Ma) with a mid-Neoproterozoic pole (from the Malani Igneous Suite at 771 ± 5; table 12). Matching the Wajrakarur pole with Keweenawan sedimentary poles and the Malani pole with the Johnny's Creek Pole and Uinta Mountain/Galeros Pole leads to the reconstruction of India relative to Laurentia and Australia as shown in figure 18. As is the case with the northern Australia poles, the proximity of the Wajrakarur kimberlite and Malani Igneous Suite poles, despite the 300 million years that separates them, is consistent with India as a fellow traveler with Laurentia along the "Grenville Loop" (fig. 17).

The paleogeographic model presented in figure 18 using this approach of Laurentia and Australia pole comparison leaves open the identity of the craton that was the conjugate to northwestern Laurentia and was rifting off in the mid Neoproterozoic. As noted in Li and Evans (2011), for south China to have been this craton it would have to be rotated substantially from the position favored in the originally postulated "missing link model" into the position shown in figure 18. Another implication of the "missing-link" model is that if both the SC-Dd and SC-Lfm poles are primary the reconstruction effectively requires rapid TPW as interpreted by Li and others (2004b) as the SC-Xd pole is a significant departure from the "Grenville Loop." Therefore the "missing-link" model for south China's position is convolved with the TPW hypothesis.

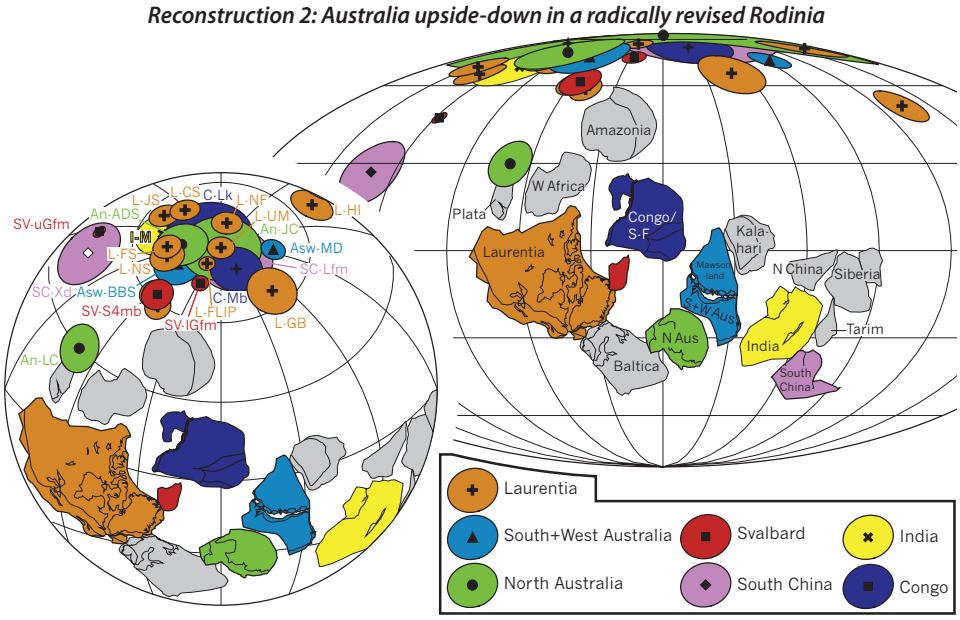

Fig. 19. Paleogeographic reconstruction discussed in sub-section *Turning Australia Upside-down* that follows the "radically revised Rodinia" of Evans (2009) with minor revisions: the relative "tale of two Australias" rotation is imposed and poles from Australia are aligned with their Meso- and Neoproterozoic time equivalents from Laurentia as in figure 18. The left equal-area projection displays select poles from Laurentia, Svalbard, northern Australia, south+west Australia, Congo, South China and India while the right Mollweide projection shows the resultant paleogeography. The abbreviations for the paleomagnetic poles are keyed out in tables 10, 11, and 12.

Turning Australia Upside-down

The other possibility for Australia's orientation relative to Laurentia at 760 Ma is the alternate polarity option favored by Evans (2009), wherein Australia is upside down relative to Laurentia. In this reconstruction, Australia does not have a direct connection to Laurentia, but is instead positioned significantly off of its eastern margin with Baltica fitting in the gap. The pairing of the An-ADS poles with Keweenawan rift sediment poles and the pairing of the Johnny's Creek pole with Laurentian sediment poles is consistent with this interpretation as shown in figure 19. This reconstruction takes the Euler poles of Evans (2009) for all cratons except for Australia. The Li and Evans (2011) "tale of two Australias" rotation is applied to the Australian continent and the position of Australia constrained with the late Mesoproterozoic poles and the Johnny's Creek pole. The North American COrdillera and BRAsiliano-Pharuside (COBRA) reconstruction of Plata and West Africa against western Laurentia replaces Australia as the conjugate continent in this reconstruction (Evans, 2009).

This polarity option has significant implications for the transition between Australia's position within Rodinia and its amalgamation into Gondwana. This polarity option was suggested by Schmidt and Clark (2000) and favored by Anderson and others (2004a) on the basis of the Silurian-Devonian APWP for Australia. In interpretations of this portion of the APWP that treat a low precision pole from the Silurian(?) Mereenie sandstone (Li and others, 1991) as robust and take data from Silurian arc volcanics of the Lolworth-Ravenswood terrane of eastern Australia's Thomson Fold Belt as representative of cratonic Australia, this polarity option reduces an implied

122° rotation in ~30 Ma to 58°. However, given the likely mobile nature of the Lolworth-Ravenswood terrane during arc accretion (McElhinny and others, 2003), and how poorly constrained the result from the Mereenie sandstone [a pole which was considered contaminated in the original analysis (Li and others, 1991) and is not used by the workers who developed it in subsequent paleogeographic reconstructions (Li and Powell, 2001)], this argument is not presently robust. Nevertheless, it should continue to be recognized that the "exit strategy" of Australia from Rodinia into Gondwanaland will be an important tool in future efforts to determine whether Australia was "rightside-up" or "upside-down" in Rodinia.

Viewing the Love's Creek Member Pole with Rose-colored Glasses and Implications for the True Polar Wander Hypothesis

The true polar wander (TPW) hypothesis for the Bitter Springs Stage, developed from the Akademikerbreen Group in Svalbard (Maloof and others, 2006), predicts that paleomagnetic poles between the Love's Creek Member (syn–Bitter Springs Stage) and the Johnny's Creek Member (post–Bitter Springs Stage) should record a 45° counter-clockwise rotation of Rodinia. As presented above, the Love's Creek Member appears to have been remagnetized in the late Cambrian through burial diagenesis. However, given the potential for coincidental overlap of the Love's Creek Member pole with the Cambrian APWP associated with Bitter Springs Stage TPW, we consider the paleogeographic implications of a primary interpretation for that pole.

The arc distance between the pole calculated from all Johnny's Creek Member component B fits and that for Love's Creek Member component C fits is 59.8° (±21°). This distance is greater than, but roughly comparable to, the 37.4° arc distance between the S4fm (post–Bitter Springs Stage) pole and the UGfm (syn–Bitter Springs Stage) pole from Svalbard and the arc distance of 45.6° between LGfm pole (pre–Bitter Springs Stage) and the UGfm (syn–Bitter Springs Stage) pole. The similarity between these arc distances is intriguing given that the TPW hypothesis predicts that poles from within and outside of the Bitter Springs Stage should span a similar arc distance as a result of the rotation wherein the total rotation is dependent on when the sediments where deposited (and magnetization acquired) with respect to the TPW.

A similar approach to a comparative pole analysis under the assumption of a coherent supercontinent can be used if rotations caused by rapid true polar wander can be confidently identified. During a TPW event, paleopoles from all continents will follow great circle paths relative Earth's spin-axis in a celestial reference frame about a single rotational axis (which corresponds to I_{min} of Earth). This rotation is in contrast to plate tectonics where continents and their paleomagnetically-derived poles move in small circles about independent poles (Euler poles). If the great circle traced out by the paleopoles can be identified on two continents, and a pole from each continent can be taken to be the same age, relative paleolongitude between continents can be constrained (that is the approach of Kirschvink and others, 1997). Figure 20 is a reconstruction that is developed assuming that the Love's Creek pole is primary and that the difference between it and the Johnny's Creek pole is a result of the same true polar wander event interpreted by Maloof and others (2006) to have caused the separation between the UGfm and S4fm poles. In this reconstruction, a geologically reasonable rotation of Svalbard is made to Laurentia (similar to that used in Maloof and others, 2006), the Johnny's Creek Member pole is aligned to overlap with the A_{95} ellipses of the pre–Bitter Springs Stage (Sv-lGfm) and post–Bitter Springs Stage (Sv-S4mb) Svalbard poles and Australia is rotated so that the A_{95} ellipse of the Love's Creek Member pole touches the great circle between the UGfm and S4fm poles. The result of this reconstruction is that the relative position of Laurentia and Australia are constrained to a position quite similar to the originally proposed SWEAT relationship (fig. 20). This approach to reconstructing the relative position between Australia and

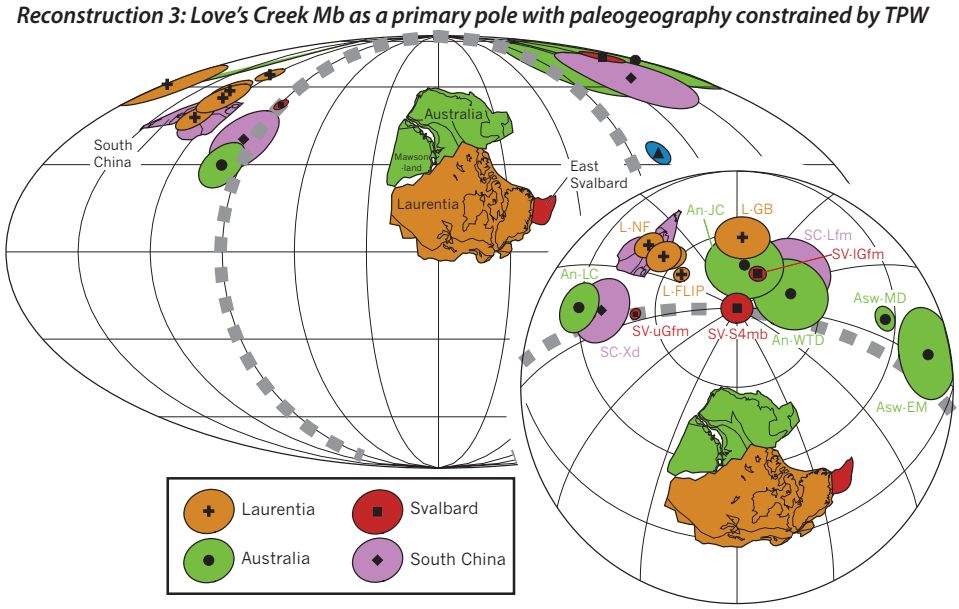

Fig. 20. Paleogeographic reconstruction taking the rose-colored glasses approach to the Love's Creek Member pole as discussed in section titled *Viewing the Love's Creek Member Pole with Rose-colored Glasses and Implications for the True Polar Wander Hypothesis*. In this reconstruction, the Love's Creek member pole is interpreted as primary and the arc distance between it and the Johnny's Creek Member pole (table 10) is taken to be a result of a true polar wander event that led to the separation of the Svalbard SV-uGfm and SV-S4mb poles (table 12). This approach allows for relative paleolongitude to be constrained. Interpreting the separation of the SC-Xd and SC-Lfm poles as due to the same true polar wander rotation leads to its position as shown. Since the "tale of two Australias" rotation is not applied, the Australia continent and poles are shown as a single color.

Laurentia is incompatible with the Li and Evans (2011) relative rotation between north and south+west Australia due to the significant overlap that results between south+west Australia and Laurentia if the rotation is applied. The choice of polarity for the paleomagnetic poles used in this analysis are consistent between Svalbard and Australia with the polarity of the syn–Bitter Springs stage poles being reversed relative to the post- and (and in the case of Svalbard) pre–Bitter Springs Stage poles. Disparate paleomagnetic poles from the 802 ± 10 Ma Xiaofeng dike and ~760–722 Liantuo Formation of South China have been presented as evidence of large-scale rapid TPW (table 12; Li and others, 2004b) that is consistent with the rotation inferred from the Svalbard poles (Maloof and others, 2006). Taking the 802 ± 10 Ma Xiaofeng dike pole to be a syn–Bitter Springs Stage pole and the the Liantuo Formation pole to be correlative with the Johnny's Creek pole results in the position of South China shown in (fig. 20) with significant distance between it and Laurentia and Australia.

CONCLUSIONS

A test for the Bitter Springs Stage true polar wander hypothesis requires that highly robust paleomagnetic data with convincingly primary magnetization are developed from both during and before/after the isotopic stage. High-quality data from the Love's Creek Member carbonates revealed two ancient magnetizations: one held by pyrrhotite and one held by magnetite. The pyrrhotite remanence formed while the rocks were at their present day structural orientation and corresponds with Carbonifer-

ous poles from Australia and the eastern Australia mobile belts. This result indicates that the majority of deformation in the basinal succession occurred prior to ~350 Ma and that the precipitation of iron-sulfides throughout Bitter Springs Formation carbonates occurred (likely as a result of fluid flow) at ~350 to 310 Ma. This timing of pyrrhotite formation corresponds to the last stages of deformation of the Alice Springs Orogeny in the hinterland of the orogeny.

In contrast to the remanence held by pyrrhotite, the magnetite remanence direction does not fall on the APWP path of Australia at the time of the Alice Springs Orogeny and was not acquired when the strata were at their present-day structural orientation. The tightest grouping of the data is achieved between 62 and 70 percent unfolding and the intermediate result may be due to structural complexity associated with vertical axis rotations rather than a result of a synfolding acquisition of magnetization. With this indication that magnetite formed prior to Alice Springs Orogeny related deformation, we are left to evaluate whether the magnetite dates to the time of deposition or formed authigenically at a later date prior to large-scale local deformation. The high degree of similarity of the magnetite remanence direction to Cambrian directions from the Amadeus Basin and an unusual correlation between thermal demagnetization spectra and polarity together suggest that the magnetite formed during the late Cambrian. This timing of magnetite formation coincides with further basinal subsidence and the passage of the Love's Creek Member through depths at which elevated temperatures could have driven the transformation of smectite to illite. Given the distance to the active orogenesis within the Petermann Orogeny, we prefer the smectite to illite magnetite formation mechanism as the driver for the growth of the magnetite if its origin is indeed authigenic. The possibility that the Love's Creek magnetite remanence is primary remains intriguing given the similar arc distance between its pole and the post–Bitter Springs Stage Johnny's Creek Member pole with the syn- and post–Bitter Springs Stage poles from Svalbard using the same choices of relative polarity. Adding to the intrigue, is the result that a true polar wander constrained paleogeographic reconstruction yields a snug geologically consistent SWEAT-style connection between Laurentia and Australia and is internally consistent with the observed changes in sea level. Such a reconstruction rules out the possibility of intra-Australian rotation or the "missing-link" South China–Laurentia connection if Australia was in a "rightside-up" position. However, without confidence that the magnetite is primary, and with reason to assign its origin to secondary magnetite formation, we present this result as a tantalizing possibility rather than a positive test of the true polar wander hypothesis. Further work on paleogeography and stratigraphic records of climate, carbon cycling and sea level before during and after the Bitter Springs Stage in more basins is necessary for hypothesis evaluation. Additionally, more radiometric age constraints that refine the duration and timing of the Bitter Springs Stage, and thus implied plate motions, can test competing hypotheses from a geodynamic perspective.

Regardless of the origin of syn–Bitter Springs Stage Love's Creek Member magnetization, paleomagnetic data from the Johnny's Creek Member of the Bitter Springs Formation yields a high-temperature remanence held by hematite that passes a tectonic fold test, fits into a reasonable position on the Meso- to Neoproterozoic APWP and is interpreted here as a primary magnetization. This paleomagnetic pole provides an important new constraint on the paleogeography of northern Australia in the time leading up to the first Neoproterozoic glaciation and is consistent with two hypotheses regarding mid-Neoproterozoic paleogeography: (1) that there was a large-scale rotation between northern and southwest Australia associated with the end-Neoproterozoic Petermann Orogeny and (2) that there was long-lived coherency of Laurentia and Australia as cotravelers within the supercontinent Rodinia.

ACKNOWLEDGMENTS

Seth Burgess, Ross Mitchell, Catherine Rose, Justin Strauss and Sarah Swanson-Hysell assisted with field work. We gratefully acknowledge assistance from the Northern Territory Geological Survey. In particular, Max Heckenberg at the Alice Springs core library and Christine Edgoose at the central office. We thank numerous pastoralists, the community of Areyonga, Ross River Tourist Resort and the Northern Territory Government for permission to conduct fieldwork on their lands. Steven Shonts and Jenn Kasbohm assisted with sample preparation. Hysteresis loops were acquired on an AGM instrument at Princeton Measurements Corporation headquarters. We thank Anthony Cumbo for access to the instrument and his help with the experiments. Low-temperature rock magnetic experiments were conducted at the Institute for Rock Magnetism, which is funded by the Instruments and Facilities Division of NSF and by the University of Minnesota. We thank Mike Jackson for his help with the experiments and their interpretation. Tim Raub and Isaac Hilburn are thanked for their technical support during measurements at the Caltech Paleomagnetism Lab. Mike McElhinny of the ANU in Canberra made his lab available for the early work on the Heavitree Formation, with a superconducting magnetometer on loan from Eugene Shoemaker of Caltech. We gratefully acknowledge the following scientists for their freely available software: Lisa Tauxe for her PmagPy software package that was utilized for the bootstrap fold tests, Craig Jones for his Paleomag X paleomagnetic data analysis program, Jean-Pascal Cogné for his Paleomac plate reconstruction software program, and Bob Kopp for the matRockmag data analysis package. The manuscript benefitted from reviews from Rob Van der Voo, Phil Schmidt and anonymous referees. The research was supported financially by NSF-EAR0514657 to A.C.M., an NSF EAPSI fellowship to N.L.S.-H., a grant from the American Philosophical Society's Lewis and Clark Fund for Exploration and Field Research in Astrobiology to N.L.S.-H. and by Princeton University.

References

Abrajevitch, A., and Kodama, K., 2009, Biochemical vs. detrital mechanism of remanence acquisition in marine carbonates: A lesson from the K-T boundary interval: Earth and Planetary Science Letters, v. 286, n. 1–2, p. 269–277, http://dx.doi.org/10.1016/j.epsl.2009.06.035

Abrajevitch, A., and Van der Voo, R., 2010, Incompatible Ediacaran paleomagnetic directions suggest an equatorial geomagnetic dipole hypothesis: Earth and Planetary Science Letters, v. 293, n. 1–2, p. 164–170, http://dx.doi.org/10.1016/j.epsl.2010.02.038

Ahmand, M., and Scrimgeour, I., 2006, Geological map of the Northern Territory: Northern Territory Geological Survey of Australia, Technical Report, 1:2,500,000 scale.

Aitken, A. R. A., Betts, P. G., and Ailleres, L., 2009, The architecture, kinematics, and lithospheric processes of a compressional intraplate orogen occurring under Gondwana assembly: The Petermann orogeny, central Australia: Lithosphere, v. 1, n. 6, p. 343–357, http://dx.doi.org/10.1130/L39.1

Alene, M., Jenkin, G. R. T., Leng, M. J., and Darbyshire, D. P. F., 2006, The Tambien Group, Ethiopia: An early Cryogenian (ca. 800-735 Ma) Neoproterozoic sequence in the Arabian-Nubian Shield: Precambrian Research, v. 147, n. 1–2, p. 79–99, http://dx.doi.org/10.1016/j.precamres.2006.02.002

Ambrose, G. J., Dunster, T. N., Munson, T. J., and Edgoose, C., 2010, Well completion reports for NTGS stratigraphic drillholes LA05DD01 and BR05DD01, southwestern Amadeus Basin: Northern Territory Geological Survey, Technical Report, Record 2010-015.

Anderson, K. L., Lackie, M. A., Clark, D. A., and Schmidt, P. W., 2003, Paleomagnetism of the Newcastle Range, northern Queensland: Eastern Gondwana in the Late Paleozoic: Journal of Geophysical Research—Solid Earth, v. 108, 2282, http://dx.doi.org/10.1029/2002JB001921

Anderson, K. L., Lackie, M. A., and Clark, D. A., 2004a, Palaeomagnetic results from the Palaeozoic basement of the southern Drummond Basin, central Queensland, Australia: Geophysical Journal International, v. 159, n. 2, p. 473–485, http://dx.doi.org/10.1111/j.1365-246X.2004.02393.x

——— 2004b, Return to Black Mountain: palaeomagnetic reassessment of the Chatsworth and Ninmaroo formations, western Queensland, Australia: Geophysical Journal International, v. 157, n. 1, p. 87–104, http://dx.doi.org/10.1111/j.1365-246X.2003.02164.x

Bagas, L., 2004, Proterozoic evolution and tectonic setting of the northwest Paterson Orogen, Western Australia: Precambrian Research, v. 128, n. 3–4, p. 475–496, http://dx.doi.org/10.1016/j.precamres.2003.09.011

Barron, E. J., 1981, Paleogeography as a climatic forcing factor: Geologische Rundschau, v. 70, n. 2, p. 737–747, http://dx.doi.org/10.1007/BF01822147

Belkaaloul, N. K., and Aissaoui, D. M., 1997, Nature and origin of magnetic minerals within the Middle Jurassic shallow-water carbonate rocks of the Paris Basin, France: implications for magnetostratigraphic dating: Geophysical Journal International, v. 130, n. 2, p. 411–421, http://dx.doi.org/10.1111/j.1365-246X.1997.tb05657.x

Bell, R., and Jefferson, C., 1987, A hypothesis for an Australia-Canadian connection in the late Proterozoic and the birth of the Pacific Ocean: Proceedings of the Pacific Rim Congress, v. 87, p. 207–222.

Berquó, T. S., Imbernon, R. A. L., Blot, A., Franco, D. R., Toledo, M. C. M., and Partiti, C. S. M., 2007, Low temperature magnetism and Mössbauer spectroscopy study from natural goethite: Physics and Chemistry of Minerals, v. 34, n. 5, p. 287–294, http://dx.doi.org/10.1007/s00269-007-0147-9

Besnus, M. J., and Meyer, A. J., 1964, Nouvelles données expérimentales sur le magnétisme de la pyrrhotine naturelle: Proceedings International Conference Magazine, v. 20, p. 507–511.

Blakemore, R., 1975, Magnetotactic bacteria: Science, v. 190, n. 4212, p. 377–379, http://dx.doi.org/10.1126/science.170679

Bond, G. C., Nickleson, P. A., and Kominz, M. A., 1984, Breakup of a supercontinent between 625 and 555 Ma: new evidence and implications for continental histories: Earth and Planetary Science Letters, v. 70, n. 2, p. 325–345, http://dx.doi.org/10.1016/0012-821X(84)90017-7

Bowring, S. A., Grotzinger, J. P., Condon, D. J., Ramezani, J., Newall, M. J., and Allen, P. A., 2007, Geochronologic constraints on the chronostratigraphic framework of the Neoproterozoic Huqf Supergroup, Sultanate of Oman: American Journal of Science, v. 307, n. 10, p. 1097–1145, http://dx.doi.org/10.2475/10.2007.01

Brookfield, M. E., 1993, Neoproterozoic Laurentia-Australia fit: Geology, v. 21, n. 8, p. 683–686, http://dx.doi.org/10.1130/0091-7613(1993)021⟨0683:NLAF⟩2.3.CO;2

Brown, L. L., and McEnroe, S. A., 2012, Paleomagnetism and magnetic mineralogy of Grenville metamorphic and igneous rocks, Adirondack Highlands, USA: Precambrian Research, v. 212–213, p. 57–74, http://dx.doi.org/10.1016/j.precamres.2012.04.012

Buchan, K. L., and Halls, H., 1990, Paleomagnetism of Proterozoic mafic dyke swarms of the Canadian Shield *in* Parker, A. J., Rickwood, P. C., and Tucker, D. H., editors, Mafic dike and Emplacement mechanisms: Rotterdam, Balkema, p. 209–230.

Buchan, K. L., Mertanen, S., Park, R. G., Pesonen, L. J., Elming, S. A., Abrahamsen, N., and Bylund, G., 2000, Comparing the drift of Laurentia and Baltica in the Proterozoic: the importance of key paleomagnetic poles: Tectonophysics, v. 319, n. 3, p. 167–198, http://dx.doi.org/10.1016/S0040-1951(00)00032-9

Buick, I. S., Storkey, A., and Williams, I. S., 2008, Timing relationships between pegmatite emplacement, metamorphism and deformation during the intra-plate Alice Springs Orogeny, central Australia: Journal of Metamorphic Geology, v. 26, n. 9, p. 915–936, http://dx.doi.org/10.1111/j.1525-1314.2008.00794.x

Burrett, C., and Berry, R., 2000, Proterozoic Australia Western United States (AUSWUS) fit between Laurentia and Australia: Geology, v. 28, n. 2, p. 103–106, http://dx.doi.org/10.1130/0091-7613(2000)028⟨0103:PAWUSA⟩2.3.CO;2

Camacho, A., Compston, W., McCulloch, M., and McDougall, I., 1997, Timing and exhumation of eclogite facies shear zones, Musgrave Block, central Australia: Journal of Metamorphic Geology, v. 15, n. 6, p. 735–751, http://dx.doi.org/10.1111/j.1525-1314.1997.00053.x

Canfield, D. E., Poulton, S. W., and Narbonne, G. M., 2007, Late-Neoproterozoic deep-ocean oxygenation and the rise of animal life: Science, v. 315, n. 5808, p. 92–95, http://dx.doi.org/10.1126/science.1135013

Cawood, P. A., and Pisarevsky, S. A., 2006, Was Baltica right-way-up or upside-down in the Neoproterozoic?: Journal of the Geological Society, London, v. 163, n. 5, p. 753–759, http://dx.doi.org/10.1144/0016-76492005-126

Chamley, H., 1989, Clay Sedimentology: Berlin, Springer-Verlag, 623 p.

Channell, J. E. T., and McCabe, C., 1994, Comparison of magnetic hysteresis parameters of unremagnetized and remagnetized limestones: Journal of Geophysical Research, v. 99, n. B3, p. 4613–4623, http://dx.doi.org/10.1029/93JB02578

Chen, Z., Li, Z. X., Powell, C. M., and Balme, B. E., 1993, Palaeomagnetism of the Brewer Conglomerate in central Australia, and fast movement of Gondwanaland during the Late Devonian: Geophysical Journal International, v. 115, n. 2, p. 564–574, http://dx.doi.org/10.1111/j.1365-246X.1993.tb01207.x

Chen, Z., Li, Z. X., and Powell, C. M., 1995, Paleomagnetism of the Upper Devonian reef complexes, Canning Basin, Western Australia: Tectonics, v. 14, n. 1, p. 154–167, http://dx.doi.org/10.1029/94TC01622

Cisowski, S., 1981, Interacting vs. non-interacting single-domain behavior in natural and synthetic samples: Physics of the Earth and Planetary Interiors, v. 26, n. 1–2, p. 56–62, http://dx.doi.org/10.1016/0031-9201(81)90097-2

Clark, D. A., 1994, Magnetic petrophysics and palaeomagnetism of the Fitzroy Leases, central Queensland—implications for exploration: CSIRO Australian Exploration and Mining Report, v. 6C, 28 p.

——— 1996, Palaeomagnetism of the Mount Leyshon Intrusive Complex, the Tuckers Igneous Complex and the Ravenswood Batholith: CSIRO Australian Exploraton and Mining Report, v. 318R.

Clark, D. A., and Lackie, M. A., 2003, Palaeomagnetism of the Early Permian Mount Leyshon Intrusive Complex and Tuckers Igneous Complex, North Queensland, Australia: Geophysical Journal International, v. 153, n. 3, p. 523–547, http://dx.doi.org/10.1046/j.1365-246X.2003.01907.x

Corkeron, M., 2007, "Cap carbonates" and Neoproterozoic glacigenic successions from the Kimberley region, north-west Australia: Sedimentology, v. 54, n. 4, p. 871–903, http://dx.doi.org/10.1111/j.1365-3091.2007.00864.x

Creveling, J. R., Mitrovica, J. X., Chan, N.-H., Latychev, K., and Matsuyama, I., 2012, Mechanisms for

oscillatory true polar wander: Nature, v. 491, n. 7423, p. 244–248, http://dx.doi.org/10.1038/nature11571

Cuadros, J., 2006, Modeling of smectite illitization in burial diagenesis environments: Geochimica et Cosmochimica Acta, v. 70, n. 15, p. 4181–4195, http://dx.doi.org/10.1016/j.gca.2006.06.1372

D'Agrella-Filho, M. S., Tohver, E., Santos, J. O. S., Elming, S.-A., Trindade, R. I. F., Pacca, I. I. G., and Geraldes, M. C., 2008, Direct dating of paleomagnetic results from Precambrian sediments in the Amazon craton: Evidence for Grenvillian emplacement of exotic crust in SE Appalachians of North America: Earth and Planetary Science Letters, v. 267, n. 1–2, p. 188–199, http://dx.doi.org/10.1016/j.epsl.2007.11.030

Dalziel, I. W. D., 1991, Pacific margins of Laurentia and East Antarctica–Australia as a conjugate rift pair: evidence and implications for an Eocambrian supercontinent: Geology, v. 19, n. 6, p. 598–601, http://dx.doi.org/10.1130/0091-7613(1991)019⟨0598:PMOLAE⟩2.3.CO;2

Davis, D. W., and Green, J. C., 1997, Geochronology of the North American Midcontinent rift in western Lake Superior and implications for its geodynamic evolution: Canadian Journal of Earth Science, v. 34, n. 4, p. 476–488, http://dx.doi.org/10.1139/e17-039

Day, R., Fuller, M., and Schmidt, V. A., 1977, Hysteresis properties of titanomagnetites: Grain size and compositional dependence: Physics of the Earth and Planetary Interiors, v. 13, n. 4, p. 260–266, http://dx.doi.org/10.1016/0031-9201(77)90108-X

Dekkers, M. J., 1989, Magnetic properties of natural goethite—II. TRM behaviour during thermal and alternating field demagnetization and low-temperature treatment: Geophysical Journal International, v. 97, n. 2, p. 341–355, http://dx.doi.org/10.1111/j.1365-246X.1989.tb00505.x

Dekkers, M. J., Mattéi, J.-L., Fillion, G., and Rochette, P., 1989, Grain-size dependence of the magnetic behavior of pyrrhotite during its low-temperature transition at 34 K: Geophysical Research Letters, v. 16, n. 8, p. 855–858, http://dx.doi.org/10.1029/GL016i008p00855

Denyszyn, S. W., Halls, H. C., Davis, D. W., and Evans, D. A. D., 2009, Paleomagnetism and U-Pb geochronology of Franklin dykes in High Arctic Canada and Greenland: a revised age and paleomagnetic pole constraining block rotations in the Nares Strait region: Canadian Journal of Earth Sciences, v. 46, n. 3, p. 689–705, http://dx.doi.org/10.1139/E09-042

Diehl, J. F., and Haig, T. D., 1994, A paleomagnetic study of the lava flows within the Copper Harbor Conglomerate, Michigan: new results and implications: Canadian Journal of Earth Sciences, v. 31, p. 369–380, http://dx.doi.org/10.1139/e94-034

Dinarès-Turell, J., and Dekkers, M. J., 1999, Diagenesis and remanence acquisition in the Lower Pliocene Trubi marls at Punta di Maiata (southern Sicily): palaeomagnetic and rock magnetic observations: Geological Society, London, Special Publications, v. 151, p. 53–69, http://dx.doi.org/10.1144/GSL.SP.1999.151.01.07

Donnadieu, Y., Goddéris, Y., Ramstein, G., Nédelec, A., and Meert, J., 2004, A "snowball Earth" climate triggered by continental break-up through changes in runoff: Nature, v. 428, p. 303–306, http://dx.doi.org/10.1038/nature02408

Duebendorfer, E. M., 2002, Regional correlation of Mesoproterozoic structures and deformational events in the Albany-Fraser orogen, Western Australia: Precambrian Research, v. 116, n. 1–2, p. 129–154, http://dx.doi.org/10.1016/S0301-9268(02)00017-7

Dunlap, W. J., and Teyssier, C., 1995, Paleozoic deformation and isotopic disturbance in the southeastern Arunta Block, central Australia: Precambrian Research, v. 71, n. 1–4, p. 229–250, http://dx.doi.org/10.1016/0301-9268(94)00063-W

Dunlap, W. J., Teyssier, C., McDougall, I., and Baldwin, S., 1991, Ages of deformation from K/Ar and $^{40}Ar/^{39}Ar$ dating of white micas: Geology, v. 19, n. 12, p. 1213–1216 http://dx.doi.org/10.1130/0091-7613(1991)019⟨1213:AODFKA⟩2.3.CO;2

——— 1995, Thermal and structural evolution of the intracratonic Arltunga Nappe Complex, central Australia: Tectonics, v. 14, n. 5, p. 1182–1204, http://dx.doi.org/10.1029/95TC00335

Dunlop, D. J., 2002a, Theory and application of the Day plot (M_{rs}/M_s versus H_{cr}/H_c) 1. Theoretical curves and tests using titanomagnetite data: Journal of Geophysical Research, v. 107, 2056, http://dx.doi.org/10.1029/2001JB000486

——— 2002b, Theory and application of the Day plot (M_{rs}/M_s versus H_{cr}/H_c) 2. Application to data for rocks, sediments, and soils: Journal of Geophysical Research, v. 107, 2057, http://dx.doi.org/10.1029/2001JB000487

Dunlop, D. J., and Özdemir, Ö., 1997, Rock Magnetism: Fundamentals and frontiers: Cambridge, United Kingdom, Cambridge University Press, Cambridge Studies in Magnetism, 573 p.

Dunlop, D. J., Özdemir, Ö., and Schmidt, P. W., 1997, Paleomagnetism and paleothermometry of the Sydney Basin 2. Origin of anomalously high unblocking temperatures: Journal of Geophysical Research, v. 102, n. B12, p. 27,285–27,295, http://dx.doi.org/10.1029/97JB02478

Elmore, R. D., Milavec, G. J., Imbus, S. W., and Engel, M. H., 1989, The Precambrian Nonesuch Formation of the North American mid-continent rift, sedimentology and organic geochemical aspects of lacustrine deposition: Precambrian Research, v. 43, n. 3, p. 191–213, http://dx.doi.org/10.1016/0301-9268(89)90056-9

Elmore, R. D., Kelley, J., Evans, M., and Lewchuk, M. T., 2001, Remagnetization and orogenic fluids: testing the hypothesis in the central Appalachians: Geophysical Journal International, v. 144, n. 3, p. 568–576, http://dx.doi.org/10.1046/j.0956-540X.2000.01349.x

Elmore, R. D., Foucher, J. L.-E., Evans, M., and Lewchuk, M., 2006, Remagnetization of the Tonoloway Formation and the Helderberg Group in the Central Appalachians: testing the origin of syntilting magnetizations: Geophysical Journal International, v. 166, n. 3, p. 1062–1076, http://dx.doi.org/10.1111/j.1365-246X.2006.02875.x

Ernst, R. E., and Buchan, K. L., 1993, Paleomagnetism of the Abitibi dyke swarm, southern Superior

Province, and implications for the Logan Loop: Canadian Journal of Earth Science, v. 30, n. 9, p. 1886–1897, http://dx.doi.org/10.1139/e93-167
Evans, D. A. D., 2003, True polar wander and supercontinents: Tectonophysics, v. 362, n. 1–4, p. 303–320, http://dx.doi.org/10.1016/S0040-1951(02)000642-X
——— 2009, The palaeomagnetically viable, long-lived and all-inclusive Rodinia supercontinent reconstruction, *in* Murphy, J. B., Keppie, J. D., and Hynes, A. J., edsitors, Ancient Orogens and Modern Analogues: Geological Society, London, Special Publications, v. 327, p. 371–404, http://dx.doi.org/10.1144/SP327.16
Evans, D. A. D., and Mitchell, R. N., 2011, Assembly and breakup of the core of Paleoproterozoic-Mesoproterozoic supercontinent Nuna: Geology, v. 39, n. 5, p. 443–446, http://dx.doi.org/10.1130/G31654.1
Evans, D. A. D., Li, Z. X., Kirschvink, J. L., and Wingate, M., 2000, A high-quality mid-Neoproterozoic paleomagnetic pole from South China, with implications for ice ages and the breakup configuration of Rodinia: Precambrian Research, v. 100, n. 1–3, p. 313–334, http://dx.doi.org/10.1016/S0301-9268(99)00079-0
Fike, D. A., Grotzinger, J. P., Pratt, L. M., and Summon, R. E., 2006, Oxidation of the Ediacaran ocean: Nature, v. 444, p. 744–747, http://dx.doi.org/10.1038/nature05345
Fillion, G., and Rochette, P., 1988, The low temperature transition in monoclinic pyrrhotite: Journal de Physique, v. C8, p. 907–908.
Fioretti, A. M., Black, L. P., Foden, J., and Visonà, D., 2005, Grenville-age magmatism at the South Tasman Rise (Australia): A new piercing point for the reconstruction of Rodinia: Geology, v. 33, n. 10, p. 769–772, http://dx.doi.org/10.1130/G21671.1
Fisher, D., 1974, Some more remarks on polar wandering: Journal of Geophysical Research, v. 79, n. 26, p. 4041–4045, http://dx.doi.org/10.1029/JB079i026p04041
Fisher, R., 1953, Dispersion on a sphere: Proceedings of the Royal Society of London, Series A, v. 217, n. 1130, p. 295–305, http://www.jstor.org/stable/99186
Gold, T., 1955, Instability of the Earth's axis of rotation: Nature, v. 175, p. 526–529, http://dx.doi.org/10.1038/175526a0
Goleby, B. R., 1980, Early Palaeozoic palaeomagnetism in south east Australia: Journal of Geomagnetism and Geoelectricity, v. 32, p. 11–21, http://dx.doi.org/10.5636/jgg.32.Supplement3_SIII11
Goodge, J. W., and Fanning, C. M., 2010, Composition and age of the East Antarctic Shield in eastern Wilkes Land determined by proxy from Oligocene-Pleistocene glaciomarine sediment and Beacon Supergroup sandstones, Antarctica: Geological Society of America Bulletin, v. 122, n. 7–8, p. 1135–1159, http://dx.doi.org/10.1130/B30079.1
Goodge, J. W., Vervoort, J. D., Fanning, C. M., Brecke, D. M., Farmer, G. L., Williams, I. S., Myrow, P. M., and DePaolo, D. J., 2008, A positive test of east Antarctica–Laurentia juxtaposition within the Rodinia supercontinent: Science, v. 321, n. 5886, p. 235–240, http://dx.doi.org/10.1126/science.1159189
Gregory, L. C., Meert, J. G., Bingen, B., Pandit, M. K., and Torsvik, T. H., 2009, Paleomagnetism and geochronology of the Malani Igneous Suite, Northwest India: Implications for the configuration of Rodinia and the assembly of Gondwana: Precambrian Research, v. 170, n. 1–2, p. 13–26, http://dx.doi.org/10.1016/j.precamres.2008.11.004
Haines, P. W., Hand, M., and Sandiford, M., 2001, Palaeozoic synorogenic sedimentation in central and northern Australia: a review of distribution and timing with implications for the evolution of intracontinental orogens: Australian Journal of Earth Sciences, v. 48, n. 6, p. 911–928, http://dx.doi.org/10.1046/j.1440-0952.2001.00909.x
Halls, H. C., 1974, A paleomagnetic reversal in the Osler Volcanic Group, northern Lake Superior: Canadian Journal of Earth Science, v. 11, n. 9, p. 1200–1207, http://dx.doi.org/10.1139/e74-113
Halverson, G. P., 2006, A Neoproterozoic Chronology, *in* Xiao, S., and Kaufman, A. J., editors, Neoproterozoic Geobiology and Paleobiology, Topics in Geobiology: Dordrecht, The Netherlands, Springer, v. 27, p. 231–271.
Halverson, G. P., Hoffman, P. F., Schrag, D. P., Maloof, A. C., and Rice, A. H. N., 2005, Toward a Neoproterozoic composite carbon-isotope record: Geological Society of America Bulletin, v. 117, n. 9–10, p. 1181–1207, http://dx.doi.org/10.1130/B25630.1
Halverson, G. P., Maloof, A. C., Schrag, D. P., Dudas, F. O., and Hurtgen, M., 2007, Stratigraphy and geochemistry of a ca 800 Ma negative carbon isotope interval in northeastern Svalbard: Chemical Geology, v. 237, n. 1–2, p. 5–27, http://dx.doi.org/10.1016/j.chemgeo.2006.06.013
Hand, M., and Sandiford, M., 1999, Intraplate deformation in central Australia, the link between subsidence and fault reactivation: Tectonophysics, v. 305, n. 1–3, p. 121–140, http://dx.doi.org/10.1016/S0040-1951(99)00009-8
Harlan, S. S., Geissman, J. W., and Snee, L. W., 2008, Paleomagnetism of Proterozoic mafic dikes from the Tobacco Root Mountains, southwest Montana: Precambrian Research, v. 163, n. 3–4, p. 239–264, http://dx.doi.org/10.1016/j.precamres.2007.12.002
Heine, C., Dietmar Müller, R., Steinberger, B., and Torsvik, T. H., 2008, Subsidence in intracontinental basins due to dynamic topography: Physics of the Earth and Planetary Interiors, v. 171, n. 1–4, p. 252–264, http://dx.doi.org/10.1016/j.pepi.2008.05.008
Henry, G. S., Mauk, F. J., and Van der Voo, R., 1977, Paleomagnetism of the upper Keweenawan sediments: The Nonesuch Shale and Freda Sandstone: Canadian Journal of Earth Science, v. 14, n. 5, p. 1128–1138, http://dx.doi.org/10.1139/e77-103
Hilgenfeldt, K., 2000, Diagenetic dissolution of biogenic magnetite in surface sediments of the Benguela upwelling system: International Journal Of Earth Sciences, v. 88, n. 4, p. 630–640, http://dx.doi.org/10.1007/s005310050293
Hill, A. C., Arouri, K., Gorjan, P., and Walter, M. R., 2000, Geochemistry of marine and nonmarine

environments of a Neoproterozoic cratonic carbonate/evaporite: the Bitter Springs Formation, Central Australia, *in* Grotzinger, J., and James, N., editors, Carbonate Sedimentation and Diagenesis in an Evolving Precambrian World: SEPM Special Publications, v. 67, p. 327–344, http://dx.doi.org/10.2110/pec.00.67.0327

Hnat, J. S., van der Pluijm, B. A., and Van der Voo, R., 2006, Primary curvature in the Mid-Continent Rift: Paleomagnetism of the Portage Lake Volcanics (northern Michigan, USA): Tectonophysics, v. 425, n. 1–4, p. 71–82, http://dx.doi.org/10.1016/j.tecto.2006.07.006

Hoffman, P. F., 1991, Did the breakout of Laurentia turn Gondwana inside out?: Science, v. 252, n. 5011, p. 1409–1412, http://dx.doi.org/10.1126/science.252.5011.1409

——— 1999, The break-up of Rodinia, birth of Gondwana, true polar wander and the snowball Earth: Journal of African Earth Sciences, v. 28, n. 1, p. 17–33, http://dx.doi.org/10.1016/S0899-5362(99)00018-4

Hoffman, P. F., Kaufman, A. J., Halverson, G. P., and Schrag, D. P., 1998, A Neoproterozoic snowball Earth: Science, v. 281, n. 5381, p. 1342–1346, http://dx.doi.org/10.1126/science.281.5381.1342

Hoffmann, K. H., Condon, D. J., Bowring, S. A., and Crowley, J. L., 2004, U-Pb zircon date from the Neoproterozoic Ghaub Formation, Namibia: Constraints on Marinoan glaciation: Geology, v. 32, n. 9, p. 817–820, http://dx.doi.org/10.1130/G20519.1

Housen, B. A., and Moskowitz, B. M., 2006, Depth distribution of magnetofossils in near-surface sediments from the Blake/Bahama Outer Ridge, western North Atlantic Ocean, determined by low-temperature magnetism: Journal of Geophysical Research, v. 111, http://dx.doi.org/10.1029/2005JG000068

Hutton, L. J., Withnall, I. W., Rienks, I. P., Bultitude, R. J., Hayward, M. A., von Gneilinski, F. E., Fordham, B. G., and Simpson, G. A., 1999, A preliminary Carboniferous to Permian magmatic framework for the Auburn-Connors Arches, Central Queensland: Armidale, New South Wales, Australia, Division of Earth Sciences, University of New England, New England Orogen 1999 Conference Proceedings, p. 223–232.

IAGA-Working-Group, Finlay, C. C., Maus, S., Beggan, C. D., Bondar, T. N., Chambodut, A., Chernova, T. A., Chulliat, A., Golovkov, V. P., Hamilton, B., Hamoudi, M., Holme, R., Hulot, G., Kuang, W., Langlais, B., Lesur, V., Lowes, F. J., Lühr, H., Macmillan, S., Mandea, M., McLean, S., Manoj, C., Menvielle, M., Michaelis, I., Olsen, N., Rauberg, J., Rother, M., Sabaka, T. J., Tangborn, A., Tøffner-Clausen, L., Thébault, E., Thomson, A. W. P., Wardinski, I., Wei, Z., and Zvereva, T. I., 2010, International Geomagnetic Reference Field: the eleventh generation: Geophysical Journal International, v. 183, n. 3, p. 1216–1230, http://dx.doi.org/10.1111/j.1365-246X.2010.04804.x

Idnurm, M., and Giddings, J. W., 1988, Australian Precambrian polar wander: a review: Precambrian Research, v. 40–41, p. 61–88, http://dx.doi.org/10.1016/0301-9268(88)90061-7

Jackson, M., 1990, Diagenetic sources of stable remanence in remagnetized Paleozoic cratonic carbonates: a rock magnetic study: Journal of Geophysical Research, v. 95, n. B3, p. 2753–2761, http://dx.doi.org/10.1029/JB095iB03p02753

Jackson, M., McCabe, C., Ballard, M. M., and Van der Voo, R., 1988, Magnetite authigenesis and diagenetic paleotemperatures across the northern Appalachian basin: Geology, v. 16, n. 7, p. 592–595, http://dx.doi.org/10.1130/0091-7613(1988)016⟨0592:MAADPA⟩2.3.CO;2

Jackson, M., and Swanson-Hysell, N. L., 2012, Rock magnetism of remagnetized carbonate rocks: Another look, *in* Elmore, R., editor, Remagnetization and Chemical Alteration of Sedimentary Rocks: Geological Society London, Special Publications, v. 371, http://dx.doi.org/10.1144/SP371.3

Jackson, M., Sun, W.-W., and Craddock, J. P., 1992, The rock magnetic fingerprint of chemical remagnetization in midcontinental Paleozoic carbonates: Geophysical Research Letters, v. 19, n. 8, p. 781–784, http://dx.doi.org/10.1029/92GL00832

Jones, C., 2002, User-driven integrated software lives: "PaleoMag" paleomagnetics analysis on the Macintosh: Computers and Geosciences, v. 28, n. 10, p. 1145–1151, http://dx.doi.org/10.1016/S0098-3004(02)00032-8

Karlstrom, K. E., Ahäll, K.-I., Harlan, S. S., Williams, M. L., McLelland, J., and Geissman, J. W., 2001, Long-lived (1.8-1.0 Ga) convergent orogen in southern Laurentia, its extensions to Australia and Baltica, and implications for refining Rodinia: Precambrian Research, v. 111, n. 1–4, p. 5–30, http://dx.doi.org/10.1016/S0301-9268(01)00154-1

Karlstrom, K. E., Harlan, S. S., Williams, M. L., McLelland, J., Geissman, J. W., and Ahäll, K.-I., 1999, Refining Rodinia: Geologic evidence for the Australia–Western US connection in the Proterozoic: GSA Today, v. 9, n. 10, p. 1–7.

Katz, B., Elmore, R. D., Cogoini, M., and Ferry, S., 1998, Widespread chemical remagnetization: Orogenic fluids or burial diagenesis of clays?: Geology, v. 26, n. 7, p. 603–606, http://dx.doi.org/10.1130/0091-7613(1998)026⟨0603:WCROFO⟩2.3.CO;2

Katz, B., Elmore, R. D., Cogoini, M., Engel, M. H., and Ferry, S., 2000, Associations between burial diagenesis of smectite, chemical remagnetization, and magnetite authigenesis in the Vocontian trough, SE France: Journal of Geophysical Research, v. 105, n. B1, p. 851–868, http://dx.doi.org/10.1029/1999JB900309

Kendall, B., Creaser, R. A., and Selby, D., 2006, Re-Os geochronology of postglacial black shales in Australia: Constraints on the timing of "Sturtian" glaciation: Geology, v. 34, n. 9, p. 729–732, http://dx.doi.org/10.1130/G22775.1

Kirschvink, J., 1978, The Precambrian-Cambrian boundary problem: paleomagnetic directions from the Amadeus Basin, Central Australia: Earth and Planetary Science Letters, v. 40, n. 1, p. 91–100, http://dx.doi.org/10.1016/0012-821X(78)90077-8

——— 1980, The least-squares line and plane and the analysis of paleomagnetic data: Geophysical Journal of the Royal Astronomical Society, v. 62, n. 3, p. 699–718, http://dx.doi.org/10.1111/j.1365-246X.1980.tb02601.x

——— 1992a, Late Proterozoic low-latitude glaciation: The snowball earth, *in* Schopf, J. W., Klein, C., and Des Marais, D., editors, The Proterozoic Biosphere: A Multidisciplinary Study: Cambridge, Cambridge University Press, p. 51–52.

——— 1992b, A paleogeographic model for Vendian and Cambrian time, *in* Schopf, J., Klein, C., and Des Marais, D., editors, The Proterozoic Biosphere: A Multidisciplinary Study: Cambridge, Cambridge University Press, p. 569–581.

Kirschvink, J. L., Ripperdan, R. L., and Evans, D. A., 1997, Evidence for a large-scale reorganization of Early Cambrian continental masses by inertial interchange true polar wander: Science, v. 277, n. 5325, p. 541–545, http://dx.doi.org/10.1126/science.277.5325.541

Kirschvink, J. L., Kopp, R., Raub, T., Baumgartner, J., and Holt, J., 2008, Rapid, precise, and high-sensitivity acquisition of paleomagnetic and rock-magnetic data: Development of a low-noise automatic sample changing system for superconducting rock magnetometers: Geochemistry, Geophysics, and Geosystems, v. 9, doi:10.1029/2007GC001856

Klootwijk, C. T., 1980, Early Palaeozoic palaeomagnetism in Australia I. Cambrian results from the Flinders Ranges, South Australia II. Late Early Cambrian results from Kangaroo Island, South Australia III. Middle to early-Late Cambrian results from the Amadeus Basin, Northern Territory: Tectonophysics, v. 64, n. 3–4, p. 249–332, http://dx.doi.org/10.1016/0040-1951(80)90100-6

Kopp, R. E., ms, 2007, The identification and interpretation of microbial biogeomagnetism: Pasadena, California, California Institute of Technology, Ph.D. thesis, 190 p.

Kopp, R. E., and Kirschvink, J. L., 2008, The identification and biogeochemical interpretation of fossil magnetotactic bacteria: Earth-Science Reviews, v. 86, n. 1–4, p. 42–61, http://dx.doi.org/10.1016/j.earscirev.2007.08.001

Korsch, R. J., and Lindsay, J. F., 1989, Relationships between deformation and basin evolution in the intracratonic Amadeus Basin, central Australia: Tectonophysics, v. 158, n. 1–4, p. 5–22, http://dx.doi.org/10.1016/0040-1951(89)90312-0

Kruiver, P. P., Dekkers, M. J., and Heslop, D., 2001, Quantification of magnetic coercivity components by the analysis of acquisition curves of isothermal remanent magnetisation: Earth and Planetary Science Letters, v. 189, n. 3–4, p. 269–276, http://dx.doi.org/10.1016/S0012-821X(01)00367-3

Lewis, J. P., Eby, M., Weaver, A. J., Johnston, S. T., and Jacob, R. L., 2004, Global glaciation in the Neoproterozoic: Reconciling previous modelling results: Geophysical Research Letters, v. 31, L08201, http://dx.doi.org/10.1029/2004GL019725

Li, Y.-L., Vali, H., Sears, S. K., Yang, J., Deng, B., and Zhang, C. L., 2004a, Iron reduction and alteration of nontronite NAu-2 by a sulfate-reducing bacterium: Geochimica et Cosmochimica Acta, v. 68, n. 15, p. 3251–3260, http://dx.doi.org/10.1016/j.gca.2004.03.004

Li, Z. X., 2000, New paleomagnetic results from the "cap dolomite" of the Neoproterozoic Walsh Tillite, northwestern Australia: Precambrian Research, v. 100, n. 1–3, p. 359–370, http://dx.doi.org/10.1016/S0301-9268(99)00081-9

Li, Z. X., and Evans, D. A. D., 2011, Late Neoproterozoic 40° intraplate rotation within Australia allows for a tighter-fitting and longer-lasting Rodinia: Geology, v. 39, n. 1, p. 39–42, http://dx.doi.org/10.1130/G31461.1

Li, Z. X., and Powell, C. M., 2001, An outline of the palaeogeographic evolution of the Australasian region since the beginning of the Neoproterozoic: Earth-Science Reviews, v. 53, n. 3–4, p. 237–277, http://dx.doi.org/10.1016/S0012-8252(00)00021-0

Li, Z. X., Schmidt, P. W., and Embleton, B. J. J., 1988, Paleomagnetism of the Hervey Group, Central New South Wales and its tectonic implications: Tectonics, v. 7, n. 3, p. 351–367, http://dx.doi.org/10.1029/TC007i003p00351

Li, Z. X., Powell, C. M., and Schmidt, P. W., 1989, Syn-deformational remanent magnetization of the Mount Eclipse Sandstone, central Australia: Geophysical Journal International, v. 99, n. 1, p. 205–222, http://dx.doi.org/10.1111/j.1365-246X.1989.tb02025.x

Li, Z. X., Powell, C. McA., Embleton, B. J. J., and Schmidt, P. W., 1991, New palaeomagnetic results from the Amadeus Basin and their implications for stratigraphy and tectonics, *in* Korsch, R. J., and Kennard, J. M., editors, Geological and Geophysical Studies in the Amadeus Basin, Central Australia: Bureau of Mineral Resources, v. 236, p. 349–360.

Li, Z. X., Zhang, L., and Powell, C. McA., 1995, South China in Rodinia: Part of the missing link between Australia–East Antarctica and Laurentia?: Geology, v. 23, n. 5, p. 407–410, http://dx.doi.org/10.1130/0091-7613(1995)023⟨0407:SCIRPO⟩2.3.CO;2

Li, Z. X., Evans, D. A. D., and Zhang, S., 2004b, A 90° spin on Rodinia: possible causal links between the Neoproterozoic supercontinent, superplume, true polar wander and low-latitude glaciation: Earth and Planetary Science Letters, v. 220, n. 3–4, p. 409–421, http://dx.doi.org/10.1016/S0012-821X(04)00064-0

Li, Z. X., Bogdanova, S. V., Collins, A. S., Davidson, A., De Waele, B., Ernst, R. E., Fitzsimons, I. C. W., Fuck, R. A., Gladkochub, D. P., Jacobs, J., Karlstrom, K. E., Lu, S., Natapov, L. M., Pease, V., Pisarevsky, S. A., Thrane, K., and Vernikovsky, V., 2008, Assembly, configuration, and break-up history of Rodinia: A synthesis: Precambrian Research, v. 160, n. 1–2, p. 179–210, http://dx.doi.org/10.1016/j.precamres.2007.04.021

Lindsay, J. F., 1987, Upper Proterozoic evaporites in the Amadeus basin, central Australia, and their role in basin tectonics: Geological Society of America Bulletin, v. 99, n. 6, p. 852–865, http://dx.doi.org/10.1130/0016-7606(1987)99⟨852:UPEITA⟩2.0.CO;2

——— 1999, Heavitree Quartzite, a Neoproterozoic (*ca* 800-760 Ma), high-energy, tidally influenced, ramp association, Amadeus Basin, central Australia: Australian Journal of Earth Sciences, v. 46, n. 1, p. 127–139, http://dx.doi.org/10.1046/j.1440-0952.1999.00693.x

——— 2002, Supersequences, superbasins, supercontinents—evidence from the Neoproterozoic–Early Palaeozoic basins of central Australia: Basin Research, v. 14, n. 2, p. 207–223, http://dx.doi.org/10.1046/j.1365-2117.2002.00170.x

Lindsay, J. F., and Korsch, R. J., 1989, Interplay of tectonics and sea-level changes in basin evolution: and

example from the intacratonic Amadeus Basin, central Australia: Basin Research, v. 2, n. 1, p. 3–25, http://dx.doi.org/10.1111/j.1365-2117.1989.tb00023.x
Liu, Q., Yu, Y., Torrent, J., Roberts, A. P., Pan, Y., and Zhu, R., 2006, Characteristic low-temperature magnetic properties of aluminous goethite [α-(Fe, Al)OOH] explained: Journal of Geophysical Research, v. 111, B12S34, http://dx.doi.org/10.1029/2006JB004560
Maboko, M. A. H., McDougall, I., Zeitler, P. K., and Williams, I. S., 1992, Geochronological evidence for ~530–550 Ma juxtaposition of two Proterozoic metamorphic terranes in the Musgrave Ranges, Central Australia: Australian Journal of Earth Sciences, v. 39, n. 4, p. 457–471, http://dx.doi.org/10.1080/08120099208728038
Macdonald, F. A., Schmitz, M. D., Crowley, J. L., Roots, C. F., Jones, D. S., Maloof, A. C., Strauss, J. V., Cohen, P. A., Johnston, D. T., and Schrag, D. P., 2010, Calibrating the Cryogenian: Science, v. 327, n. 5970, p. 1241–1243, http://dx.doi.org/10.1126/science.1183325
Maher, B. A., Karloukovski, V. V., and Mutch, T. J., 2004, High-field remanence properties of synthetic and natural submicrometre haematites and goethites: significance for environmental contexts: Earth and Planetary Science Letters, v. 226, n. 34, p. 491–505, http://dx.doi.org/10.1016/j.epsl.2004.05.042
Maidment, D. W., Williams, I. S., and Hand, M., 2007, Testing long-term patterns of basin sedimentation by detrital zircon geochronology, Centralian Superbasin, Australia: Basin Research, v. 19, n. 3, p. 335–360, http://dx.doi.org/10.1111/j.1365-2117.2007.00326.x
Maloof, A. C., Halverson, G. P., Kirschvink, J. L., Schrag, D. P., Weiss, B. P., and Hoffman, P. F., 2006, Combined paleomagnetic, isotopic and stratigraphic evidence for true polar wander from the Neoproterozoic Akademikerbreen Group, Svalbard, Norway: Geological Society of America Bulletin, v. 118, n. 9–10, p. 1099–1124, http://dx.doi.org/10.1130/B25892.1
Maloof, A. C., Kopp, R. E., Grotzinger, J. P., Fike, D. A., Bosak, T., Vali, H., Poussart, P. M., Weiss, B. P., and Kirschvink, J. L., 2007, Sedimentary iron cycling and the origin and preservation of magnetization in platform carbonate muds, Andros Island, Bahamas: Earth and Planetary Science Letters, v. 259, n. 3–4, p. 581–598, http://dx.doi.org/10.1016/j.epsl.2007.05.021
Marshall, H. G., Walker, J. C. G., and Kuhn, W. R., 1988, Long-term climate change and the geochemical cycle of carbon: Journal of Geophysical Research, v. 93, n. D1, p. 791–801, http://dx.doi.org/10.1029/JD093iD01p00791
Matsuyama, I., Mitrovica, J. X., Daradich, A., and Gomez, N., 2010, The rotational stability of a triaxial ice-age earth: Journal of Geophysical Research, v. 115, B05401, http://dx.doi.org/10.1029/2009JB006564
McCabe, C., and Channell, J. E. T., 1994, Late Paleozoic remagnetization in limestones of the Craven Basin (northern England) and the rock magnetic fingerprint of remagnetized sedimentary carbonates: Journal of Geophysical Research, v. 99, n. B3, p. 4603–4612, http://dx.doi.org/10.1029/93JB02802
McCabe, C., and Elmore, R. D., 1989, The occurrence and origin of Late Paleozoic remagnetization in the sedimentary rocks of North America: Reviews of Geophysics, v. 27, n. 4, p. 471–494, http://dx.doi.org/10.1029/RG027i004p00471
McCabe, C., and Van der Voo, R., 1983, Paleomagnetic results from the upper Keweenawan Chequamegon Sandstone: implications for red bed diagenesis and Late Precambrian apparent polar wander of North America: Canadian Journal of Earth Science, v. 20, n. 1, p. 105–112, http://dx.doi.org/10.1139/e83-010
McCabe, C., Van der Voo, R., Peacor, D. R., Scotese, C. R., and Freeman, R., 1983, Diagenetic magnetite carries ancient yet secondary remanence in some Paleozoic sedimentary carbonates: Geology, v. 11, n. 4, p. 221–223, http://dx.doi.org/10.1130/0091-7613(1983)11⟨221:DMCAYS⟩2.0.CO;2
McElhinny, M. W., 1964, Statistical significance of the fold test in paleomagnetism: Geophysical Journal of the Royal Astronomical Society, v. 8, n. 3, p. 338–340, http://dx.doi.org/10.1111/j.1365-246X.1964.tb06300.x
McElhinny, M. W., Powell, C. McA., and Pisarevsky, S. A., 2003, Paleozoic terranes of eastern Australia and the drift history of Gondwana: Tectonophysics, v. 362, n. 1–4, p. 41–65, http://dx.doi.org/10.1016/S0040-1951(02)00630-3
McFadden, P. L., and McElhinny, M. W., 1988, The combined analysis of remagnetization circles and direct observations in paleomagnetism: Earth and Planetary Science Letters, v. 87, n. 1–2, p. 161–172, http://dx.doi.org/10.1016/0012-821X(88)90072-6
——— 1990, Classification of the reversal test in palaeomagnetism: Geophysical Journal International, v. 103, n. 3, p. 725–729, http://dx.doi.org/10.1111/j.1365-246X.1990.tb05683.x
McLaren, S., Sandiford, M., Dunlap, W. J., Scrimgeour, I., Close, D., and Edgoose, C., 2009, Distribution of Palaeozoic reworking in the Western Arunta Region and northwestern Amadeus Basin from $^{40}Ar/^{39}Ar$ thermochronology: implications for the evolution of intracratonic basins: Basin Research, v. 21, n. 3, p. 315–334, http://dx.doi.org/10.1111/j.1365-2117.2008.00385.x
McWilliams, M. O., and Dunlop, D. J., 1975, Precambrian paleomagnetism: Magnetizations reset by the Grenville Orogeny: Science, v. 190, n. 4211, p. 269–272, http://dx.doi.org/10.1126/science.190.4211.269
Meert, J. G., Van der Voo, R., and Ayub, S., 1995, Paleomagnetic investigation of the Neoproterozoic Gagwe lavas and Mbozi complex, Tanzania and the assembly of Gondwana: Precambrian Research, v. 74, n. 4, p. 225–244, http://dx.doi.org/10.1016/0301-9268(95)00012-T
Ménabréaz, L., Thouveny, N., Camoin, G., and Lund, S. P., 2010, Paleomagnetic record of the late Pleistocene reef sequence of Tahiti (French Polynesia): A contribution to the chronology of the deposits: Earth and PlanetaryScience Letters, v. 294, n. 1–2, p. 58–68, http://dx.doi.org/10.1016/j.epsl.2010.03.002
Miller, J. D., and Kent, D. V., 1988, Regional trends in the timing of Alleghenian remagnetization in the Appalachians: Geology, v. 16, n. 7, p. 588–591, http://dx.doi.org/10.1130/0091-7613(1988)016⟨0588:RTITTO⟩2.3.CO;2

Miller, K. C., and Hargraves, R. B., 1994, Paleomagnetism of some Indian kimberlites and lamproites: Precambrian Research, v. 69, n. 1–4, p. 259–267, http://dx.doi.org/10.1016/0301-9268(94)90090-6
Mitchell, R. N., Evans, D. A. D., and Kilian, T. M., 2010, Rapid early Cambrian rotation of Gondwana: Geology, v. 38, n. 8, p. 755–758, http://dx.doi.org/10.1130/G30910.1
Mitrovica, J. X., Wahr, J., Matsuyama, I., and Paulson, A., 2005, The rotational stability of an ice-age earth: Geophysical Journal International, v. 161, n. 2, p. 491–506, http://dx.doi.org/10.1111/j.1365-246X.2005.02609.x
Montgomery, P., Hailwood, E. A., Gale, A. S., and Burnett, J. A., 1998, The magnetostratigraphy of Coniacian late Campanian chalk sequences in southern England: Earth And Planetary Science Letters, v. 156, n. 3–4, p. 209–224, http://dx.doi.org/10.1016/S0012-821X(98)00008-9
Moores, E. M., 1991, Southwest U.S.–East Antarctic (SWEAT) connection: A hypothesis: Geology, v. 19, n. 5, p. 425–428, http://dx.doi.org/10.1130/0091-7613(1991)019⟨0425:SUSEAS⟩2.3.CO;2
Morris, W. A., and Roy, J. L., 1977, Discovery of the Hadrynian Polar Track and further study of the Grenville problem: Nature, v. 266, p. 689–692, http://dx.doi.org/10.1038/266689a0
Mound, J. E., and Mitrovica, J. X., 1998, True polar wander as a mechanism for second-order sea-level variations: Science, v. 279, n. 5350, p. 534–537, http://dx.doi.org/10.1126/science.279.5350.534
Murthy, G., Gower, C., Tubrett, M., and Pätzold, R., 1992, Paleomagnetism of Eocambrian Long Range dykes and Double Mer Formation from Labrador, Canada: Canadian Journal of Earth Sciences, v. 29, n. 6, p. 1224–1234, http://dx.doi.org/10.1139/e92-098
Muttoni, G., 1995, "Wasp-waisted" hysteresis loops from a pyrrhotite and magnetite-bearing remagnetized Triassic limestone: Geophysical Research Letters, v. 22, n. 23, p. 3167–3170, http://dx.doi.org/10.1029/95GL03073
Muxworthy, A. R., and McClelland, E., 2000, Review of the low-temperature magnetic properties of magnetite from a rock magnetic perspective: Geophysical Journal International, v. 140, n. 1, p. 101–114, http://dx.doi.org/10.1046/j.1365-246x.2000.00999.x
Myers, J. S., Shaw, R. D., and Tyler, I. M., 1996, Tectonic evolution of Proterozoic Australia: Tectonics, v. 15, n. 6, p. 1431–1446, http://dx.doi.org/10.1029/96TC02356
Narbonne, G. M., and Gehling, J. G., 2003, Life after snowball: The oldest complex Ediacaran fossils: Geology, v. 31, n. 1, p. 27–30, http://dx.doi.org/10.1130/0091-7613(2003)031⟨0027:LASTOC⟩2.0.CO;2
Nicholson, S. W., Schultz, K. J., Shirey, S. B., and Green, J. C., 1997, Rift-wide correlation of 1.1 Ga Midcontinent rift system basalts: implications for multiple mantle sources during rift development: Canadian Journal of Earth Science, v. 34, n. 4, p. 504–520, http://dx.doi.org/10.1139/e17-041
Otofuji, Y.-i., Takemoto, K., Zaman, H., Nishimitsu, Y., and Wada, Y., 2003, Cenozoic remagnetization of the Paleozoic rocks in the Kitakami massif of northeast Japan, and its tectonic implications: Earth and Planetary Science Letters, v. 210, n. 1–2, p. 203–217, http://dx.doi.org/10.1016/S0012-821X(03)00125-0
Özdemir, O., and Dunlop, D. J., 1996, Thermoremanence and Néel temperature of goethite: Geophysical Research Letters, v. 23, n. 9, p. 921–924, http://dx.doi.org/10.1029/96GL00904
Palmer, H. C., and Davis, D. W., 1987, Paleomagnetism and U-Pb geochronology of volcanic rocks from Michipicoten Island, Lake Superior, Canada: precise calibration of the Keweenawan polar wander track: Precambrian Research, v. 37, n. 2, p. 157–171, http://dx.doi.org/10.1016/0301-9268(87)90077-5
Palmer, H. C., Merz, B. A., and Hayatsu, A., 1977, The Sudbury dikes of the Grenville Front region: paleomagnetism, petrochemistry, and K-Ar age studies: Canadian Journal of Earth Sciences, v. 14, n. 8, p. 1867–1887, http://dx.doi.org/10.1139/e77-158
Pavlov, V., and Gallet, Y., 2010, Variations in geomagnetic reversal frequency during the Earth's middle age: Geochemistry Geophysics Geosystems, v. 11, http://dx.doi.org/10.1029/2009GC002583
Pisarevsky, S. A., Wingate, T. D., Powell, C. M., Johnson, S., and Evans, D. A. D., 2003a, Models of Rodinia assembly and fragmentation, *in* Yoshida, M., Windley, B. E., and Dasgupta, S., editors, Proterozoic East Gondwana: Supercontinent Assembly and Breakup: The Geological Society, London, Special Publications, v. 206, p. 35–55, http://dx.doi.org/10.1144/GSL.SP.2003.206.01.04
Pisarevsky, S. A., Wingate, M. T. D., and Harris, L. B., 2003b, Late Mesoproterozoic (*ca* 1.2 Ga) palaeomagnetism of the Albany-Fraser orogen: no pre-Rodinia Australia–Laurentia connection: Geophysical Journal International, v. 155, n. 1, p. F6–F11, http://dx.doi.org/10.1046/j.1365-246X.2003.02074.x
Pisarevsky, S. A., Wingate, M. T. D., Stevens, M. K., and Haines, P. W., 2007, Palaeomagnetic results from the Lancer 1 stratigraphic drillhole, Officer Basin, Western Australia, and implications for Rodinia reconstructions: Australian Journal of Earth Sciences, v. 54, n. 4, p. 561–572, http://dx.doi.org/10.1080/08120090701188962
Preiss, W. V., 2000, The Adelaide Geosyncline of South Australia and its significance in Neoproterozoic continental reconstruction: Precambrian Research, v. 100, n. 1–3, p. 21–63, http://dx.doi.org/10.1016/S0301-9268(99)00068-6
Preiss, W. V., Walter, M. R., Coats, R. P., and Wells, A. T., 1978, Lithological correlations of Adelaidean glaciogenic rocks in parts of the Amadeus, Ngalia, and Georgina basins: Bureau of Minearl Resources Journal of Australian Geology and Geophysics, v. 3, p. 45–53.
Raimondo, T., Collins, A. S., Hand, M., Walker-Hallam, A., Smithies, R. H., Evins, P. M., and Howard, H. M., 2009, Ediacaran intracontinental channel flow: Geology, v. 37, n. 4, p. 291–294, http://dx.doi.org/10.1130/G25452A.1
——— 2010, The anatomy of a deep intracontinental orogen: Tectonics, v. 29, TC4024, http://dx.doi.org/10.1029/2009TC002504
Rainbird, R. H., Jefferson, C. W., and Young, G. M., 1996, The early Neoproterozoic sedimentary Succession B of northwestern Laurentia: Correlations and paleogeographic significance: Geological Society of America Bulletin, v. 108, n. 4, p. 454–470, http://dx.doi.org/10.1130/0016-7606(1996)108⟨0454:TENSSB⟩2.3.CO;2
Raub, T. D., Kirschvink, J. L., and Evans, D. A. D., 2007, True polar wander: Linking deep and shallow

geodynamics to hydro- and bio-spheric hypotheses, *in* Kono, M., editor, Geomagnetism: Treatise on Geophysics, v. 5, p. 565–589, http://dx.doi.org/10.1016/B978-044452748-6.00099-7
Rochette, P., and Fillion, G., 1989, Field and temperature behavior of remanence in synthetic goethite: Paleomagnetic implications: Geophysical Research Letters, v. 16, n. 8, p. 851–854, http://dx.doi.org/10.1029/GL016i008p00851
Rochette, P., Fillion, G., Mattéi, J.-L., and Dekkers, M. J., 1990, Magnetic transition at 30–34 Kelvin in pyrrhotite: insight into a widespread occurrence of this mineral in rocks: Earth and Planetary Science Letters, v. 98, n. 3–4, p. 319–328, http://dx.doi.org/10.1016/0012-821X(90)90034-U
Roy, J. L., and Robertson, W. A., 1978, Paleomagnetism of the Jacobsville Formation and the apparent polar wander path for the interval ~1100 to ~670 m.y. for North America: Journal of Geophysical Research, v. 83, n. B3, p. 1289–1304, http://dx.doi.org/10.1029/JB083iB03p01289
Sandiford, M., and Hand, M., 1998, Controls on the locus of intraplate deformation in central Australia: Earth and Planetary Science Letters, v. 162, n. 1–4, p. 97–110, http://dx.doi.org/10.1016/S0012-821X(98)00159-9
Schmidt, P. W., and Clark, D. A., 2000, Paleomagnetism, apparent polar-wander path, and paleolatitude, *in* Veevers, J. J., editor, Billion-Year Earth History of Australia and Neighbours in Gondwanaland: Sydney, Australia, GEMOC Press, p. 12–17.
Schmidt, P. W., and Williams, G. E., 1996, Palaeomagnetism of the ejecta-bearing Bunyeroo Formation, late Neoproterozoic Adelaide fold belt, and the age of the Acraman impact: Earth and Planetary Science Letters, v. 144, n. 3–4, p. 347–357, http://dx.doi.org/10.1016/S0012-821X(96)00169-0
Schmidt, P. W., Embleton, B. J. J., Cudahy, T. J., and Powell, C. McA., 1986, Prefolding and Premegakinking Magnetizations from the Devonian Comerong Volcanics, New South Wales, Australia, and their bearing on the Gondwana Pole Path: Tectonics, v. 5, n. 1, p. 135–150, http://dx.doi.org/10.1029/TC005i001p00135
Schmidt, P. W., Embleton, B. J. J., and Palmer, H. C., 1987, Pre- and post-folding magnetizations from the early Devonian Snowy River Volcanics and Buchan Caves Limestone, Victoria: Geophysical Journal of the Royal Astronomical Society, v. 91, n. 1, p. 155–170, http://dx.doi.org/10.1111/j.1365-246X.1987.tb05218.x
Schmidt, P. W., Clark, D. A., and Rajagopalan, S., 1993, An historical perspective of the early Palaeozoic APWP of Gondwana: New results from the early Ordovician Black Hill Norite, South Australia: Exploration Geophysics, v. 24, p. 257–262, http://dx.doi.org/10.1071/EG993257
Schmidt, P. W., Williams, G. E., Camacho, A., and Lee, J. K. W., 2006, Assembly of Proterozoic Australia: implications of a revised pole for the ~1070 Ma Alcurra Dyke Swarm, central Australia: Geophysical Journal International, v. 167, n. 2, p. 626–634, http://dx.doi.org/10.1111/j.1365-246X.2006.03192.x
Schmidt, P. W., Williams, G. E., and McWilliams, M. O., 2009, Palaeomagnetism and magnetic anisotropy of late Neoproterozoic strata, South Australia: Implications for the palaeolatitude of late Cryogenian glaciation, cap carbonate and the Ediacaran System: Precambrian Research, v. 174, n. 1–2, p. 35–52, http://dx.doi.org/10.1016/j.precamres.2009.06.002
Schrag, D. P., Berner, R. A., Hoffman, P. F., and Halverson, G. P., 2002, On the initiation of a snowball Earth: Geochemistry, Geophysics, and Geosystems, v. 3, 1036,http://dx.doi.org/10.1029/2001GC000219
Sears, J. W., and Price, R. A., 2000, New look at the Siberian connection: No SWEAT: Geology, v. 28, n. 4, p. 423–426, http://dx.doi.org/10.1130/0091-7613(2000)28⟨423:NLATSC⟩2.0.CO;2
Sohl, L. E., Christie-Blick, N., and Kent, D. V., 1999, Paleomagnetic polarity reversals in Marinoan (ca. 600 Ma) glacial deposits of Australia: implications for the duration of low-latitude glaciation in Neoproterozoic time: Geological Society of America Bulletin, v. 111, n. 8, p. 1120–1139, http://dx.doi.org/10.1130/0016-7606(1999)111⟨1120:PPRIMC⟩2.3.CO;2
Southgate, P. N., 1989, Relationships between cyclicity and stromatolite form in the Late Proterozoic Bitter Springs Formation, Australia: Sedimentology, v. 36, n. 2, p. 323–339, http://dx.doi.org/10.1111/j.1365-3091.1989.tb00610.x
Srodon, J., and Eberl, D. D., 1984, Illite: Reviews in Mineralogy and Geochemistry, v. 13, p. 495–544.
Steinberger, B., and O'Connell, R. J., 1997, Changes of the Earth's rotation axis owing to advection of mantle density heterogeneities: Nature, v. 387, p. 169–173, http://dx.doi.org/10.1038/387169a0
——— 1998, Advection of plumes in mantle flow: implications for hotspot motion, mantle viscosity and plume distribution: Geophysical Journal International, v. 132, n. 2, p. 412–434, http://dx.doi.org/10.1046/j.1365-246x.1998.00447.x
——— 2002, The convective mantle flow signal in rates of true polar wander, *in* Mitrovica, J. X., and Vermeersen, B. L. A., editors, Ice Sheets, Sea Level and the Dynamic Earth: Geodynamics Research Series, v. 29, p. 233–256, http://dx.doi.org/10.1029/029GD15
Steinberger, B., and Torsvik, T. H., 2008, Absolute plate motions and true polar wander in the absence of hotspot tracks: Nature, v. 452, p. 620–623, http://dx.doi.org/10.1038/nature06824
——— 2010, Toward an explanation for the present and past locations of the poles: Geochemistry Geophysics Geosystems, v. 11, Q06W06, http://dx.doi.org/10.1029/2009GC002889
Swanson-Hysell, N. L., Maloof, A. C., Weiss, B. P., and Evans, D. A. D., 2009, No asymmetry in geomagnetic reversals recorded by 1.1-billion-year-old Keweenawan basalts: Nature Geoscience, v. 2, p. 713–717, http://dx.doi.org/10.1038/ngeo622
Swanson-Hysell, N. L., Rose, C. V., Calmet, C. C., Halverson, G. P., Hurtgen, M. T., and Maloof, A. C., 2010, Cryogenian glaciation and the onset of carbon-isotope decoupling: Science, v. 328, n. 5978, p. 608–611, http://dx.doi.org/10.1126/science.1184508
Tanaka, H., and Idnurm, M., 1994, Palaeomagnetism of Proterozoic mafic intrusions and host rocks of the Mount Isa Inlier, Australia: revisited: Precambrian Research, v. 69, n. 1–4, p. 241–258, http://dx.doi.org/10.1016/0301-9268(94)90089-2
Tarduno, J. A., and Myers, M., 1994, A primary magnetization fingerprint from the Cretaceous Laytonville

Limestone: Further evidence for rapid oceanic plate velocities: Journal of Geophysical Research, v. 99, n. B11, p. 21,691–21,703, http://dx.doi.org/10.1029/94JB01939
Tauxe, L., 2010, Essentials of Paleomagnetism: Berkeley, California, University of California Press, 489 p.
Tauxe, L., and Kodama, K. P., 2009, Paleosecular variation models for ancient times: Clues from Keweenawan lava flows: Physics of the Earth and Planetary Interiors, v. 177, n. 1–2, p. 31–45, http://dx.doi.org/10.1016/j.pepi.2009.07.006
Tauxe, L., and Watson, G. S., 1994, The fold test: an eigen analysis approach: Earth and Planetary Science Letters, v. 122, n. 3–4, p. 331–341, http://dx.doi.org/10.1016/0012-821X(94)90006-X
Tauxe, L., Mullender, T. A. T., and Pick, T., 1996, Potbellies, wasp-waists, and superparamagnetism in magnetic hysteresis: Journal of Geophysical Research, v. 101, n. B1, p. 571–583, http://dx.doi.org/10.1029/95JB03041
Thrupp, G. A., Kent, D. V., Schmidt, P. W., and Powell, C. McA., 1991, Palaeomagnetism of red beds of the Late Devonian Worange Point Formation, SE Australia: Geophysical Journal International, v. 104, n. 1, p. 179–202, http://dx.doi.org/10.1111/j.1365-246X.1991.tb02503.x
Tohver, E., Weil, A. B., Solum, J. G., and Hall, C. M., 2008, Direct dating of carbonate remagnetization by $^{40}Ar/^{39}Ar$ analysis of the smectite-illite transformation: Earth and Planetary Science Letters, v. 274, n. 3–4, p. 524–530, http://dx.doi.org/10.1016/j.epsl.2008.08.002
Tsai, V. C., and Stevenson, D. J/, 2007, Theoretical constraints on true polar wander: Journal of Geophysical Research—Solid Earth, v. 112, B05415, http://dx.doi.org/10.1029/2005JB003923
Van der Voo, R., 1990, The reliability of paleomagnetic data: Tectonophysics, v. 184, n. 1, p. 1–9, http://dx.doi.org/10.1016/0040-1951(90)90116-P
Vanyo, J. P., and Awramik, S. M., 1982, Length of day and obliquity of the ecliptic 850 Ma ago: preliminary results of a stromatolite growth model: Geophysical Research Letters, v. 9, n. 10, p. 1125–1128, http://dx.doi.org/10.1029/GL009i010p01125
——— 1985, Stromatolites and Earth-Sun-Moon dynamics: Precambrian Research, v. 29, n. 1–3, p. 121–142, http://dx.doi.org/10.1016/0301-9268(85)90064-6
Veevers, J. J., and Eittreim, S. L., 1988, Reconstruction of Antarctica and Australia at breakup (95 ± 5 Ma) and before rifting (160 Ma): Australian Journal of Earth Sciences, v. 35, n. 3, p. 355–362, http://dx.doi.org/10.1080/08120098808729453
Verwey, E. J. W., 1939, Electronic conduction of magnetite (Fe_3O_4) and its transition point at low temperatures: Nature, v. 144, n. 3642, p. 327–328, http://dx.doi.org/10.1038/144327b0
Wahyono, H., ms, 1992, Palaeomagnetism and anisotropy of magnetic susceptibility of the Bathurst Batholith and its contact aureole: Macquarie Park, Australia, Macquarie University, Master's thesis, 102 p.
Walker, J. C. G., Hays, P. B., and Kasting, J. F., 1981, A negative feedback mechanism for the long-term stabilization of Earth's surface temperature: Journal of Geophysical Research, v. 86, n. C10, p. 9776–9782, http://dx.doi.org/10.1029/JC086iC10p09776
Walter, M. R., 1972, Stromatolites and the biostratigraphy of the Australian Precambrian and Cambrian: Palaeontological Association, Special Papers in Palaeontology, n. 11, Palaeontological Association, 190 p.
Walter, M. R., Veevers, J. J., Calver, C. R., and Grey, K., 1995, Neoproterozoic stratigraphy of the Centralian Superbasin, Australia: Precambrian Research, v. 73, n. 1–4, p. 173–195, http://dx.doi.org/10.1016/0301-9268(94)00077-5
Warnock, A. C., Kodama, K. P., and Zeitler, P. K., 2000, Using thermochronometry and low-temperature demagnetization to accurately date Precambrian paleomagnetic poles: Journal of Geophysical Research, v. 105, n. B8, p. 19,435–19,453, http://dx.doi.org/10.1029/2000JB900114
Weaver, R., Roberts, A. P., and Barker, A. J., 2002, A late diagenetic (syn-folding) magnetization carried by pyrrhotite: implications for paleomagnetic studies from magnetic iron sulphide-bearing sediments: Earth and Planetary Science Letters, v. 200, p. 371–386, http://dx.doi.org/10.1016/S0012-821X(02)00652-0
Weil, A. B., and Van der Voo, R., 2002, Insights into the mechanism for orogen-related carbonate remagnetization from growth of authigenic Fe-oxide: A scanning electron microscopy and rock magnetic study of Devonian carbonates from northern Spain: Journal of Geophysical Research, v. 107, 2063, http://dx.doi.org/10.1029/2001JB000200
Weil, A. B., Van der Voo, R., Mac Niocaill, C., and Meert, J., 1998, The Proterozoic supercontinent Rodinia: Paleomagnetically derived reconstructions for 1100 to 800 Ma: Earth and Planetary Science Letters, v. 154, n. 1–4, p. 13–24, http://dx.doi.org/10.1016/S0012-821X(97)00127-1
Weil, A. B., Geissman, J. W., Heizler, M., and Van der Voo, R., 2003, Paleomagnetism of Middle Proterozoic mafic intrusions and Upper Proterozoic (Nankoweap) red beds from the Lower Grand Canyon Supergroup, Arizona: Tectonophysics, v. 375, n. 1–4, p. 199–220, http://dx.doi.org/10.1016/S0040-1951(03)00339-1
Weil, A. B., Geissman, J. W., and Van der Voo, R., 2004, Paleomagnetism of the Neoproterozoic Chuar Group, Grand Canyon Supergroup, Arizona: implications for Laurentia's Neoproterozoic APWP and Rodinia break-up: Precambrian Research, v. 129, n. 1–2, p. 71–92, http://dx.doi.org/10.1016/j.precamres.2003.09.016
Weil, A. B., Geissman, J. W., and Ashby, J. M., 2006, A new paleomagnetic pole for the Neoproterozoic Uinta Mountain supergroup, Central Rocky Mountain States, USA: Precambrian Research, v. 147, n. 3–4, p. 234–259, http://dx.doi.org/10.1016/j.precamres.2006.01.017
Wells, A. T., Forman, D. J., Ranford, L. C., and Cook, P. J., 1970, Geology of the Amadeus Basin, Central Australia: Bureau of Mineral Resources, Australia Bulletin 100, 222 p.
White, R. W., Clarke, G. L., and Nelson, D. R., 1999, SHRIMP U-Pb zircon dating of Grenville-age events in

the western part of the Musgrave Block, central Australia: Journal of Metamorphic Geology, v. 17, n. 5, p. 465–481, http://dx.doi.org/10.1046/j.1525-1314.1999.00211.x

Wingate, M. T. D., and Giddings, J. W., 2000, Age and paleomagnetism of the Mundine Well dyke swarm, Western Australia: Implications for an Australia-Laurentia connection at 755 Ma: Precambrian Research, v. 100, n. 1–3, p. 335–357, http://dx.doi.org/10.1016/S0301-9268(99)00080-7

Wingate, M. T. D., Pisarevsky, S. A., and Evans, D. A. D., 2002, Rodina connections between Australia and Laurentia: no SWEAT, no AUSWUS?: Terra Nova, v. 14, n. 2, p. 121–128, http://dx.doi.org/10.1046/j.1365-3121.2002.00401.x

Wingate, M. T. D., Pisarevsky, S. A., and De Waele, B., 2010, Paleomagnetism of the 765 Ma Luakela volcanics in Northwest Zambia and implications for Neoproterozoic positions of the Congo Craton: American Journal of Science, v. 310, n. 10, p. 1333–1344, http://dx.doi.org/10.2475/10.2010.05

Woods, S. D., Elmore, R. D., and Engel, M. H., 2002, Paleomagnetic dating of the smectite-to-illite conversion: Testing the hypothesis in Jurassic sedimentary rocks, Skye, Scotland: Journal of Geophysical Research, v. 107, n. B5, http://dx.doi.org/10.1029/2000JB000053

Xu, W., Van der Voo, R., and Peacor, D. R., 1998, Electron microscopic and rock magnetic study of remagnetized Leadville carbonates, central Colorado: Tectonophysics, v. 296, n. 3–4, p. 333–362, http://dx.doi.org/10.1016/S0040-1951(98)00146-2

Zegers, T. E., Dekkers, M. J., and Bailly, S., 2003, Late Carboniferous to Permian remagnetization of Devonian limestones in the Ardennes: Role of temperature, fluids, and deformation: Journal of Geophysical Research, v. 108, 2357, http://dx.doi.org/10.1029/2002JB002213

Zijderveld, J., 1967, A. C. demagnetization of rocks: analysis of results, *in* Collinson, D. W., Creer, K. M., and Runcorn, S. K., editors, Methods in Paleomagnetism: New York, Elsevier, p. 256–286.